General Disclaimer

One or more of the Following Statements may affect this Document

- This document has been reproduced from the best copy furnished by the organizational source. It is being released in the interest of making available as much information as possible.

- This document may contain data, which exceeds the sheet parameters. It was furnished in this condition by the organizational source and is the best copy available.

- This document may contain tone-on-tone or color graphs, charts and/or pictures, which have been reproduced in black and white.

- This document is paginated as submitted by the original source.

- Portions of this document are not fully legible due to the historical nature of some of the material. However, it is the best reproduction available from the original submission.

Produced by the NASA Center for Aerospace Information (CASI)

NAS 12-602
CR 86318



AUTOMATIC LANDING

R-651

SOME APPLICATIONS OF
MATHEMATICAL OPTIMIZATION
TO AUTOMATIC LANDING SYSTEMS

By
Duncan MacKinnon

November 1969

RECEIVED
NASA STI FACILITY

INSTRUMENTATION LABORATORY
Massachusetts Institute of Technology

N70-17917
(ACCESSION NUMBER)
115
(PAGES)
NASA-CR-86318
(NASA CR OR TMX OR AD NUMBER)
(THRU)
1
(CODE)
21
(CATEGORY)
FACILITY FORM 602

NASA - CR - 86318

R-651

SOME APPLICATIONS OF MATHEMATICAL OPTIMIZATION TO AUTOMATIC LANDING SYSTEMS

by

Duncan MacKinnon

November 1969

INSTRUMENTATION LABORATORY
MASSACHUSETTS INSTITUTE OF TECHNOLOGY
CAMBRIDGE, MASSACHUSETTS, 02139

NAS-12-602

Approved: _____
Associate Director

Approved: _____
Deputy Director

ACKNOWLEDGMENT

The author wishes to acknowledge the sponsorship of Robert Pawlak of the Electronics Research Center of the National Aeronautics and Space Administration, whose interest in the applications of inertial navigation to all-weather landing resulted in the establishment of the project reported herein.

The mathematical models of the Convair 880 vehicle were formulated by Paul A. Madden, who also provided a great deal of help in constructing the contract system optimization algorithms. The author also acknowledges the programming help provided by Eugenia Freiburghouse.

The author also extends his thanks to Dr. Terrance Carney, who contributed numerous valuable suggestions during the preparation of this work.

This report was prepared under DSR Project 55-30500, sponsored by the Electronics Research Center of the National Aeronautics and Space Administration through Contract NAS 12-602 with the Instrumentation Laboratory of Massachusetts Institute of Technology in Cambridge, Massachusetts.

The publication of this report does not constitute approval by the National Aeronautics and Space Administration of the findings or the conclusions contained therein. It is published only for the exchange and stimulation of ideas.

PRECEDING PAGE BLANK NOT FILMED.

TABLE OF CONTENTS

Chapter		Page
1.	INTRODUCTION	
1.1	Automatic Landing System Ecology	1
1.2	High Precision Flight Path Trajectory Control	3
2.	APPLICATION OF OPTIMIZATION THEORY TO HYBRID NAVIGATION SYSTEM DESIGN	
2.1	Introduction	7
2.2	Inertial System Error Model	7
2.3	Radio Aid Model	9
2.4	Minimum Integral Square Estimation of Inertial System Errors	10
2.5	Weighted Least Mean Square Estimation	12
2.6	Derivation of the Kalman-Bucy Filter for Continuous Dynamical Systems	16
2.7	Optimal Estimation of Inertial System Acceleration, Velocity and Position Errors	18
2.8	Response Characteristics of Optimal Estimators	25
2.9	Gyro Drift Rate Induced Estimator Error	33
2.10	Optimal Estimator Sensitivity to Model Errors	40
2.11	Discrete Optimal Estimation Algorithms	40
3.	NECESSARY CONDITONS FOR THE EXISTENCE OF OPTIMAL STOCHASTIC CONTROL SYSTEMS	
3.1	Introduction	45
3.2	Response of a Linear System to Environmental Noise	46
3.3	Evaluation of the Covariance Matrix x	46
3.4	Problem Formulation	47
3.5	The First Necessary Condition for the Existence of a Weak Relative Minimum	48
3.6	The Canonical Equations of the First Variation	49
4.	NUMERICAL PROCEDURES FOR PARAMETER OPTIMIZATION	
4.1	Introduction	51
4.2	Numerical Optimization Techniques	51

Chapter Page

4.3 The Method of Steepest Descent 54
4.4 Method of the Average Gradients. 54
4.5 The Generalized Method of Newton Raphson 57
4.6 Method of Conjugate Gradients 57
4.7 Method of Davidon 62
4.8 The Method of Powell. 64
4.9 A Simple Illustrative Example 67
4.10 Selection of the Optimization Algorithm. 72

5. OPTIMIZATION OF A VERTICAL POSITION CONTROL SYSTEM FOR AUTOMATIC LANDINGS

5.1 Introduction 77
5.2 Vertical Trajectory Control 77
5.3 Vertical Trajectory Control System Structure 80
5.4 Optimizing the Vertical Position Control System. 82

6. SUMMARY, CONCLUSIONS, AND AREAS FOR FURTHER INVESTIGATION

APPENDIX A: LONGITUDINAL EQUATIONS OF MOTION WITH AUTOMATIC TRAJECTORY CONTROL

A.1 Introduction 101
A.2 Vehicle Trajectory Equations 101
A.3 Vehicle Longitudinal Equations of Motion 102
A.4 Velocity Control System 103
A.5 Hinge Moment Equations 103
A.6 Control Surface Servo 104
A.7 Aerodynamic Noise 104
A.8 Sensor Noise 105
A.9 Control Law 107
A.10 State Variable Equations 107

REFERENCES 108

CHAPTER 1

INTRODUCTION

1.1 Automatic Landing System Ecology

The problems associated with air traffic control and, in particular, the automatic landing problem, have attracted a considerable amount of interest since the end of the second world war. Recently, interest in the problem has blossomed, sparked by development programs for the SST, the jumbo jets and the severe air terminal problems precipitated by bad weather and/or poor utilization of terminal facilities. The pressure of traffic in the Chicago-Washington triangle on the current outmoded Air Traffic Control (ATC) system has also led to interest in new systems for the 1980's which will undoubtedly include automatic landing among other aspects of automated flight management. The range of technical resources currently applied to the problem is apparent in the papers presented at conferences and in publications throughout the world (refs. 1, 2, 3, 4, 5, 6, 9, 16, 19, 20, 26).*

The search for automatic landing systems is also greatly encouraged by the rather dramatic accidents which occur periodically during instrument approaches. The author can recall at least five examples in the United States alone during the last year which resulted in over one hundred fatalities. During the last week of work on this report two additional instrument approach accidents were reported which resulted in complete destruction of the aircraft and a loss of ninety-one lives.** Attention is thus focussed on improving guidance performance under conditions when human control is marginal.***

---

*The numbers refer to entries in the table of References.

**Boston Globe, November 11, 1969: Fairchild 227B airliner strikes peak during approach to Glen Falls, N.Y. with a loss of fourteen lives; Nigerian VC 10 crashes on approach to Lagos airport with a loss of seventy-seven lives.

***It is anticipated that the reliability and performance of fully automated landing systems can be made high enough to win the confidence of aircrews and the public alike. This implies a level of performance significantly higher than that achieved by man-in-the-loop systems.

The automatic landing problem is a major facet of the Terminal Area Control problem which in turn is part of the overall Air Traffic Control problem. From a control engineer's point of view, the problems may be unified as a generalized trajectory control problem. The vehicle may be considered as existing in a small subset of a generalized state space which is translated from the departure point to the point of flight termination. The vehicle must always remain in the small subset in order to satisfy the constraints which arise from a number of sources including:

1. Position constraints arising from:
   a. Permissible traffic patterns.
   b. Other traffic
   c. Noise abatement
   d. Ground obstructions
2. Velocity constraints as a result of:
   a. Vehicle operating restrictions.
   b. Velocity characteristics of other traffic
3. Angular constraints imposed by:
   a. Vehicle operating restrictions
   b. Passenger comfort
   c. Ground obstructions

to name only a few. One possible formalization of the problem is as follows.

Air Traffic-Control Problem: Find a control $u \epsilon C [t_i, t_f]$ * and the corresponding trajectory $x_d \epsilon C [t_i, t_f]$ which transfers the state from the initial value x_i at the departure point $(t = t_i)$ to the final state x_f at the arrival point, $t_f > t_i$.

The vehicle trajectory x must satisfy the system of vehicle differential equations

$$\dot{x} = f(x, u) \qquad (1.1.1)$$

subject to the boundary conditions

$$x(t_i) = x_i \qquad (1.1.2)$$

$$x(t_f) = x_f \qquad (1.1.3)$$

* The notation $u \epsilon C [t_i, t_f]$ indicates that u is a continuous function of the interval $t_i \leq t \leq t_f$.

and the constraint set

$$|x - x_d| < L_a^* \tag{1.1.4}$$

$$|\dot{x}| < L_b \tag{1.1.5}$$

where L_a and L_b are functions of time.

The initial and terminal times are subject to variation, but variations are penalized by a function P where

$$P = P(t_i, t_f, t_{id}, t_{fd}) \tag{1.1.6}$$

t_{id} and t_{fd} are the desired departure and arrival times respectively.

It is apparent from the above that the trajectory design of x_d must reflect constraints (1.1.1), (1.1.4) and (1.1.5) in addition to the boundary conditions (1.1.2) and (1.1.3).

The trajectory control system must be accurate enough to satisfy (1.1.4) and (1.1.5) in spite of the deterministic and stochastic disturbances which the vehicle will encounter during flight. An automatic landing system is a flight trajectory control system which is distinguished primarily by the higher levels of accuracy associated with the control of position and attitude. The MIT/NASA-ERC study has been primarily directed towards the development of techniques for achieving the required high levels of accuracy.

1.2 High Precision Flight Path Trajectory Control

It has been shown in previous documents in this series that the attainment of precise flight paths demands consideration of a multitude of problems.

Precise trajectory control requires a control system which is insensitive to extraneous environmental disturbances and the design of an appropriate coupling or feedforward compensation network to introduce the desired trajectory to the control system. The desired trajectory must also reflect limitations imposed on the vehicle's path by structural, effector saturation and passenger comfort considerations to ensure its flyability. Care must be exercised to ensure that the input trajectory does not result in prolonged vehicle control system saturation which could lead to instability and/or the accumulation of large environmental-disturbance-induced errors. Modern navigation system design techniques must also be used to furnish high quality position, velocity and acceleration data. The flight path control system must then be redesigned to reflect the improved nature of the navigation data.

---

* The notation $|y| < L$ is defined by $|y_i| < L_i$ for all elements y_i of y.

The philosophy behind the improved design is of interest. The control system is subject to two types of inputs. The first, desired trajectory information, is subject to the designer who can shape the flight path to reflect the limitations imposed by the vehicle and the terminal area geometry.

The second input arises from stochastic and deterministic environmental effects such as wind gusts and shear which are beyond the control of the designer. Thus it is apparent that the control problem may be dichotomized, to some extent, into the areas of position control in the presence of disturbances and trajectory-feedforward-compensator design.

A block diagram of an advanced automatic flight path control system is shown in fig 1-2-1. The system is distinguished by the presence of a nonlinear trajectory generator (ground or airborne), a feedforward compensator, an integrated radio inertial sensor, and an optimized stochastic position control system.

Nonlinear trajectory generation has been considered in previous reports in this series and by MacKinnon in refs. 3, 10. Recently the work has been extended by Erzberger to the design of overall terminal area horizontal flight paths.[6] Erzberger has also investigated vertical plane trajectories for noise abatement.

The reference trajectory must be introduced into the control system in such a way as to ensure that the ability of the control system to follow the reference path is maximized. This goal is satisfied by the feedforward compensator which has been discussed in previous reports in this series and will be discussed further in future documents.

The integrated navigation system combines data from terminal area radio navigation aids and on-board inertial measurements to provide relatively noise-free estimates of inertial position, velocity and acceleration relative to the runway. Navigation system integration has been investigated by Burrows et al. and in the previous two reports in this series. In Chapter 2, two classes of optimal estimators, as well as the optimal estimators themselves, are presented. The optimal estimation of inertial sensor errors in position, velocity, and acceleration is investigated.

The availability of relatively precise linear position, velocity, and acceleration data provides the basis for a control system design which is less sensitive to environmental disturbances. The optimization of a control system subject to stochastic environmental disturbances is pursued from the parameter optimization approach in Chapters 3, 4, and 5.

While the techniques presented in this report are applied to the landing problem, the concepts are applicable to the design of any flight trajectory control system.

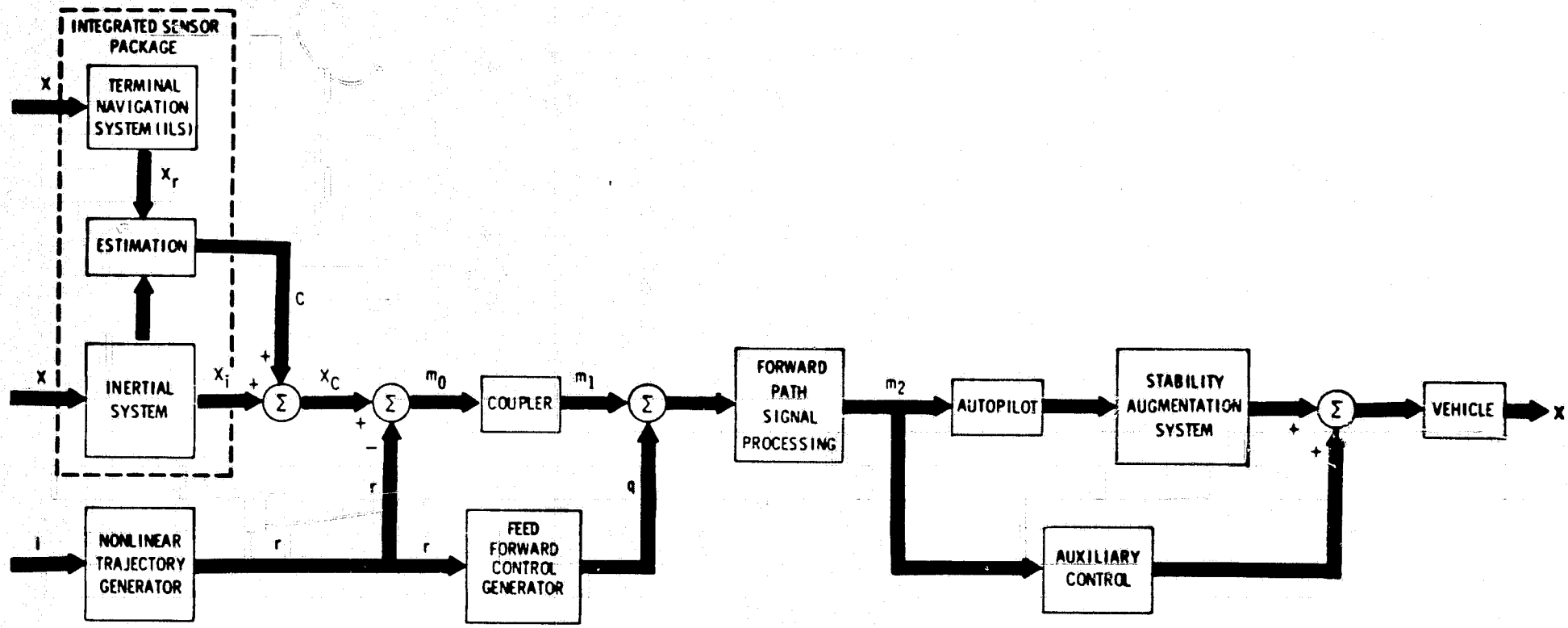


Fig. 1-2-1 Modern aircraft flight path control system configuration.

PRECEDING PAGE BLANK NOT FILMED.

CHAPTER 2

APPLICATION OF OPTIMIZATION THEORY TO HYBRID NAVIGATION SYSTEM DESIGN

2.1 Introduction

The generation of precise, noise- and delay-free information describing the geographic coordinates of a vehicle in space presents a formidable obstacle to the development of a high-performance automatic landing system. Radio aids such as ILS, VOR, DME, VORTAC, LORAN, OMEGA, etc., do not provide the degree of precision and noise level placed on the feedback variables of a high open-loop gain control system. Inertial navigation systems, on the other hand, generate position, velocity and acceleration information which is relatively free from high frequency noise and time lags; however, low-frequency gyro drift-induced errors preclude the direct application of inertial data for precise area navigation. After a typical flight, position errors measured in nautical miles and velocity discrepancies of knots are common in the horizontal plane. Errors in the vertical are often larger as a result of the unstable character of the vertical error equations of an inertial navigator.

A procedure is desired which combines the high accuracy of the radio-aid signal averaged over a period of time (or distance) with the wide band dynamic response range of an inertial measurement device. Such a procedure is found within the framework of modern integrated navigation system design. This chapter develops a number of techniques for systematically estimating the errors in an inertial system. The resultant estimates may then be utilized to correct the inertial system outputs. The corrected outputs provide the desired feedback variables for a high precision control system which may be designed using the methods presented in Chapters 3, 4, and 5.

2.2 Inertial System Error Model

Inertial systems are subject to low-frequency gyro drift and misalignment induced errors which deteriorate the validity of position, velocity and acceleration data based on inertial measurements. Since the frequencies associated with the gross fluctuations in gyro drift rate and the Shuler oscillations are long compared to the duration of a landing, it is possible to simplify the inertial system model for

analysis purposes to a set of three independent single axis systems.

Let the state vector of a single axis inertial system be designated x_i

$$x_i = \begin{bmatrix} x_{i1} \\ x_{i2} \\ x_{i3} \end{bmatrix} \tag{2.2.1}$$

where x_{i1}, x_{i2}, x_{i3} are inertially measured position, velocity and acceleration respectively. The state variables satisfy the set of linear differential equations

$$\dot{x}_i = F_i\, x_i + G_i\, u_i + H_i\, x \tag{2.2.2}$$

where F_i, G_i and H_i are constant matrices; u_i, is a random gyro drift. The elements x_1, x_2, and x_3 of the three dimensional vector x represent the true values of inertial position, velocity and acceleration respectively along the designated axis. The matrices F_i, G_i, and H_i have the form

$$F_i = \begin{bmatrix} 0 & 1 & 0 \\ 0 & 0 & 1 \\ 0 & 0 & 0 \end{bmatrix} \tag{2.2.3}$$

$$G_i = \begin{bmatrix} 0 \\ 0 \\ g \end{bmatrix} \tag{2.2.4}$$

$$H_i = \begin{bmatrix} 0 & 0 & 0 \\ 0 & 0 & 1 \\ 0 & 0 & 0 \end{bmatrix} \tag{2.2.5}$$

where g is a constant.

The utilization of inertial data for control applications is possible only if the inertial system errors can be corrected. It is convenient to define an <u>error state vector</u> e_i whose three components e_{i1}, e_{i2} and e_{i3} represent the errors in position, velocity and acceleration respectively. e_i is independent of x in a well-designed inertial system and satisfies the linear differential equation

$$\dot{e}_i = F_i\, e_i + G_i\, u_i \tag{2.2.6}$$

subject to the boundary condition

$$e_i(0) = e_{i0} \tag{2.2.7}$$

the error due to initial misalignment and miscalibration.

2.3 Radio Aid Model

The radio aid is an observer with dynamics. The observer measures a variable x and is subject to noise introduced in the measurement which is assumed to be exponentially correlated. The correlation is performed by augmenting the state of the observer. The aid also generates internal noise which is assumed to appear at the output as low level white noise v_r. The observer is modelled by a set of linear differential equations.

$$\dot{x}_r = F_r x_r + G_r u_r + H_{ri} x \tag{2.3.1}$$

where x_r is the radio-aid state vector, u_r is uncorrelated white noise, and x is the inertial state observed by the aid. F_r, G_r, and H_{ri} are matrices which may be time-varying. The output of the radio aid is a scalar measurement which is a linear combination of the elements of the state x_r.

$$z_r = H_r x_r + v_r \tag{2.3.2}$$

where v_r is uncorrelated white measurement noise.

2.4 Minimum Integral Square Estimation of Inertial System Errors

In references 4 and 5, the application of minimum integral square error estimation techniques to the estimation of inertial navigation system errors was introduced. In this section the method is briefly reviewed; and the effects of inertial system quality, radio, and inertial sensor model accuracy on performance are considered.

The inertial system error state vector can be estimated by comparing the measured inertial position with the position generated by a radio aid. Let the radio aid be described by a differential equation of the form

$$\dot{x}_r = F_r x_r + G_r u_r + H_{ri} x \tag{2.4.1}$$

as described in Section 2.3. The scalar output of the radio aid is a linear combination of the elements of x_r plus a white noise source v_r.

$$z_r = H_r x_r + v_r \tag{2.4.2}$$

In order to make the estimation process independent of vehicle motion, the inertial measurement x_i is passed through a linear model of the radio aid.

$$\dot{x}_m = F_r\ x_m + H_{ri} x_i \qquad (2.4.3)$$

The radio aid measurement based on inertial data is then

$$z_m = H_r\ x_m \qquad (2.4.4)$$

If the inertial system were perfect, x_i would be equal to x. If, in addition, the radio aid noise u_r were zero, the difference between the state vectors x_m and x_r would approach zero asymptotically.* Thus the outputs of the model z_m and the actual receiver z_r would correspond exactly. However, in a real system, the inertial errors, e_i, and radio aid noise, u_r and v_r, will result in discrepancies. Let the error between z_m and z_r be designated ϵ.

$$\epsilon = z_m - z_r \qquad (2.4.5)$$

As a result of dynamic matching, the error, ϵ, is independent of the value of the inertial state, x. This approach thus avoids the necessity of modelling the vehicle dynamics.

Since the noise characteristics of navigation aids vary significantly from site to site, the minimum integral square error estimator is derived without considering the radio aid noise u_r and the measurement noise v_r. The effects of noise are then investigated by considering the noise to be a disturbance affecting the estimation process.

Assuming that the radio-aid noise and the gyro drift rates are zero, the error ϵ may be expressed in the form

$$\epsilon(t) = h'(t) e_i(0) \qquad (2.4.6)$$

where h is a three - dimensional vector of response functions. The element h_i is the response component of z_m due to a unit step in the i^{th} element of the inertial system error e_i. Equation (2.4.6) provides the basis for the formulation of an optimization problem whose solution is the best integral square error estimate of the inertial system error state.

---

*assuming that the system in (2.4.1) is asymptotically stable

Problem: Find an estimate of the initial error $e_{ie}(0)$ which minimizes the integral performance index

$$J = \int_0^t \left[\epsilon(\alpha) - h'(\alpha)\, e_{ie}(0) \right]^2 d\alpha \qquad (2.4.7)$$

Consider the first variation in J with respect to $e_{ie}(0)$

$$\delta J \int_0^t 2 \left[\epsilon(\alpha) h'(\alpha) - e_{ie}(0)' h(\alpha) h'(\alpha) \right] \delta e_{ie}(0)\, d\alpha \qquad (2.4.8)$$

To satisfy the First Necessary Condition of the Calculus of Variations, the first variation in J must vanish for arbitrary perturbations in $e_{ie}(0)$. This requirement is satisfied if

$$e_{ie}(0) = \left[\int_0^t h(\alpha) h'(\alpha)\, d\alpha \right]^{-1} \int_0^t h(\alpha) \epsilon(\alpha)\, d\alpha \qquad (2.4.9)$$

If the radio aid noise, $x_m(0)$ and the gyro drift rates are all zero, it is apparent that

$$e_{ie}(0) = e_i(0) \qquad (2.4.10)$$

As indicated in ref 5 the initial estimate of $e_i(0)$ will not exist since the matrix $h(0)h(0)'$ is singular. However, as time passes, convergence is achieved and (2.4.10) is satisfied.

If the radio aid noise is nonzero, the estimate $e_{ie}(0)$ will not equal the $e_i(0)$, but will equal the minimum integral square error estimate of $e_i(0)$.

The current estimate of the inertial system errors is obtained by extrapolating the initial error using the state transition matrix associated with the set of differential equations (2.2.6).

$$e_{ie}(t) = Te_{ie}(0) \tag{2.4.11}$$

where

$$T = \begin{bmatrix} -1 & -t & \frac{t^2}{2} \\ 0 & -1 & -t \\ 0 & 0 & -1 \end{bmatrix} \tag{2.4.12}$$

The estimated inertial position, velocity, and acceleration state, x_{ie}, is then obtained by subtracting the predicted value of the error, e_{ie}, from the inertial system state x_i. Thus

$$x_{ie} = x_i - e_{ie} \tag{2.4.13}$$

Since the value of $h(\alpha)$ is independent of the current state, the complete minimum ISE estimator may be represented by a time-varying linear model.

Let

$$K(t) = \left[\int_0^t h(\alpha)h'(\alpha)d\alpha \right]^{-1} \tag{2.4.14}$$

be a matrix of time varying gains. The estimator may then be represented as shown in Fig. 2-4-1.

2.5 Weighted Least Mean Squares Estimation

The estimation of inertial system errors using radio aid measurements by a minimum integral square error approach was considered in Section 2.4. In this section the concept of weighted least squares estimation is introduced. The results are then extended to the estimation of the state of a linear dynamical system in the

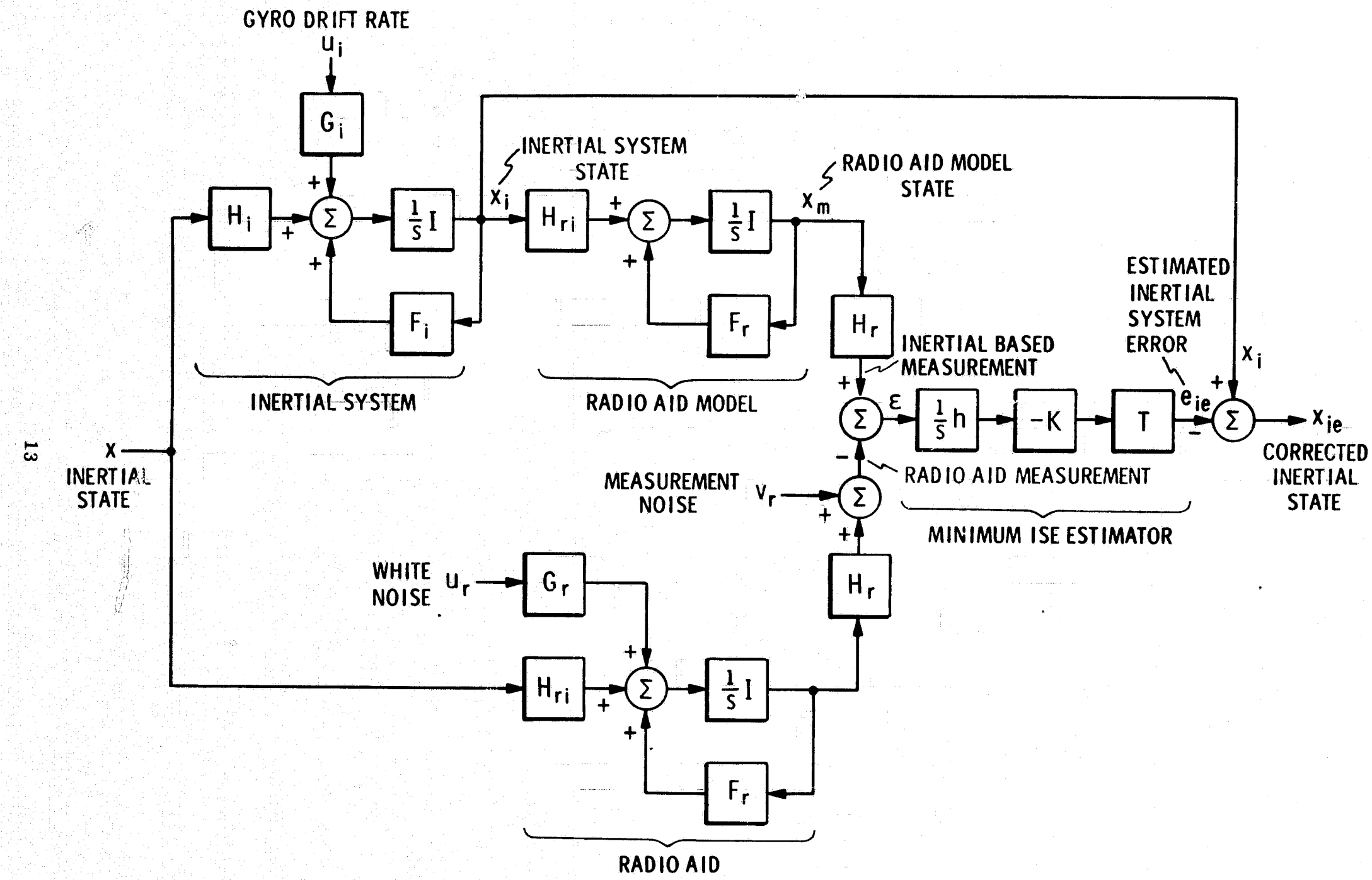


Fig. 2-4-1 Minimum integral square error estimator.

next section leading to the formulation of the Kalman-Bucy Filter which is then used to estimate the error state of an inertial system using radio data.

Let x be a vector of variables to be estimated and let x_e be the estimate of x. Let the error e between the estimate and the actual value of x be defined

$$e = x_e - x \tag{2.5.1}$$

Measurements are made of x by an observer of the form

$$z = Hx + v \tag{2.5.2}$$

where v is zero-mean white noise, uncorrelated with x.

A useful optimization goal is the minimization of the sum of the mean square values of the elements of the error vector. The performance index J in this case is

$$J = E(e'e) \tag{2.5.3}$$

which may also be written

$$J = \text{trace } E(ee') \tag{2.5.4}$$

where the operation trace signifies the summation of the terms on the main diagonal of the matrix E(ee'). An optimization problem is thus formulated.

Problem: Find the estimate x_e based on current and previous observations of the state variable x which minimize the performance index

$$J = \text{trace } E(ee') \tag{2.5.5}$$

Assume that the optimal estimate x_e is a linear combination of the current measurement z and a previous best estimate x_ℓ

$$x_e = x_\ell + K(z - Hx_\ell) \tag{2.5.6}$$

where K is a matrix to be determined. Using equations (2.5.1) and (2.5.2) the equation (2.5.6) may be written

$$e = [I + KH]\, e_\ell + Kv \tag{2.5.7}$$

Since v is white noise it is uncorrelated with the previous error e_ℓ

$$E(e_\ell v') = E(ve_\ell') = 0 \tag{2.5.8}$$

so that

$$E(ee') = E(e_\ell e_\ell') + KHE(e_\ell e_\ell') + E(e_\ell e_\ell')H'K' + K\left[HE(e_\ell e_\ell')H' + E(vv')\right]K' \tag{2.5.9}$$

Let the current covariance of e be P and the previous value be P_ℓ then the covariance P may be written

$$E(ee') = P = P_\ell + KHP_\ell + P_\ell H'K' + K(HP_\ell H' + R)K' \tag{2.5.10}$$

Consider the first variation in the performance index J due to a perturbation δK in the optimal gain matrix K.

$$\delta J = \text{trace}\left(\delta K \frac{\partial}{\partial K} P\right) \tag{2.5.11}$$

$$= 2\,\text{trace}\left(\delta K\left[HP_\ell + \left[HP_\ell H' + R\right]K'\right]\right) \tag{2.5.12}$$

Since

$$\text{trace } KHP_\ell = \text{trace } P_\ell H'K' \tag{2.5.13}$$

The first variation vanishes with respect to the perturbation δK if the coefficient of δK is equal to zero or

$$K = -P_\ell H'\left[HP_\ell H' + R\right]^{-1} \tag{2.5.14}$$

Equation (2.5.14) describes the optimal gain matrix for the minimum mean square error estimator. The fact that δJ does vanish implies that the assumed estimation formula is, indeed, an optimal estimation scheme.

The corrected covariance matrix is then obtained by substituting (2.5.14) in (2.5.10), with the result:

$$P = P_\ell - P_\ell H'(HP_\ell H' + R)^{-1} HP_\ell \tag{2.5.15}$$

2.6 Derivation of the Kalman-Bucy Filter for Continuous Dynamical Systems

Let the dynamical system be described by a set of linear differential equations of the form:

$$\dot{x} = Fx + Gu \tag{2.6.1}$$

where x is an n-dimensional state vector and u is an m-dimensional vector of Gaussian white noise disturbances. The boundary condition on x is

$$x(0) = x_0 \tag{2.6.2}$$

Let the mean of u be designated u_m

$$E(u) = u_m \tag{2.6.3}$$

The autocorrelation matrix of u(t) then has the form

$$E\Big([u(t) - u_m][u(\tau) - u_m]\Big) = Q\delta(t-\tau) \tag{2.6.4}$$

where $\delta(t-\tau)$ is the Dirac Delta Function.

Let x_ℓ be the best estimate of x at time t. If no further measurements of x or u are made the best estimate x_e of x is given by the solution of the differential equation

$$\dot{x}_e = Fx_e + Gu_m \tag{2.6.5}$$

with the boundary condition

$$x_e(t) = x_\ell \tag{2.6.6}$$

The best estimate of the error e between x and x_e is the solution of the differential equation

$$\dot{e} = \dot{x} - \dot{x}_e = Fe + G[u - u_m] \tag{2.6.7}$$

subject to

$$e(t) = e_\ell \tag{2.6.8}$$

the last estimate of the error. The derivative of the covariance of the error e is then

$$\begin{aligned} \frac{d}{dt}E(ee') &= E(e\dot{e}' + \dot{e}e') \\ &= E(Fee' + ee'F' + G[u - u_m][u - u_m]'G') \end{aligned} \tag{2.6.9}$$

Setting $P = E(ee')$ gives the differential equation satisfied by the covariance

$$\dot{P} = FP + PF' + GQG' \qquad (2.6.10)$$

where

$$P(t) = E(e_l e_l') \qquad (2.6.11)$$

Suppose that a measurement z is made of x at $t + \Delta t$

$$z = Hx + v \qquad (2.6.12)$$

where v is zero-mean white noise with an autocorrelation matrix of the form

$$E[v(t)v(\tau)'] = R\delta(t-\tau) \qquad (2.6.13)$$

and the covariance matrix P is corrected using formula (2.5.16).

The value of P at $t + \Delta t + \epsilon$ where Δt, ϵ are small positive numbers and $0 < \epsilon \ll \Delta t$ is:

$$P(t + \Delta t + \epsilon) \approx P(t) + [FP(t) + P(t)F' + GQG']\Delta t$$
$$- [P(t)H'[HP(t)H' + R_e]^{-1}HP(t)] \qquad (2.6.14)$$

where $R_\epsilon = E(vv')$ the covariance matrix of v. Then

$$\frac{1}{\Delta t}[P(t + \Delta t + \epsilon) - P(t)] = FP(t) + P(t)F' + GQG'$$
$$- P(t)H'[HP(t)H'\Delta t + R_e\Delta t]^{-1}HP(t) \qquad (2.6.15)$$

Noting that

$$\lim_{\Delta t \to 0} HP(t)H'\Delta t = 0$$

and letting

$$\lim_{\Delta t \to 0} R_e\Delta t = R$$

and taking the limit at $\Delta t \to 0$ gives

$$\dot{P} = FP + PF' + GQG' - PH'R^{-1}HP \qquad (2.6.16)$$

By a similar process it may be shown that the estimate x_e satisfies the differential equation

$$\dot{x}_e = Fx_e + Gu_m + PH'R^{-1}[z - Hx_e] \qquad (2.6.17)$$

Equations (2. 6. 16) and (2. 6. 17) are the equations of the continuous Kalman Filter for the system of equations (2. 6. 1) and (2. 6. 11). Since the gain $K = PH'R^{-1}$ does not depend on x or x_e, it is apparent that the Kalman Filter may be represented by the linear system shown in fig. 2-6-1.

2.7 Optimal Estimation of Inertial System Acceleration, Velocity and Position Errors

To illustrate some of the properties of the optimal estimators described in Sections 2. 4, 2. 5, and 2. 6, an example was constructed. It was decided to estimate the inertial system errors in position, velocity and acceleration since these are the most significant errors in commercially available aircraft inertial navigation systems.

The estimation algorithms were illustrated by estimating the inertial system errors in a direction normal to an ILS Localizer center plane.* The problem geometry is illustrated in fig. 2-7-1.

The radio aid was characterized by a first order lag shown in fig. 2-7-2. The input to the receiver is radio angle α_y.

The radio aid differential equations are then

$$\dot{x}_r = F_r x_r + G_r u_r + H_{ri} x \qquad (2.7.1)$$

where

$$F_r = \begin{bmatrix} 2.0 & 2.0 \\ 0 & 0.333 \end{bmatrix} \qquad (2.7.2)$$

$$G_r = \begin{bmatrix} 0 \\ 0.333 \end{bmatrix} \qquad (2.7.3)$$

$$H_{ri} = \begin{bmatrix} \frac{2.0}{R} & 0 & 0 \\ 0 & 0 & 0 \end{bmatrix} \qquad (2.7.4)$$

*While the estimation process is applied to the ILS Localizer it is apparent that the glideslope problem may be handled in exactly the same way. In fact the analysis with minor changes applies to any navigation aid which gives angular data such as VOR, VORTAC, etc. The application of estimation using DME or area navigator data follows directly if the position measurement noise is appropriately defined as a function of position.

The second element in x_r is the exponentially correlated noise introduced by "beam bending" described in ref. 5 .

The inertial system model is described in Section 2.2 and has the form

$$\dot{x}_i = F_i x_i + G_i u_i + H_i x \tag{2.7.5}$$

where

$$x = \begin{bmatrix} y \\ \dot{y} \\ \ddot{y} \end{bmatrix} \tag{2.7.6}$$

$$F_i = \begin{bmatrix} 0 & 1 & 0 \\ 0 & 0 & 1 \\ 0 & 0 & 0 \end{bmatrix} \tag{2.7.7}$$

$$G_i = \begin{bmatrix} 0 \\ 0 \\ 32.2 \end{bmatrix} \tag{2.7.8}$$

$$H_i = \begin{bmatrix} 0 & 0 & 0 \\ 0 & 0 & 1 \\ 0 & 0 & 0 \end{bmatrix} \tag{2.7.9}$$

The random gyro drift rate u_i is in radians per second.

Suppose that the position output of the inertial navigator is applied to a model of the radio aid

$$\dot{x}_m = F_r x_m + H_{ri} x_i \tag{2.7.10}$$

and the output of the ILS receiver x_{r1} is multiplied by the range R* to the localizer transmitter antenna. The measured signal component due to inertial system errors and ILS localizer noise is then

$$\epsilon = x_{m1} - R x_{r1} \tag{2.7.11}$$

This signal is the information used by the minimum ISE and Kalman-Bucy optimal estimators.

---

*The range R could be provided by a DME located at the localizer transmitter antenna, area navigation data or height of the glideslope beam center plane, for example. The accuracy of R is not too critical in any case.

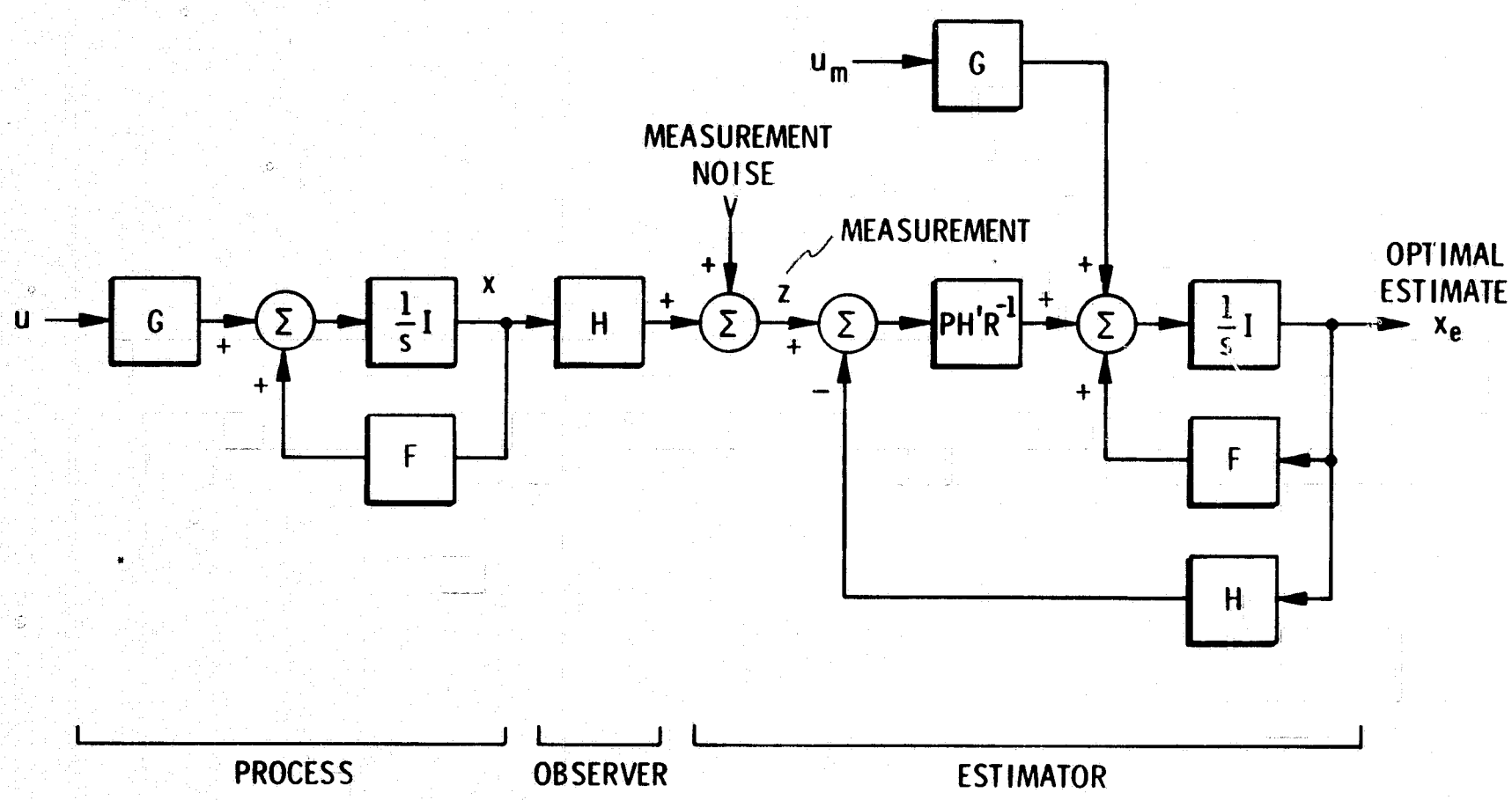


Fig. 2-6-1 Block diagram of a minimum least-mean-squares estimator.

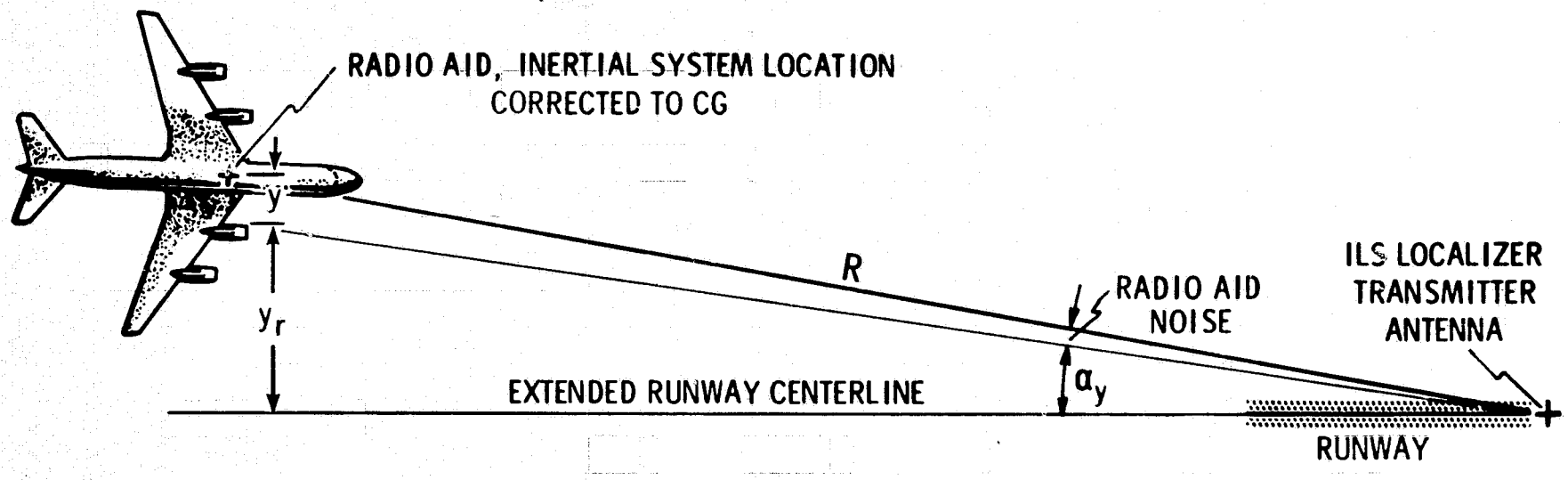


Fig. 2-7-1 Sample problem geometry.

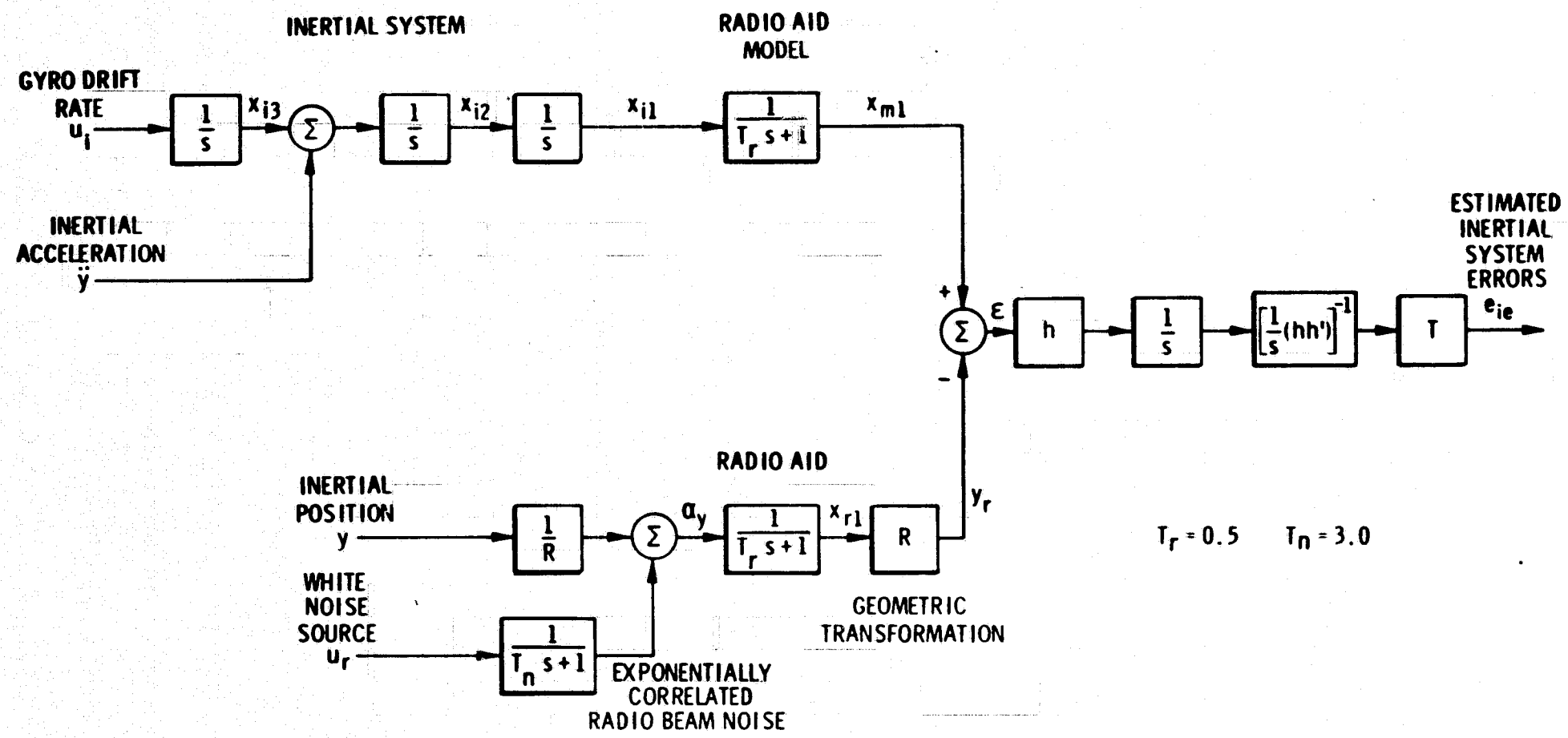


Fig. 2-7-2 Block diagram of minimum ISE estimator for estimating inertial system errors using ILS data.

The minimum ISE estimator was constructed using the procedure in Section 2.4. The estimated initial value of the inertial error was calculated using equation (2.4.9).

$$e_{ie}(0) = \left[\int_0^t h(\alpha)h(\alpha)d\alpha\right]^{-1} \int_0^t h(\alpha)\epsilon(\alpha)d\alpha \qquad (2.7.12)$$

here $\epsilon(\alpha)$ is defined in fig. 2-7-2 and the equation (2.7.11).

The vector of influence functions h in (2.7.11) is the solution of the set of linear differential equations

$$\dot{h} = F_h h + G_h u \qquad (2.7.13)$$

where

$$F_h = \begin{bmatrix} -2.0 & 0 & 0 \\ 1.0 & 0 & 0 \\ 0 & 1.0 & 0 \end{bmatrix} \qquad (2.7.14)$$

$$G_h = \begin{bmatrix} 2.0 \\ 0 \\ 0 \end{bmatrix} \qquad (2.7.15)$$

and u is the unit step function

$$u(t) = \begin{cases} 0 & t<0 \\ 1 & t \geqq 0 \end{cases} \qquad (2.7.16)$$

subject to the initial condition

$$h(0) = 0 \qquad (2.7.17)$$

The current estimate $e_{ie}(t)$ of the inertial system error e_i was computed by extrapolating an estimate of the initial value of the error

$$e_{ie}(t) = T\, e_{ie}(0) \qquad (2.7.18)$$

T is defined in (2.4.16). A schematic diagram of the minimum ISE estimator is shown in fig. 2-7-2.

The Kalman-Bucy Estimator is defined by (2.6.16) and (2.6.17)

$$\dot{P} = FP + PF' + GQG' - PH' R^{-1} HP \qquad (2.7.19)$$

$$\dot{x}_e = Fx_e + Gu_m + PH' R^{-1}\left[z - Hx_e\right] \qquad (2.7.20)$$

where F, G, and H are defined

$$F = \begin{bmatrix} F_i & 0 \\ H_{ri} & F_r \end{bmatrix} \tag{2.7.21}$$

$$G = \begin{bmatrix} G_i & 0 \\ 0 & G_r \end{bmatrix} \tag{2.7.22}$$

$$H = [0\ 0\ 0\ 1\ 0] \tag{2.7.23}$$

and

$$x_e = \begin{bmatrix} e_{ie} \\ e_{re} \end{bmatrix} \tag{2.7.24}$$

$$e_{ie} = \begin{bmatrix} e_{i1} \\ e_{i2} \\ e_{i3} \end{bmatrix} \text{ estimated} \tag{2.7.25}$$

$$e_{re} = \begin{bmatrix} x_{m1} - Rx_{r1} \\ x_{m2} - Rx_{r2} \end{bmatrix} \text{ estimated} \tag{2.7.26}$$

$$u = \begin{bmatrix} u_i \\ u_r \end{bmatrix} \tag{2.7.27}$$

$$v = \begin{bmatrix} v_r \end{bmatrix} \tag{2.7.28}$$

$$z = [\epsilon] \tag{2.7.29}$$

The vector u_m is the expectation E(u). The measurement noise v_r is an undefined white noise signal appearing at the radio aid output.

The boundary condition on (2.7.19) is the initial estimate of the error covariance matrix. Since the dynamic response characteristics of the filter depend strongly upon the initial values of P a large value,

$$\begin{bmatrix} 4 \times 10^4 & & & & & \\ & 1 \times 10^4 & & & & \\ & & 1 \times 10^3 & & & \\ & & & 4 \times 10^4 & & \\ & & & & 4 \times 10^4 & \end{bmatrix} = P(0) \tag{2.7.30}$$

was selected. The large initial value of the diagonal terms of P resulted in rapid estimation of initial inertial system errors.

The measurement noise covariance matrix R was assumed to be very small. The value of R was set equal to

$$R = E(vv') = .002 \tag{2.7.31}$$

The disturbance convariance matrix Q was equal to

$$Q = E(uu') = \begin{bmatrix} 0.0001 & 0 \\ 0 & 6.0\ E(\alpha_y^2) \end{bmatrix} \tag{2.7.32}$$

A block diagram of the Kalman-Bucy Estimator is shown in figure 2-7-3.

2.8 Response Characteristics of Optimal Estimators

The response characteristics of the estimator were investigated by forming the difference between the estimated inertial system error e_{ie} and the actual error e_i.

The transient response characteristics were investigated by setting $u_r = u_i = 0$ and establishing initial errors in the inertial system measurements of position, velocity and acceleration. The results of these tests are shown in figs. 2-8-1 to 2-8-6. Since the estimators are linear systems the responses shown provide a basis for the function space containing the responses to all possible combinations of inertial errors.

The response of the estimators to radio aid noise was investigated by considering u_r to be stationary process. The mean square value of the radio beam angle α_y was identified by a constant $E(\alpha_y{}^2)$. The mean square error in the radio position at a radial distance R from the ILS transmitter antenna is then

$$E(y_r{}^2) = R^2 E(\alpha_y^2) \tag{2.8.1}$$

where y_r is the position deviation from the beam center plane computed using the relationship

$$y_r = R\alpha_y \tag{2.8.2}$$

As discussed in ref. 5 the beam noise was assumed to be exponentially correlated with respect to distance. The characteristic distance was ≈800 ft. which corresponds to a correlation time of approximately 3.0 seconds at normal approach speeds. The rate of change of radius was assumed to be constant

$$\dot{R} = -278.4 \text{ ft/sec.} \tag{2.8.3}$$

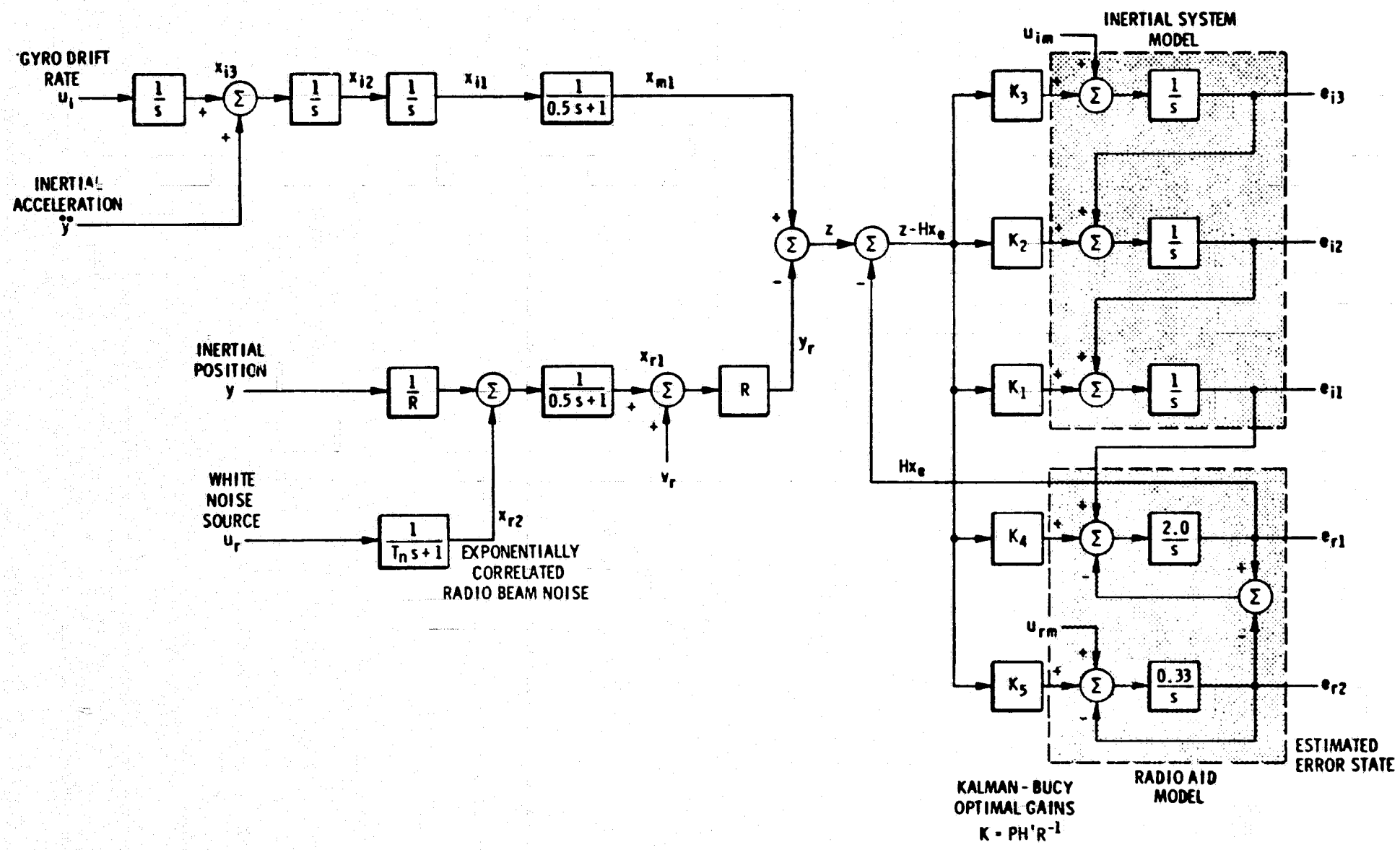


Fig. 2-7-3 Kalman-Bucy Estimator for estimating inertial system errors using radio aid data.

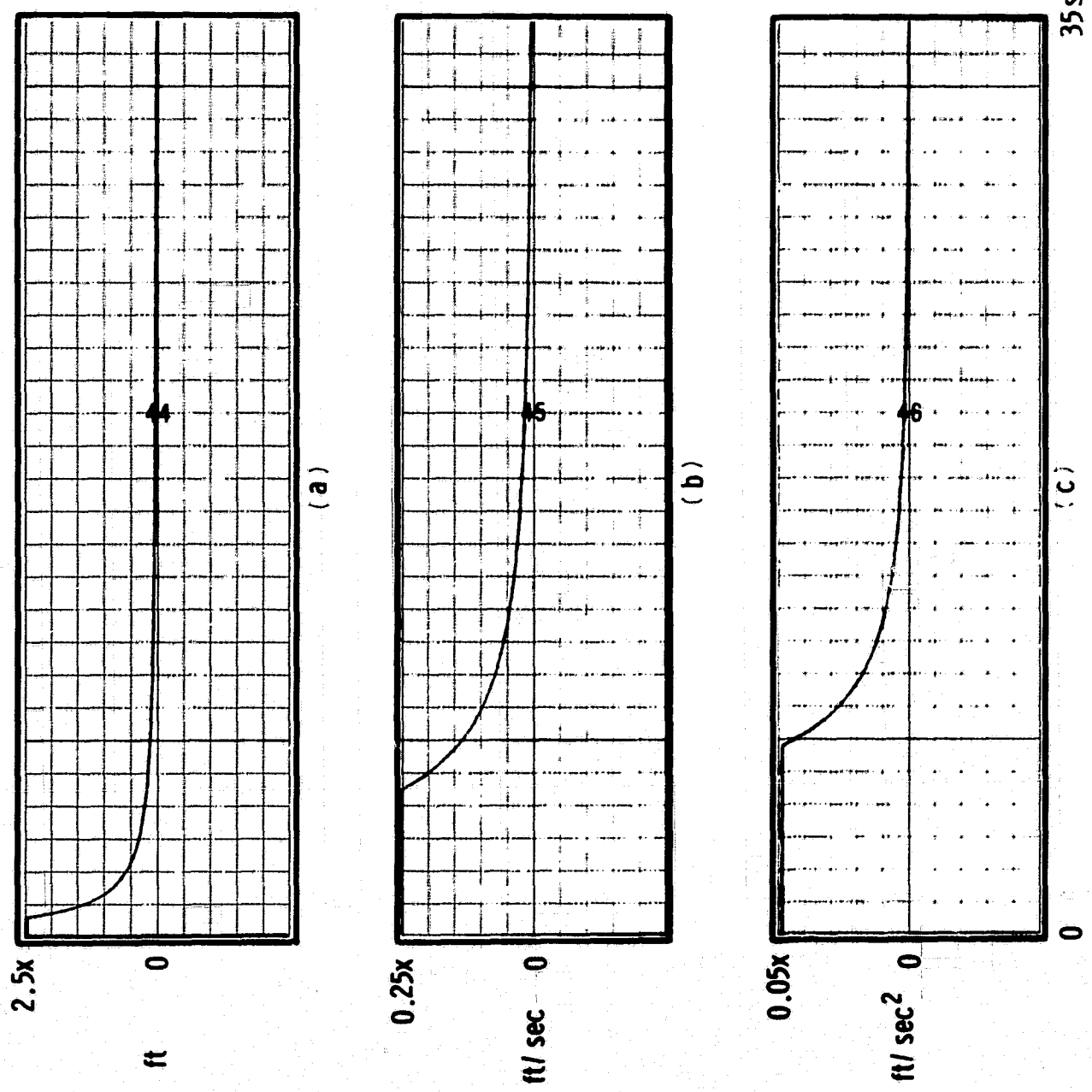


Fig. 2-8-1 Errors in minimum ISE estimation of inertial system biases in (a) position, (b) velocity and (c) acceleration due to an initial position bias error of x feet, versus time.

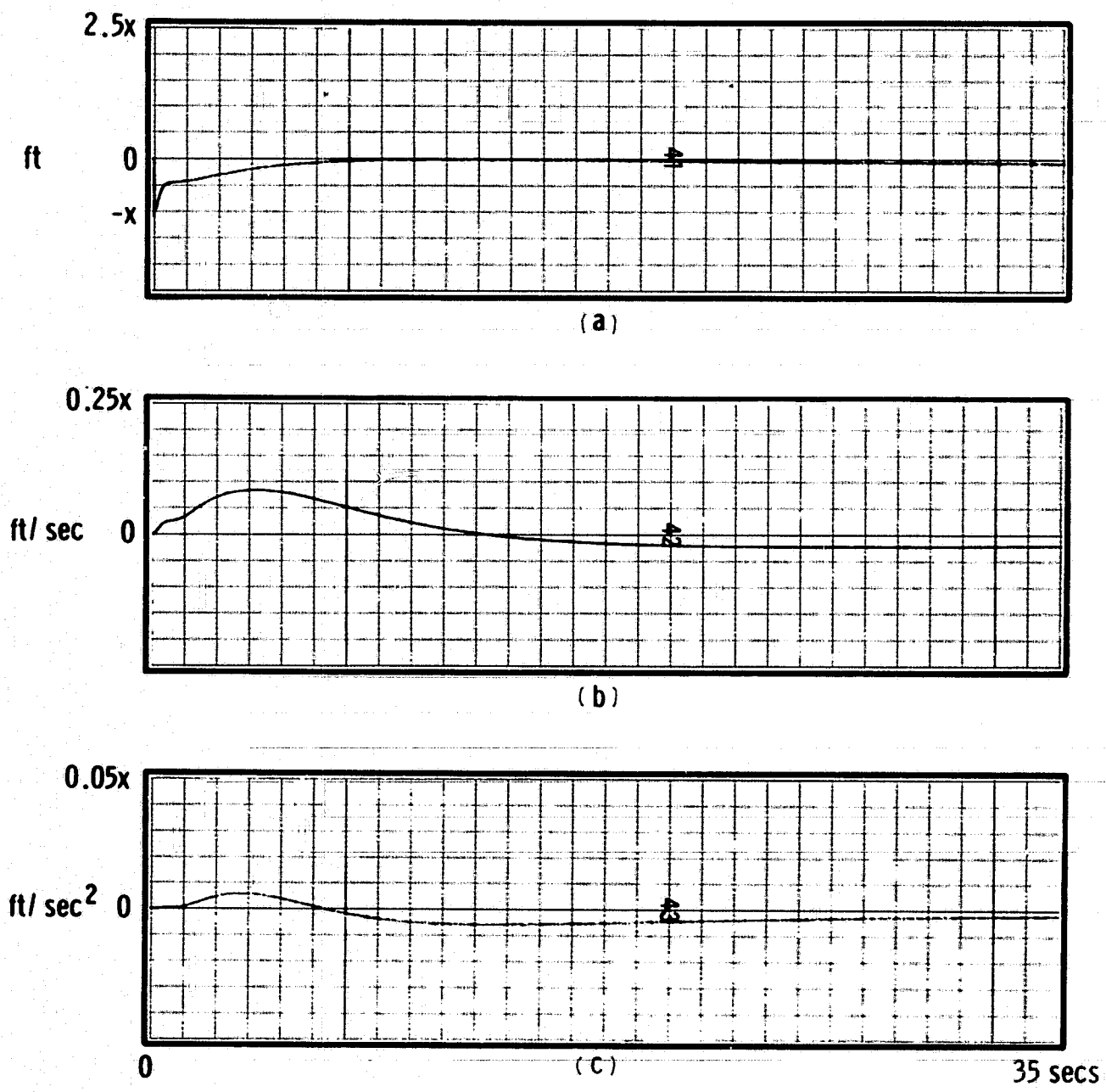


Fig. 2-8-2 Errors in Kalman-Bucy estimation of inertial system biases in (a) position, (b) velocity and (c) acceleration due to an initial position error of x feet, versus time.

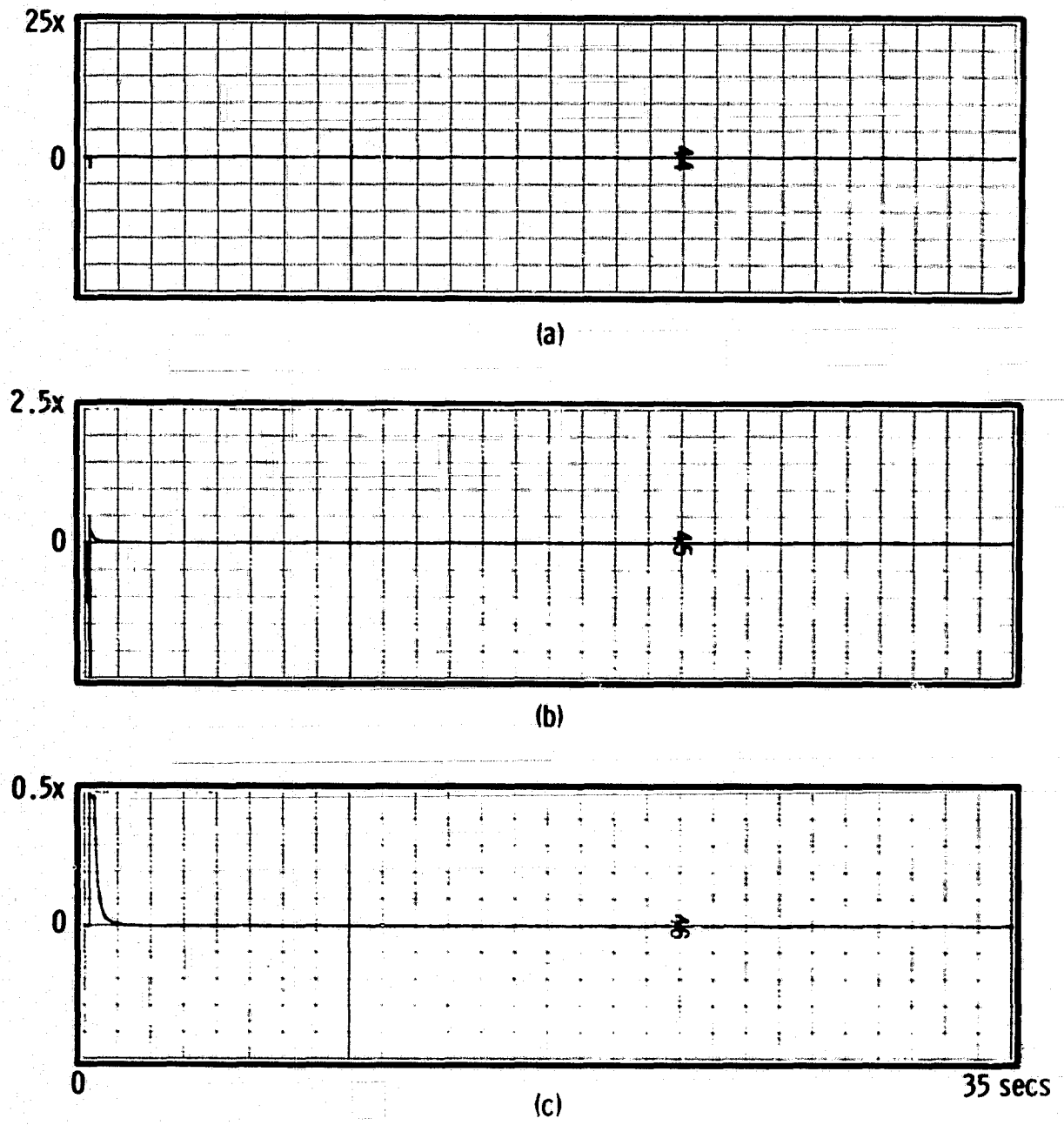
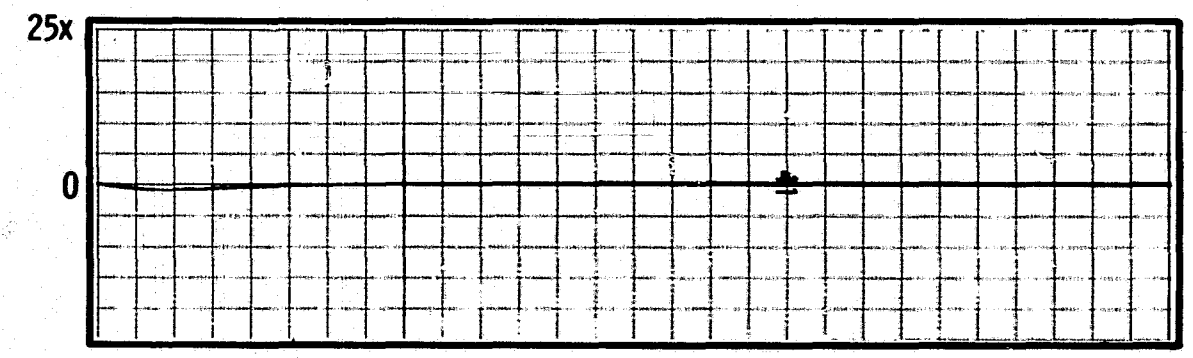
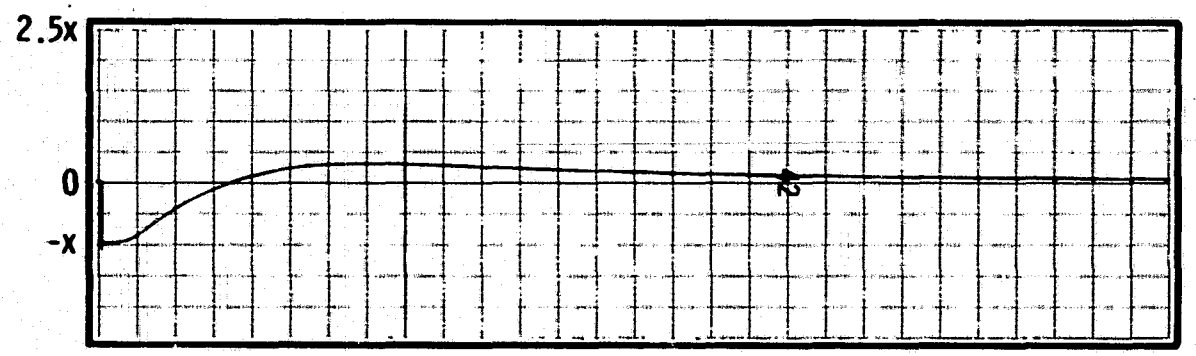


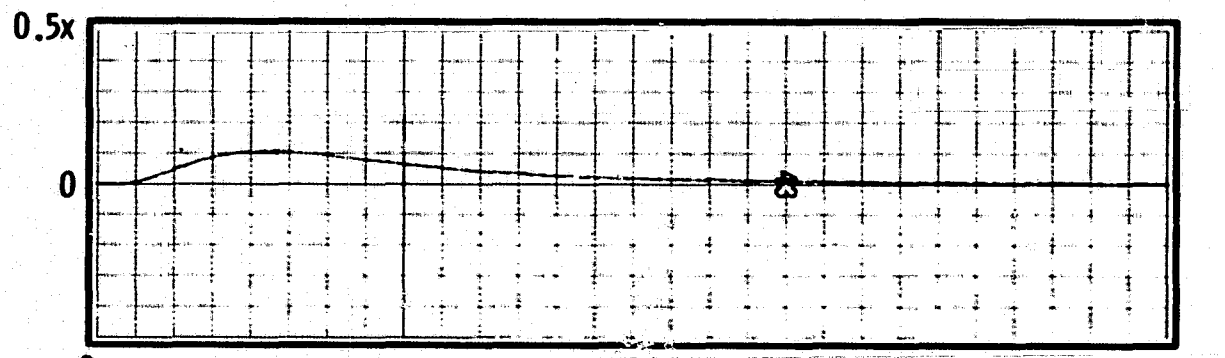
Fig. 2-8-3 Errors in minimum ISE estimation of inertial system biases in (a) position, (b) velocity and (c) acceleration due to an initial velocity bias error of x feet/second.



(a)



(b)



(c)

Fig. 2-8-4 Errors in Kalman-Bucy estimation of inertial system biases in (a) position, (b) velocity and (c) acceleration due to an initial velocity bias error of x feet/second.

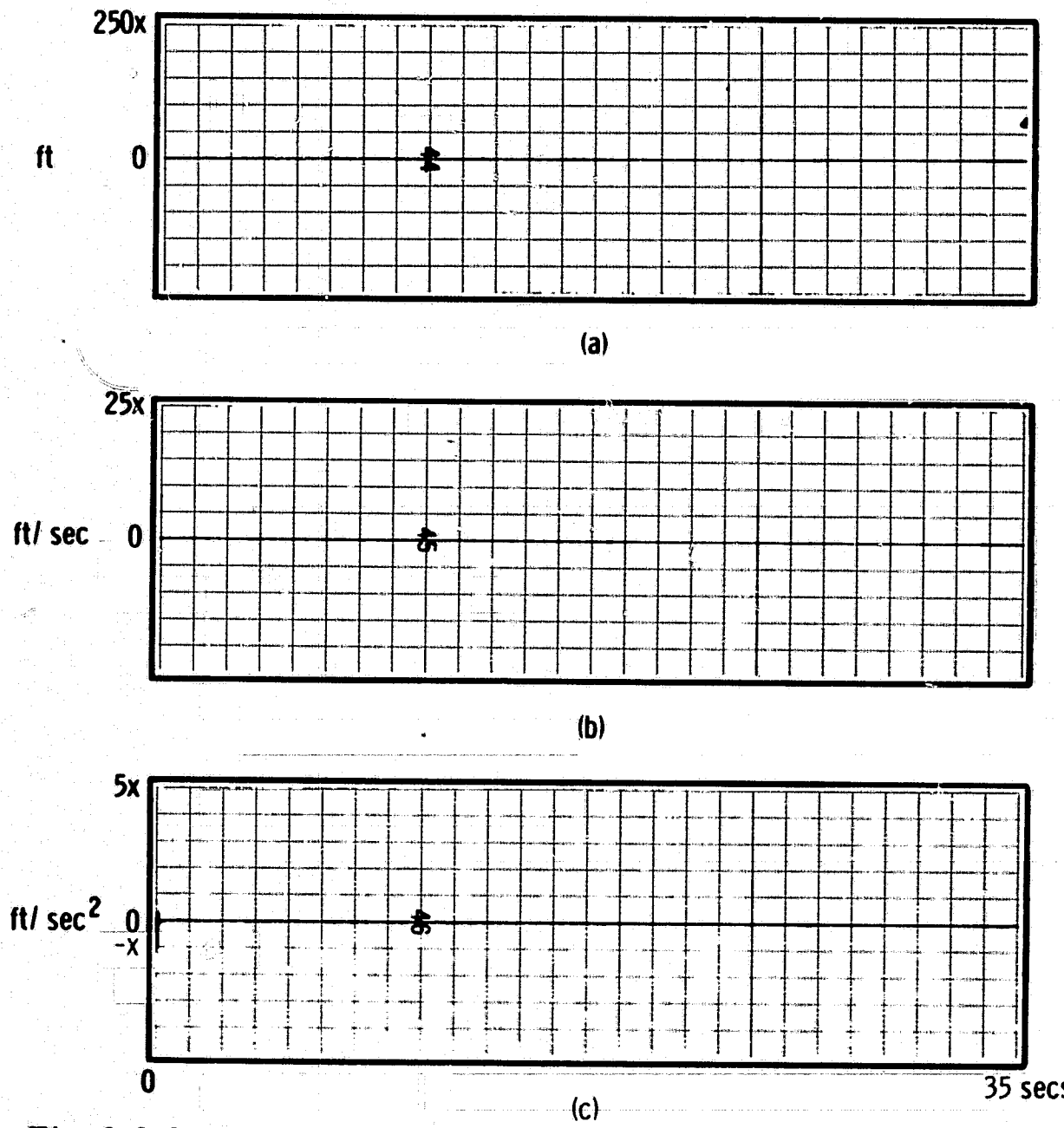


Fig. 2-8-5 Errors in minimum ISE estimation of inertial system errors in (a) position, (b) velocity and (c) acceleration due to an initial acceleration bias error of x feet/second^2.

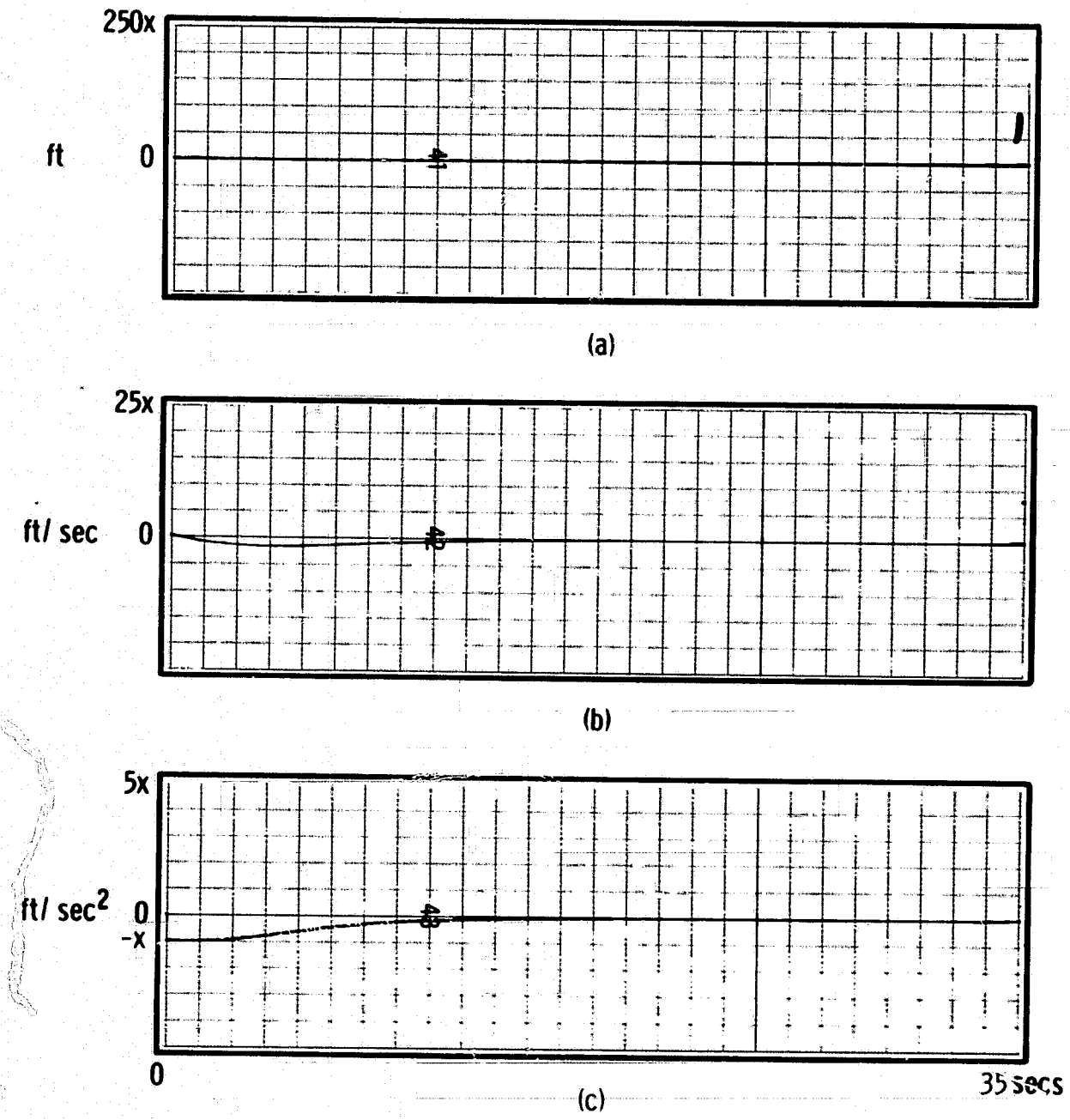


Fig. 2-8-6 Errors in Kalman-Bucy estimation of inertial system errors in (a) position, (b) velocity and (c) acceleration due to an initial acceleration bias error of x ft/sec^2.

The response of the estimators to beam noise is shown in figs. 2-8-7, 2-8-8, and 2-8-9. In order to obtain a quantitative comparison of estimator performance the mean square values of the errors in the estimates of inertial position, velocity and acceleration biases were calculated by time averaging using the expression*

$$E(x^2) \approx \frac{1}{T}\int_{10}^{T} x(\alpha)^2 \, d\alpha \qquad (2.8.4)$$

The results of these experiments are shown in figs. 2-8-5 and 2-8-6. As a result of linearity the results may be normalized with respect to the mean square value of beam angle. Such a procedure permits the results to be extended to any quality of ILS including the new microwave ILS.

2.9 Gyro Drift Rate Induced Estimator Error

Gyro drift rate is an important criterion of inertial system performance. A typical commercial quality navigator will use gyros with an average drift rate of the order of one minute of arc per hour. The estimators described in Section 2.7 provide estimates of the inertial system errors in position, velocity and acceleration normal to the localizer center plane. It is relevant to pose the question: What is the effect of gyro drift rate on the estimated inertial navigator errors? Since the estimators are linear systems, the component of error δe_{ie} introduced by the average value of gyro drift u_{im} in the estimates e_{ie} is described by an expression of the form

$$\delta e_{ie}(t) = g(t)\, u_{im} \qquad (2.9.1)$$

where $g(t)$ is a vector of time varying functions. The form of g is shown in figs. 2-9-1 and 2-9-2 which show that the gyro drift introduces errors which grow as t, t^2, and t^3 in the estimated acceleration, velocity and position biases respectively. The accumulated errors after the passage of 10 and 100 seconds to two mean gyro drift rates are tabulated in table 2-9.1.

Such figures would not preclude the application of low quality** inertial components in an inertially aided automatic landing system. In any case, it appears

---

*The time averaging process was initiated at t = 10.0 seconds to reduce the effect of the transient in the minimum ISE estimates.

**Gyro drift rates less than 10.0 degrees/hour.

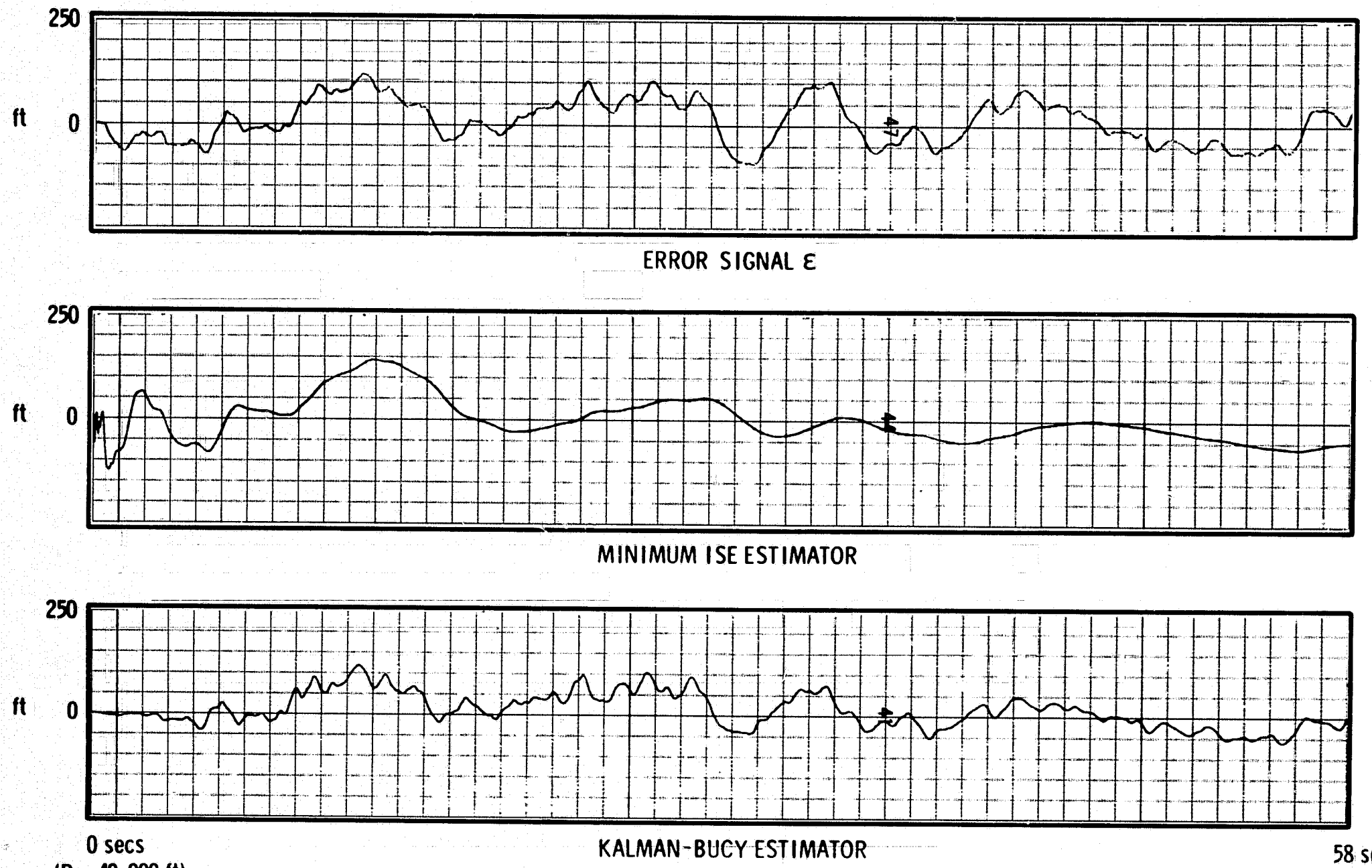


Fig. 2-8-7 Error signal ϵ and error in estimated inertial system position bias versus time. The bias errors in the inertial system are zero so that $\epsilon = -y_r$.

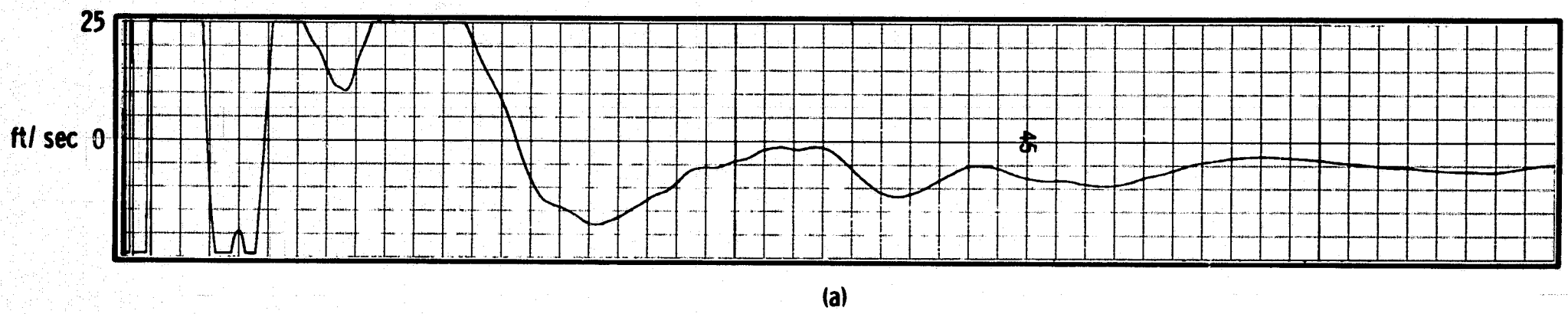
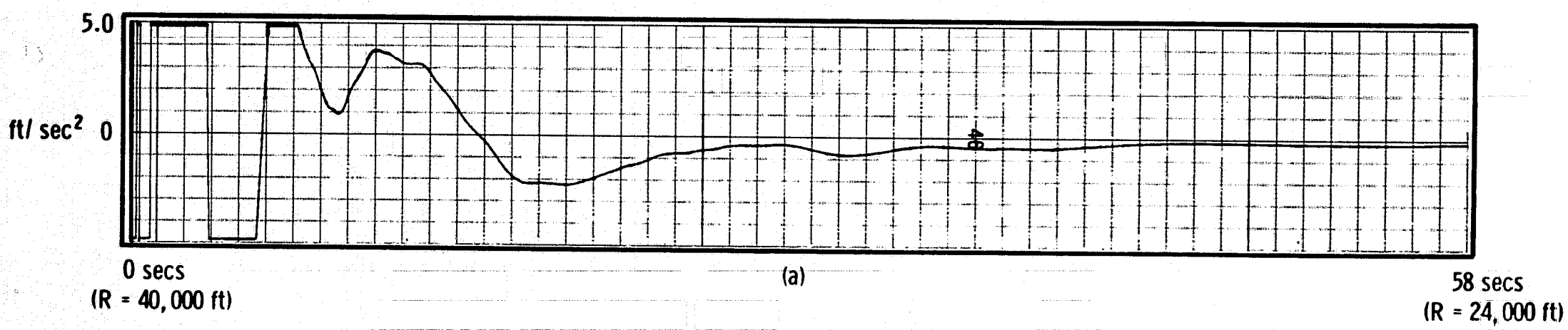


Fig. 2-8-8 Error in estimated inertial system velocity bias versus time for (a) the minimum ISE estimator and (b) the Kalman-Bucy Estimator. The actual inertial system biases are all zero.



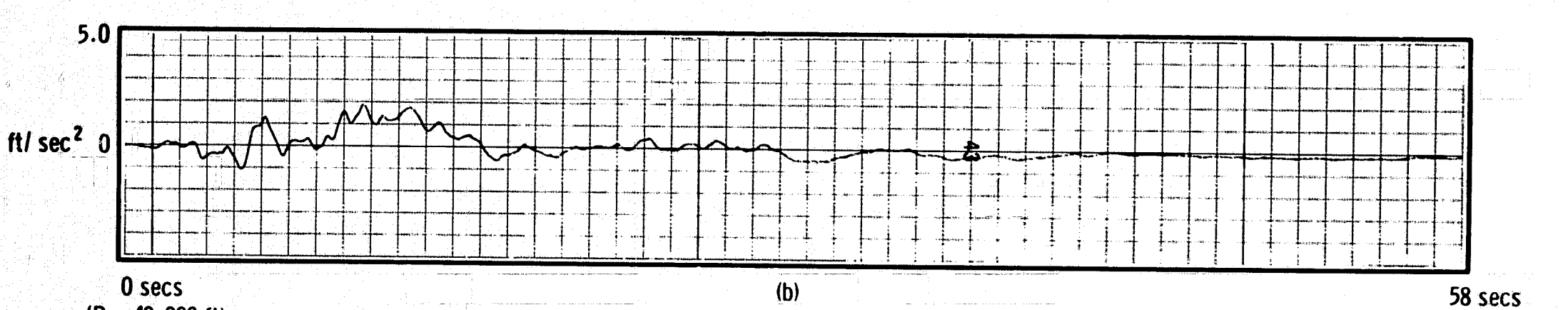
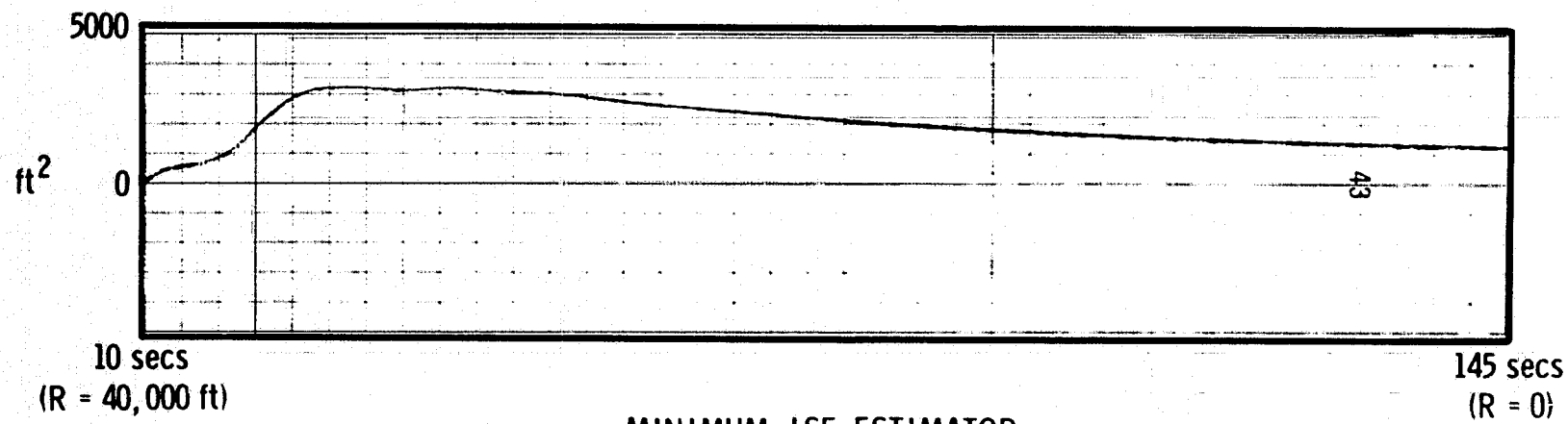
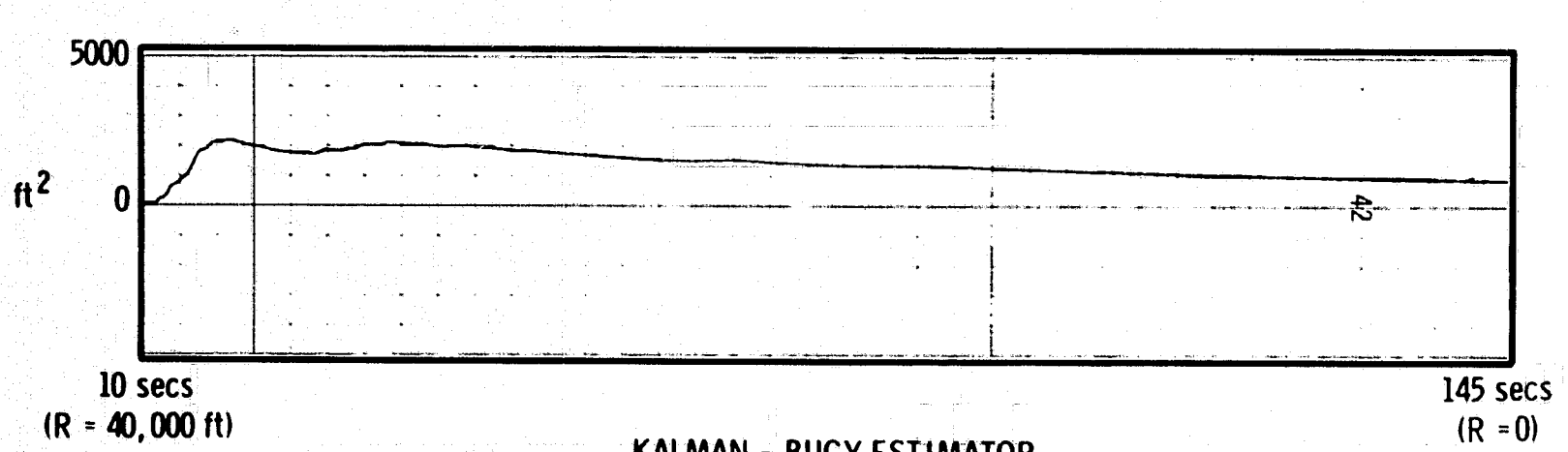


Fig. 2-8-9 Error in estimated inertial system acceleration bias versus time for (a) the minimum ISE estimator and (b) the Kalman-Bucy Estimator. The actual inertial system biases are zero.



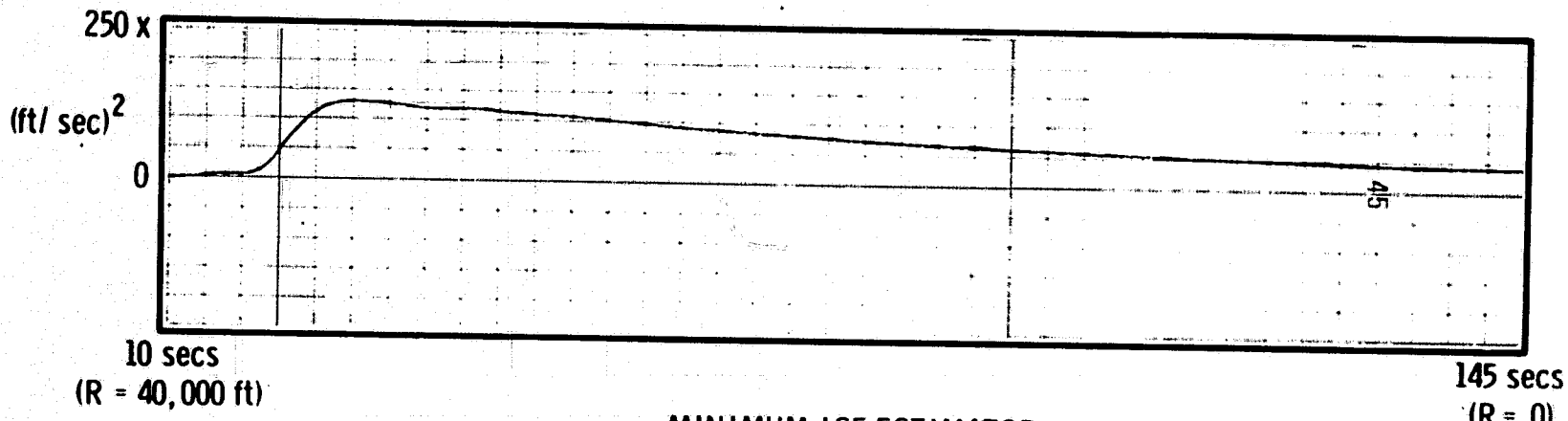
MINIMUM ISE ESTIMATOR



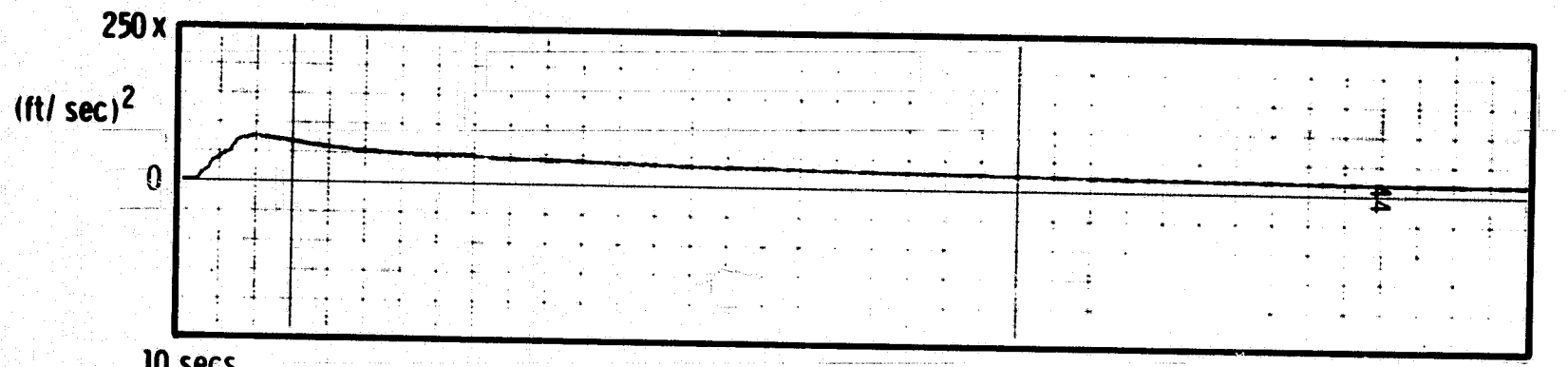
KALMAN - BUCY ESTIMATOR

$E(a_y^2) = 4 \times 10^{-4}$ RAD^2

Fig. 2-8-10 Equation (2.8.4) versus time for x equal to the error in estimated position bias. The actual inertial system biases are zero.



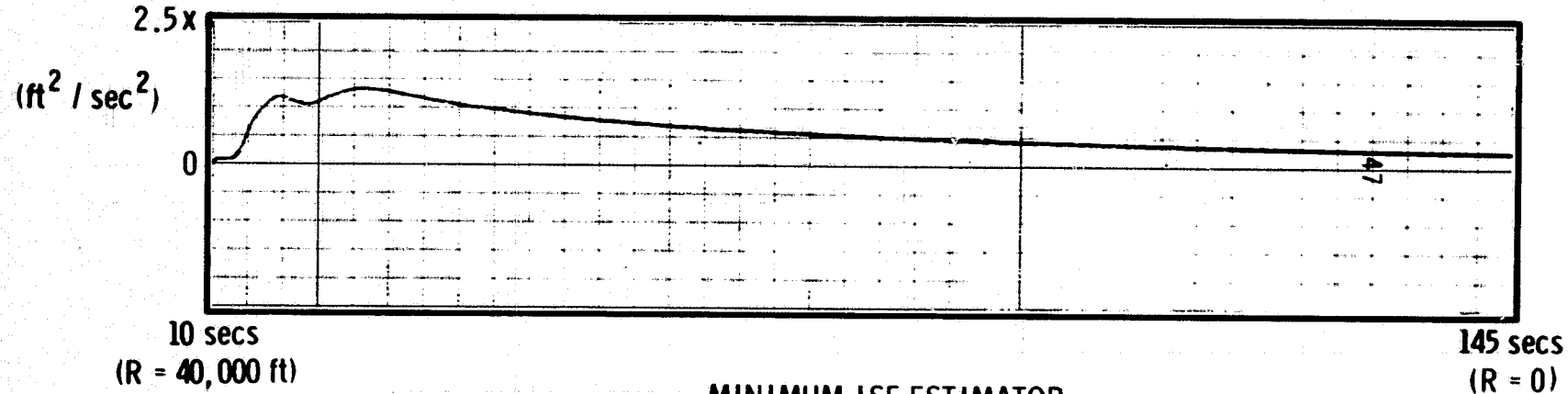
MINIMUM ISE ESTIMATOR



KALMAN - BUCY ESTIMATOR

$E(\alpha_y^2) = 4 \times 10^{-4}$ RAD^2

Fig. 2-8-11 Equation (2. 8. 4) versus time for x equal to the error in estimated velocity bias. The actual inertial system biases are zero.



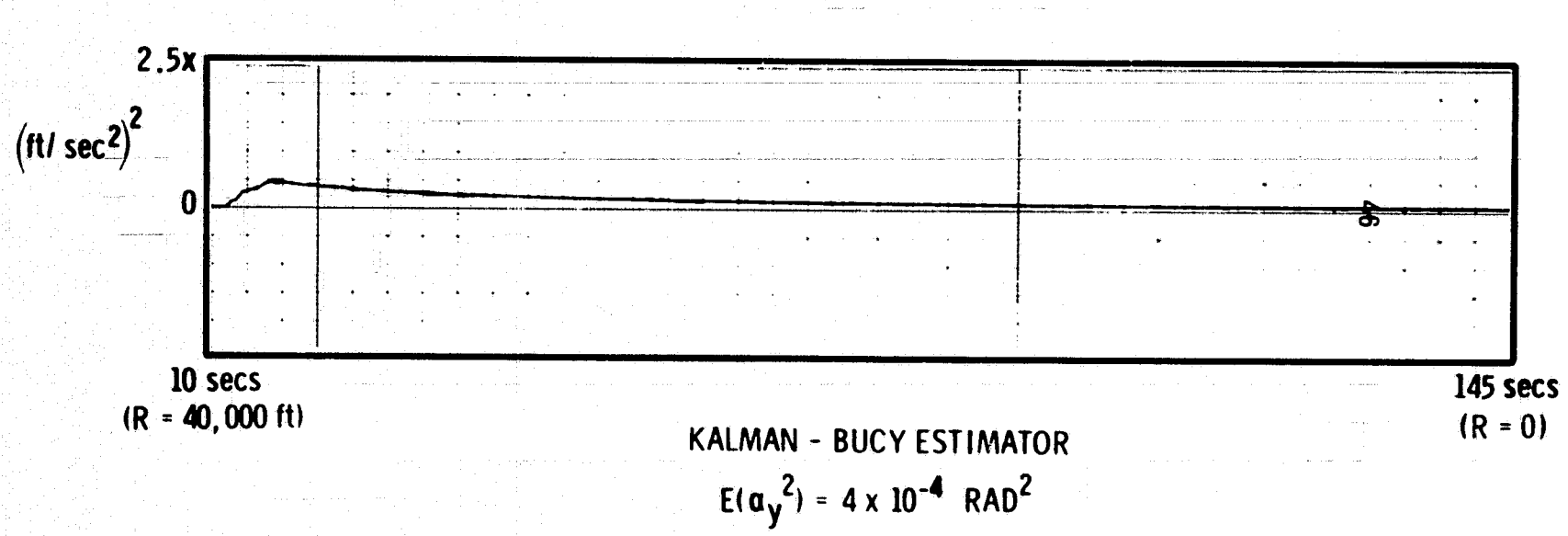


Fig. 2-8-12 Equation (2.8.4) versus time for x equal to the error in estimated acceleration bias. The actual inertial system biases are zero.

to be quite feasible to estimate gyro drift rate by increasing the dimension of the estimator by 1, thus eliminating this source of error.

2.10 Optimal Estimator Sensitivity to Model Errors

The optimal estimators described above require models of various system components in order to carry out the estimation process.

The minimum ISE estimator requires a model of the inertial system and the radio aid receiver to generate the error ϵ in (2.4.5) and the vector of functions h in (2.4.6)

The Kalman Estimator requires a model of the exponentially-correlated radio aid signal noise as well as models of the inertial system and the radio aid.

The current study did not permit a complete analysis of the effects of model errors. A brief discussion is presented here.

If the first order models for the ILS receiver and the exponentially-correlated ILS noise source are assumed to be valid, it is apparent that model errors may arise from variations in the time constants associated with the first order lags or variations in scale factors such as the ILS receiver gain and radius R_t, to the ILS transmitter antenna, for example.

The effects of the variations are twofold. First the model errors can introduce discrepancies in the estimates of the inertial system biases in the absence of vehicle motion and radio aid noise. The second problem is associated with the coupling of vehicle motion into the estimator since complete cancellation of the vehicle motion at the ϵ summing junction will not occur.

Work is continuing on this important problem and the results will be presented in a later report.

2.11 Discrete Optimal Estimation Algorithms

Future aircraft navigation and control systems will undoubtedly use a digital computer as the primary computational system element The application of a digital computer presents some unique problems not encountered by analog devices. Since most current digital computers are serial devices, mathematical operations are performed in a sequence rather than in parallel. As a result, limitations are imposed on the number of operations which can be performed per unit of time. These limitations are very important if the results of the computation are to interact with a physical system which, of course, operates in real time.

---

*The errors due to random components and the constant components of higher derivatives would still be present.

Table 2-9.1 Accumulated errors in bias estimates due to gyro drift rates.

elapsed estimation time	10 seconds		100 seconds	
average gyro drift rate u_{im}	1 minute per hour	60 minutes per hour	1 minute per hour	60 minutes per hour
acceleration estimate error δe_{i3}	-0.000013 ft/s^2	-0.00078 ft/s^2	-0.00013 ft/s^2	0.0078 ft/s^2
velocity estimate error δe_{i2}	-0.0000052 ft/s	-0.0031 ft/s	-0.0052 ft/s	-0.31 ft/s
position estimate error δe_{i1}	-0.0000024 ft	-0.000144 ft	-0.0024 ft	-0.144 ft

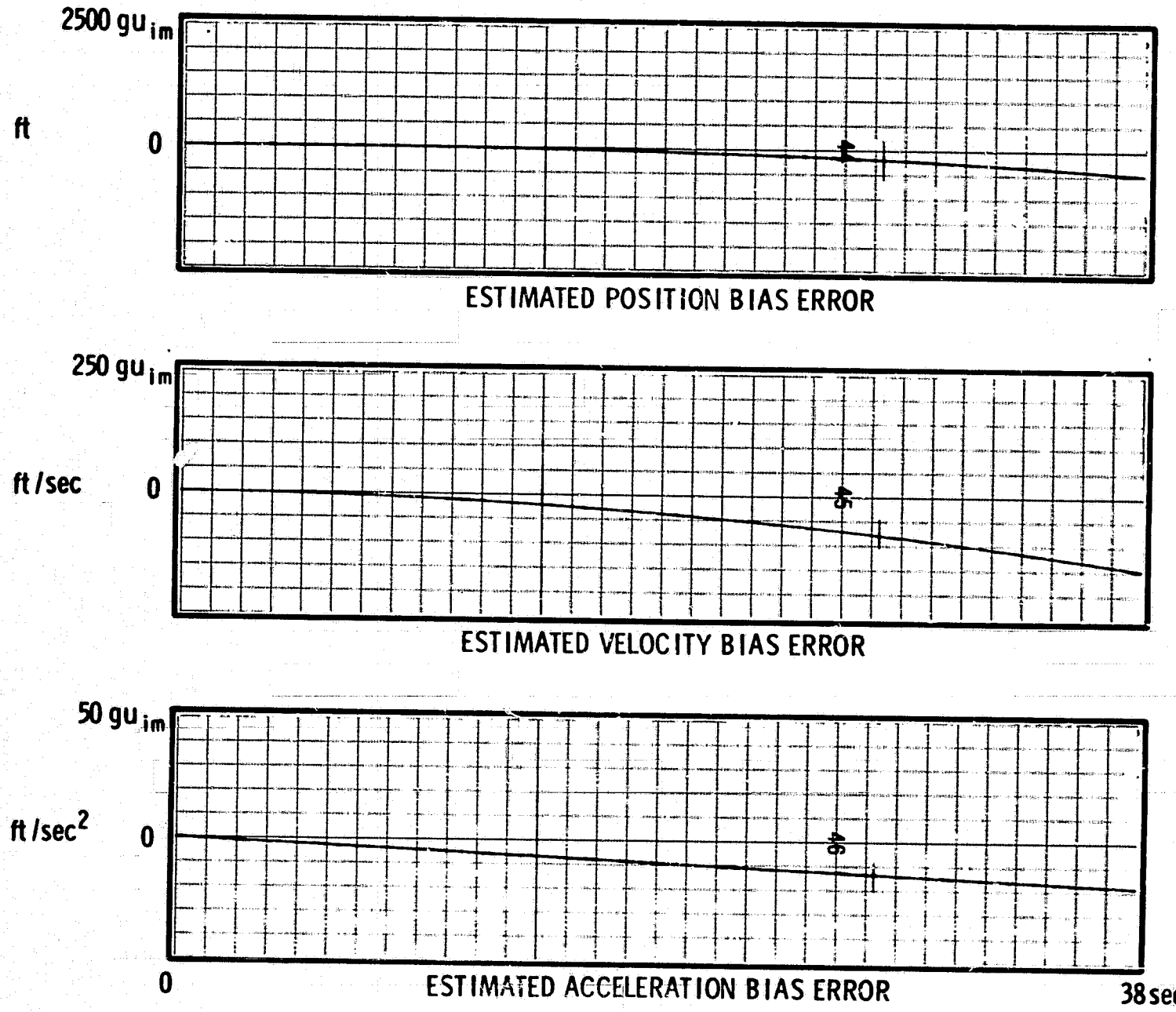


Fig. 2-9-1 Minimum ISE estimator error responses to a constant gyro-induced drift gu_{im} ft/sec^3 where g = 32.2 and u_{im} is the gyro drift rate in radians/second.

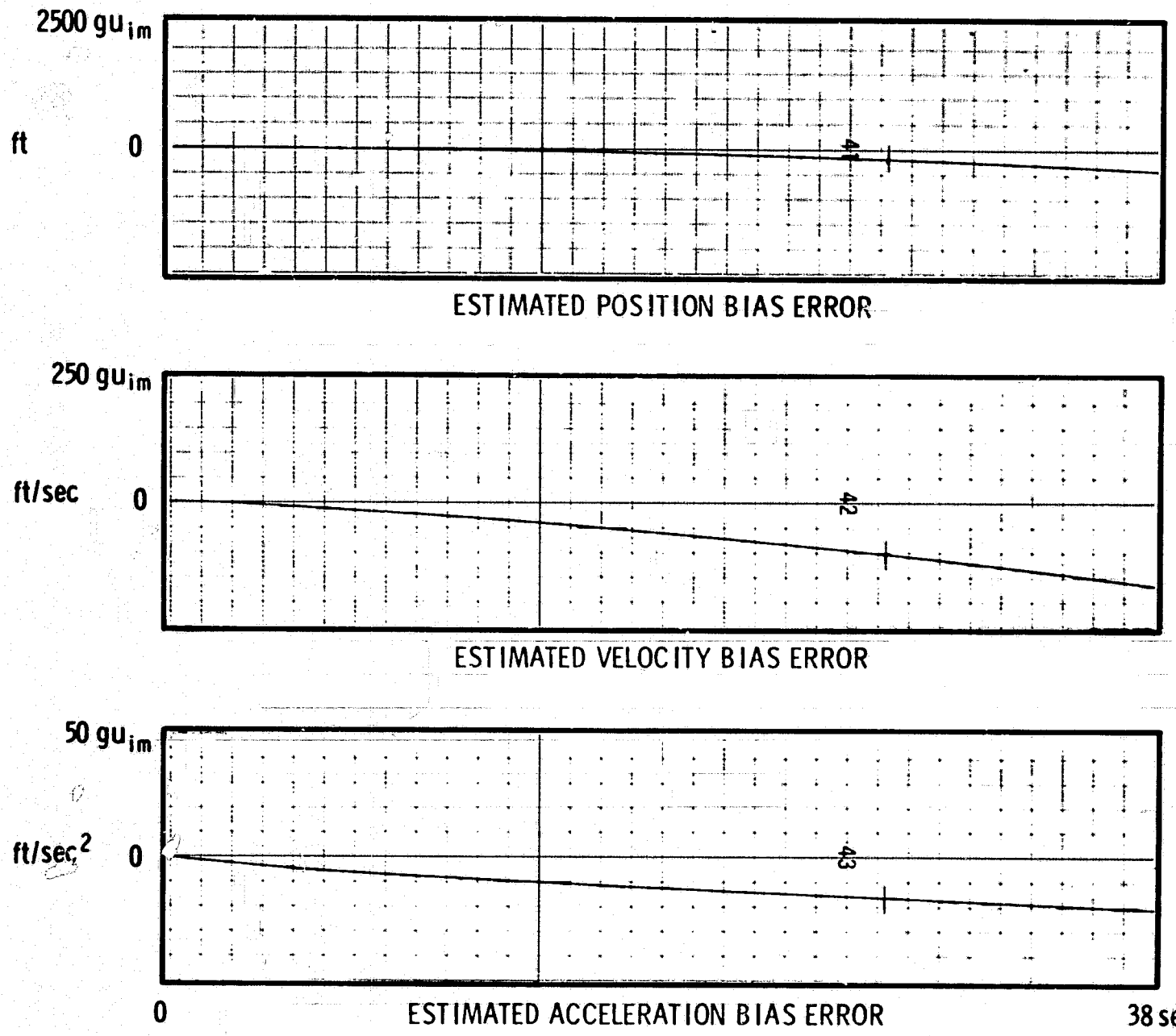


Fig. 2-9-2 Kalman-Bucy Estimator error responses to a constant drift gu_{im} ft/sec^3.

Numerical integration is a particularly time-consuming operation. Thus the integrations indicated in (2.4.9), and the solution of the differential equations in (2.6.15) and (2.6.16) are not usually feasible. It is common to avoid these difficulties by approximating the continuous system equations by algebraic difference equations. The differential equation

$$\dot{x} = Fx \tag{2.11.1}$$

$$x(0) = x_0 \tag{2.11.2}$$

may be replaced by the difference equation

$$x(t + \Delta t) = \Phi x(t) \tag{2.11.3}$$

where Φ is given by

$$\Phi(\Delta t) = \int_0^{\Delta t} F\, \Phi(\alpha)\, d\alpha \tag{2.11.4}$$

subject to the boundary condition

$$\Phi(0) = I \tag{2.11.5}$$

where I is the identity matrix. Since Δt may be relatively large compared to the integration step size, a considerable amount of computer time may be saved.

The primary problem associated with application of the algebraic difference equation approach is the fact that the solution (2.11.3) is only available at times $t + k\Delta t$ where k is an integer. As a result some care must be exercised in the selection of Δt, the interpolation of solutions between the sample times $t = k\Delta t$ and the control of the noise introduced by sampling. The optimal design of digital state estimators shall be the subject of a future report.

CHAPTER 3

NECESSARY CONDITIONS FOR THE EXISTENCE OF OPTIMAL STOCHASTIC CONTROL SYSTEMS

3.1 Introduction

An integrated navigation system, consisting of one or more radio aids and an inertial measurement unit, provides position, velocity, and acceleration information which is relatively noise- and lag-free compared to the radio aid-derived information. In order to take maximum advantage of the improved quality of the integrated sensor data, the control system which uses this information to guide the vehicle along a desired trajectory must be optimized. Such a redesigned system will feature higher feedback path gains than a system relying on a radio aid as its prime navigation reference. As a result, sensitivity to environmental disturbances will be reduced.

In the previous work, [4, 5] the optimization of a landing system featuring an integrated navigation system was discussed from a heuristic point of view using the classical method of frequency domain analysis. In this report a time domain state space approach and systematic mathematical optimization techniques are adopted to achieve a rigorous solution. The primary problem shall be the minimization of the mean square value of certain trajectory errors resulting from stochastic disturbances in a worst case environment which impinge on the vehicle. The mean square error values shall be minimized by adjusting control law parameters subject to mean square error constraints on control variables such as aileron and elevator deflection.

By the application of optimization techniques it shall be possible to form a rigorous basis of comparing both conventional and inertially-aided control system configurations.

In addition, optimization techniques provide a tool for synthesizing systems which achieve optimum performance with respect to an index which reflects design limitations on system structure and the mean square value of dynamic parameters such as control surface deflection.

The following sections will introduce methods for determining the behavior of a physical system subject to stochastic disturbances, formulate the parameter optimization problem, and investigate the necessary conditions for the existence of

an optimal solution.

Unlike the linear optimal control approach,[11, 19, 20] the parameter optimization techniques will not require the measurement or estimation of all the elements of the state vector of the aircraft, or precise knowledge of the time history of the environmental disturbances on the vehicle.

3.2 Response of a Linear System to Environmental Noise:

In order to facilitate this analysis, the characteristics of the response of a linear system to environmental noise must be delineated mathematically. Consider the system of linear differential equations

$$\dot{x} = Fx + Gu \qquad (3.2.1)$$

where x is a vector describing the state of the system, and u is a vector of Gaussian white noise inputs; u is assumed to be uncorrelated with the state x. The matrix F describes the structure of the system, while the matrix G indicates the manner in which the disturbances act on the system.

The covariance matrix X of x is defined by the relationship

$$X = E(xx') \qquad (3.2.2)$$

where E is the mathematical expectation operator. It is apparent that X is a symmetric matrix, a property which may be used advantageously in computations.

3.3 Evaluation of the Covariance Matrix X

A key problem in the solution of stochastic control problems is the evaluation of the covariance matrix X. Such evaluation has been investigated using frequency domain techniques and results for transfer functions may be obtained by evaluating tabulated parameter functions as described in ref. 27 . Such a procedure, while feasible for simple systems, has the disadvantage of requiring precise knowledge of the system transfer functions and is quite laborious for complicated systems. These difficulties may be avoided by observing that the covariance matrix X satisfies the set of linear differential equations[18]

$$\dot{X} = FX + XF' + GQG' \qquad (3.3.1)$$

subject to the boundary condition

$$X(0) = X_0 \tag{3.3.2}$$

Of prime interest in control system investigations are time-invariant or stationary systems. A linear system of the form (3.2.1) is time-invariant if the matrices F and G are constant. If the system is time-invariant and asymptotically stable, and the correlation matrix Q is also constant, the matrix X will approach a constant as $t \to \infty$. This implies that the derivative $\dot{X}$ of X vanishes as $t \to \infty$ or that the final value of X satisfies the set of linear algebraic equations.[18]

$$FX + XF' + GQG' = 0 \tag{3.3.3}$$

The process is then said to be statistically stationary in the limit $t \to \infty$.

The solution X satisfying (3.3.3) is conveniently obtained by integrating in the forward direction until the value of X reaches a steady state.

3.4 Problem Formulation

Let the performance index, J, be defined as a linear combination of the elements of the covariance matrix, X. Such a performance index may be expressed in the form

$$J = \text{trace } CX \tag{3.4.1}$$

where

$$\text{trace } CX = \sum_{i=1}^{n} \left(CX\right)_{ii} \tag{3.4.2}$$

the scalar sum of the elements on the main diagonal of the matrix CX. The value of J depends upon the element values of the matrices C and X. C is selected to reflect the control goals of the system operating in the stochastic environment, while the value of X depends upon the matrices F, G, and Q as indicated in section 3.3. The matrices G and Q are assumed to be constant while the matrix F is a function of an adjustable parameter vector, p.

The problem may then be defined as follows

Definition of the Problem:

Find a set of parameters, p, which minimize the performance index

$$J = \text{trace } CX \tag{3.4.3}$$

subject to the constraint

$$FX + XF' + GQG' = 0 \tag{3.4.4}$$

where p is vector of adjustable parameters
F is a matrix which is a function of the parameter vector, p
X is the covariance matrix of the system state vector x
Q is the covariance matrix of the white noise process, u
G is a matrix specifying the coupling between the system and the dimensional stochastic disturbance vector, u.

3.5 The First Necessary Condition for the Existence of a Weak Relative Minimum

In the calculus of functions of a single variable, the necessary condition for a weak relative minimum is the vanishing of the first derivative of the function with respect to the variable. In the case of functionals such as

$$J = \text{trace } CX \tag{3.5.1}$$

the general concept of a derivative can be extended using the Calculus of Variations.[13]

A parameter value p_{opt} is said to produce a weak relative minimum if the change in J for small perturbations δp, in p_{opt} satisfies the following inequality:

$$J\left(p_{opt} + \delta p\right) \geq J\left(p_{opt}\right) \tag{3.5.2}$$

The necessary condition for the existence of a weak relative minimum in J may be deduced by expanding the perturbation δJ due to δp in a Taylor's series.

$$\delta J = \delta p' J_p + \text{higher order terms in } \delta p \tag{3.5.3}$$

The notation J_p signifies the gradient of J with respect to p.

$$J_p = \begin{bmatrix} \frac{\partial J}{\partial p_1} \\ \vdots \\ \frac{\partial J}{\partial p_n} \end{bmatrix} \qquad (3.5.4)$$

If δp is sufficiently small the higher order terms in δp may be neglected and δJ approximated by

$$\delta J \approx \delta p' J_p. \qquad (3.5.5)$$

In order to satisfy the inequality it is apparent that J_p must vanish for $p = p_{opt}$.

$$J_p\left(p_{opt}\right) = 0 \qquad (3.5.6)$$

This condition is called the First Necessary Condition of the Calculus of Variations.

3.6 The Canonical Equations of the First Variation

In the problem defined in sec 3.4, the minimization of the performance index is carried out subject to the constraint imposed by the system dynamics in 3.4.4 . These restrictions may be introduced by adjoining the constants to the performance index through the artifice of a Lagrange Multiplier Matrix, P.[15] The performance index is then written

$$J = \text{trace}\left[CX + P\left[FX + XF' + GQG'\right]\right] \qquad (3.6.1)$$

The first variation in the performance index may then be written by considering perturbations in P, X, and p.

$$\begin{aligned} \delta J = \text{trace} \Big[& \delta P\left[FX + XF' + GQG'\right] \\ & + \delta X\left[C + PF + F'P\right] \\ & + \sum_{i=1}^{\ell}\left[\delta p_i\left[PX + XP\right]\frac{\partial}{\partial p_i}F'\right] \Big] \end{aligned} \qquad (3.6.2)$$

The last term may be identified as

$$\delta p' J_p = \text{trace} \sum_{i=1}^{\ell} \delta p_i \left[PX + XP\right] \frac{\partial}{\partial p_i} F' \qquad (3.6.3)$$

where each element of the vector J_p is defined

$$J_{p_i} = \frac{\partial}{\partial p_i} J$$

$$= \text{trace} \left[PX + XP\right] \frac{\partial}{\partial p_i} F' \qquad (3.6.4)$$

Since the matrices $\frac{\partial}{\partial p_i} F$ are relatively easy to compute, equation (3.6.4) provides a convenient basis for evaluating the gradient, J_p, of the performance index.

In order for the first variation to vanish with respect to arbitrary perturbations in δp, δX, and δF, the following set of Canonical Equations of the First Variation must be satisfied.

Canonical Equations of the First Variation

$$FX + XF' + GQG' = 0 \qquad (3.6.5)$$

$$PF + F'P + C = 0 \qquad (3.6.6)$$

$$J_p = 0 \qquad (3.6.7)$$

In the next chapter, numerical procedures are presented which systematically satisfy the necessary conditions of the first variation.

CHAPTER 4

NUMERICAL PROCEDURES FOR PARAMETER OPTIMIZATION

4.1 Introduction

In the preceding chapter, the canonical equations of the first variation were derived. In the following sections, computational algorithms are introduced which systematically search for a solution of the canonical equations. The numerical techniques are then compared by applying the various algorithms to the optimization of a simple stochastic control system.

4.2 Numerical Optimization Techniques

The field of numerical optimization encompasses a large number of different algorithms and applications. To a large extent, the application of numerical optimization techniques to the solution of practical engineering problems is a relatively recent phenomenon arising from the development of high speed, large scale, electronic digital computers which are capable of performing the optimization computations in a reasonable length of time.

A review of the algorithms presented in the following sections reveals a structural commonality shown in fig. 4-2-1. Each algorithm requires the computation of the value of the performance index, J, and the gradient, J_p, of J with respect to the parameter vector, p. These calculations are conveniently performed using the canonical equations of the first variation in Section 3.6.

The calculation of J is illustrated in fig. 4-2-2. The covariance matrix, X, is the solution of the matrix algebraic equation.

$$\dot{X} = FX + XF' + GQG' = 0. \qquad (4.2.1)$$

The value of X is obtained by integrating the differential equation describing the behavior of X as a function of time to a steady state solution; a procedure suggested by Kalman and Bertram*. A similar procedure is used to evaluate the solution of the Lagrange multiplier equation

$$\dot{P} = F'P + PF + C = 0. \qquad (4.2.2)$$

*The actual computations are carried out using a combination of numerical integration and the state transition approach, to save time.

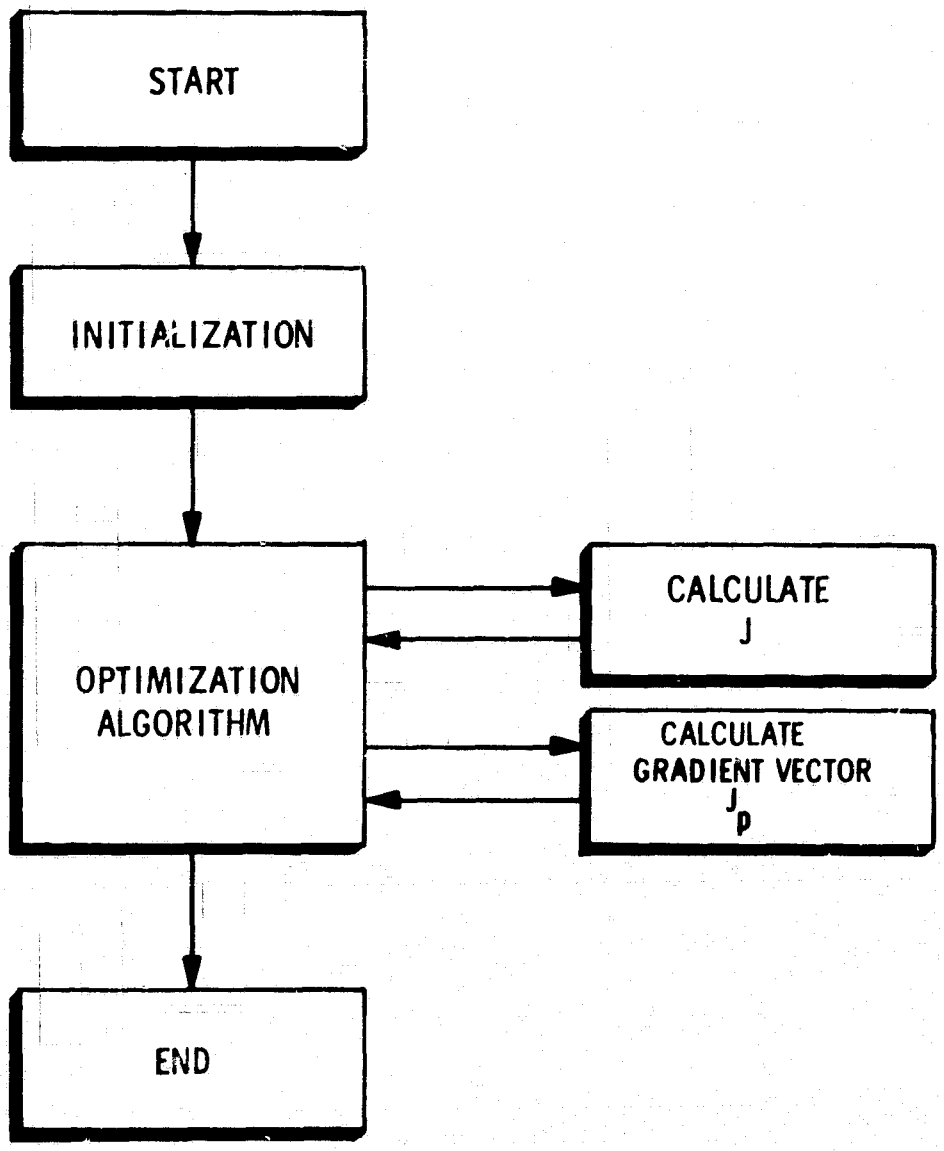


Fig. 4-2-1 Good structural characteristics of optimization algorithms.

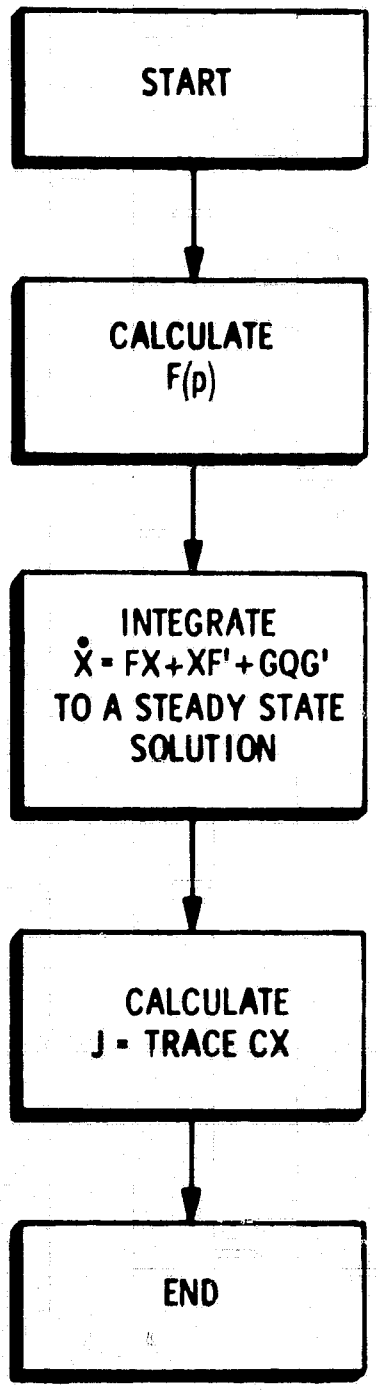


Fig. 4-2-2 Numerical computation of the performance index J.

The gradient is then calculated using relationship (3.6.4)

$$\frac{\partial J}{\partial p_i} = \text{trace}\left[P\frac{\partial}{\partial p_i}FX + PX\frac{\partial}{\partial p_i}F'\right] \qquad (4.2.3)$$

The computations involved are illustrated in fig. 4-2-3.

4.3 The Method of Steepest Descent

Perhaps the most basic method of minimizing the value of a function is the method of steepest descent,[14] which is based on the Taylor series expansion of the variation δJ in the performance index due to a small perturbation, δp, in the parameter vector. If δp is sufficiently small the value of δJ is approximately equal to

$$\delta J \approx \delta p' J_p \qquad (4.3.1)$$

Suppose the change in δp is equal to

$$\delta p = -\epsilon J_p \qquad (4.3.2)$$

where ϵ is a positive number. If ϵ is selected so that δp is small, the approximation (4.3.1) is satisfied. Then δJ becomes

$$\delta J \approx -\epsilon J_p' J_p$$

Since the inner product of J_p with itself, is always positive the perturbation δJ is negative and the value of $J(p+\delta p)$ will be less than the value of $J(p)$. This process may be iterated to produce a monotonically decreasing sequence of values for J. Since the sequence is continuously decreasing the algorithm always converges to a minimum, providing such a minimum exists.

A flow diagram of a steepest descent algorithm is shown is fig. 4-3-1. The variable NIC counts the number of successful iterations ($\delta J < 0$) while NHC keeps track of the number of iterations in which the size of δp is too large to satisfy approximation (4.3.1). If δp is too large ϵ is halved, the evaluation of J is repeated. The algorithm terminates when NIC or NHC exceeds the maximum values NIM or NHM respectively.

4.4 Method of The Average Gradients

One of the important problems associated with the method of steepest descent is the "valley problem". Such a problem occurs if the orientation of the direction of maximum descent path is approximately normal to the gradient vector at the current value of p. If the step size is too great the value of p is transferred to the other side of the "valley" where a similar situation is often encountered.

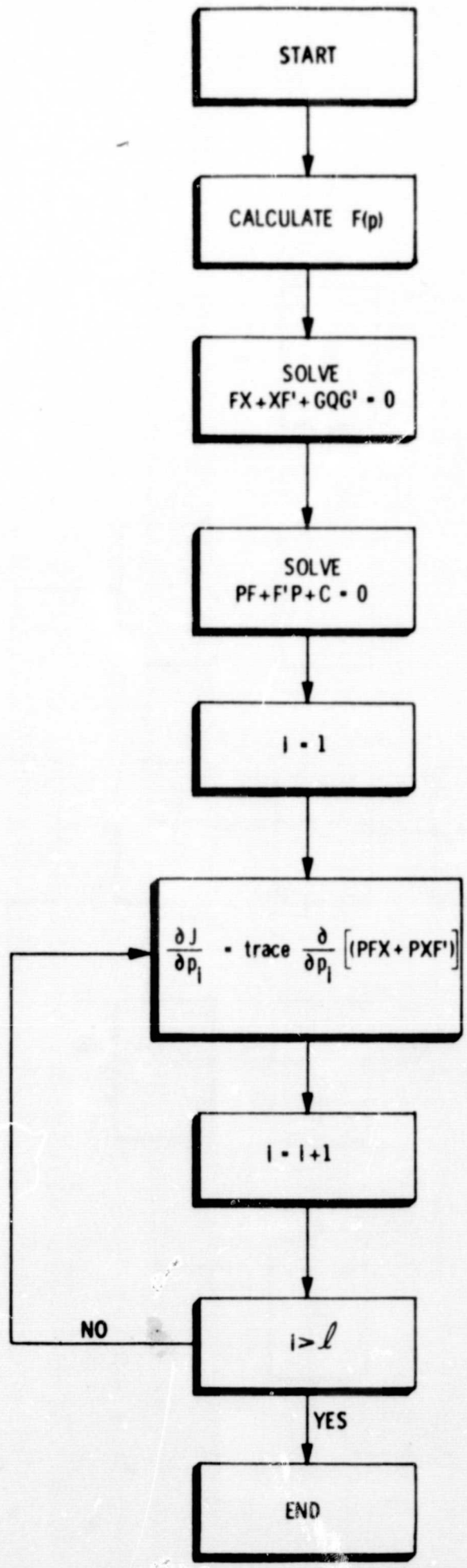


Fig. 4-2-3 Numerical computation of J_p.

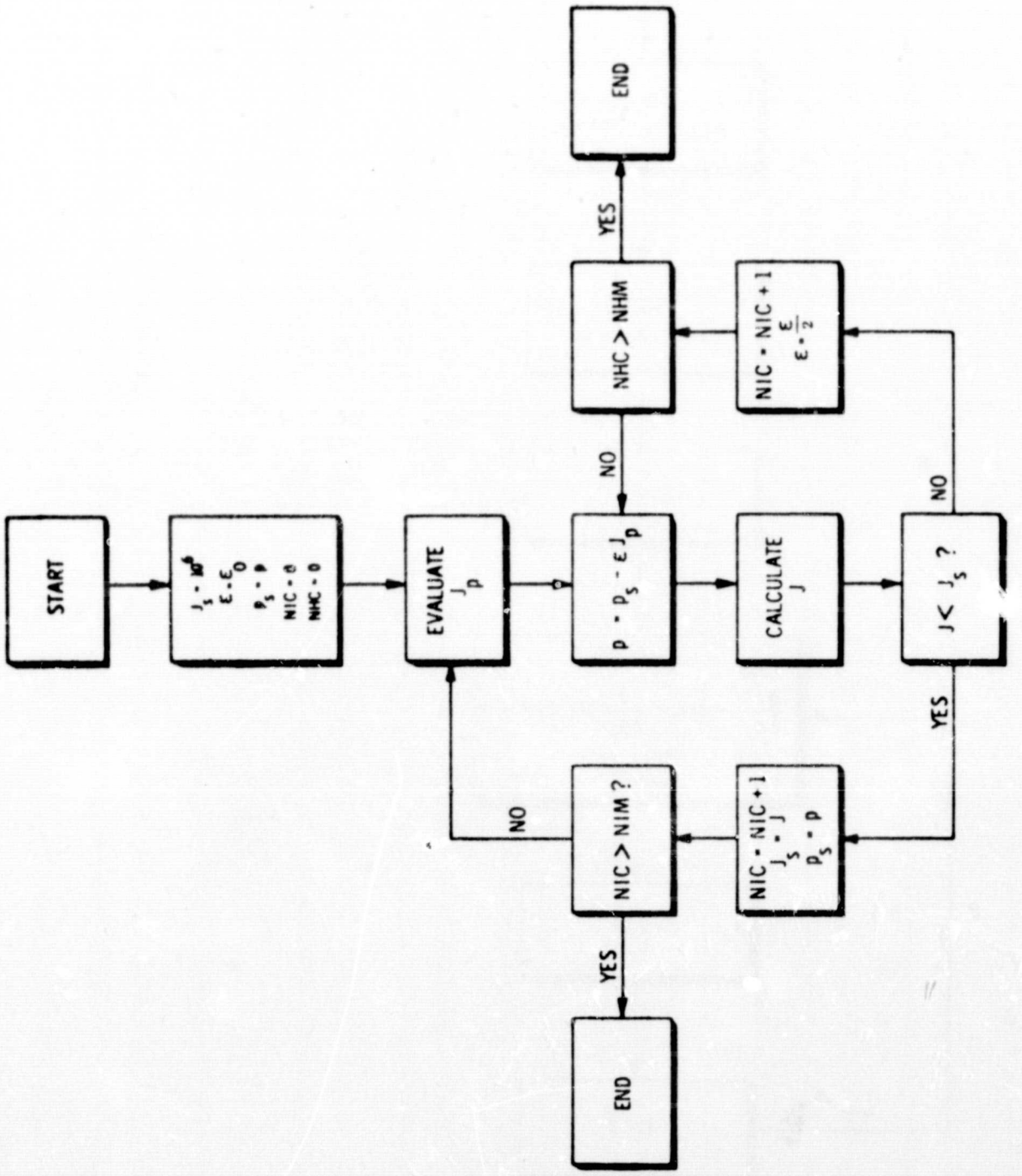


Fig. 4-3-1 Method of steepest descent.

The algorithm may thus continue to traverse back and forth across the "valley" converging very slowly to the minimum. This difficulty may be advoided by using a direction which is the average of the current gradient and the gradient used in the last sucessful iteration.[15]

A flow diagram of the average gradient algorithm is shown in fig. 4-4-1. The previous gradient, J_{ps}, is equal to the present gradient initially so that the first step utilizes the steepest descent algorithm.

4.5 The Generalized Method of Newton Raphson[12]

Convergence rates can usually be improved by considering the second as well as the first variations in the performance index. The expanded perturbation in J due to δp is then of the form

$$\delta J \approx \delta p' J_p + \frac{1}{2} \delta p' J_{pp} \delta p \qquad (4.5.1)$$

where J_{pp} is the matrix of second partial derivatives of the performance index J. J_{pp} is evaluated by finite differences or by using a combination of finite differences and closed form generation of J_p. If the variation in J is required to vanish,

$$\delta p = - J_{pp}^{-1} J_p. \qquad (4.5.2)$$

Since the approximation (4.5.1) is only valid for small δp, the step size is controlled by introducing a positive constant ϵ writing

$$\delta p = -\epsilon \; J_{pp}^{-1} J_p$$

If the performance index is quadratic in p and ϵ is equal to unity, the algorithm will converge in one step to the optimum value. In any case, the algorithm will exhibit one-step convergence if p is near p_{opt}.* The algorithm is illustrated in fig. 4-5-1.

4.6 Method of Conjugate Gradients[18]

This numerical technique is a systematic optimization procedure which displays some of the favorable characteristics of the Newton Raphson algorithm without the necessity of inverting the matrix of the second derivatives, J_{pp}. If the performance index, J, is quadratic in the parameter vector, p, the method will minimize J in ℓ steps where ℓ is the dimension of p.

The algorithm operates by generating a set of "J_{pp} - orthogonal" or "J_{pp} - conjugate" vectors $q_1, \ldots, q_\ell$, in the ℓ-dimensional Euclidean solution space.

---

*Since the performance index will be essentially quadratic in δp when p is near p_{opt}.

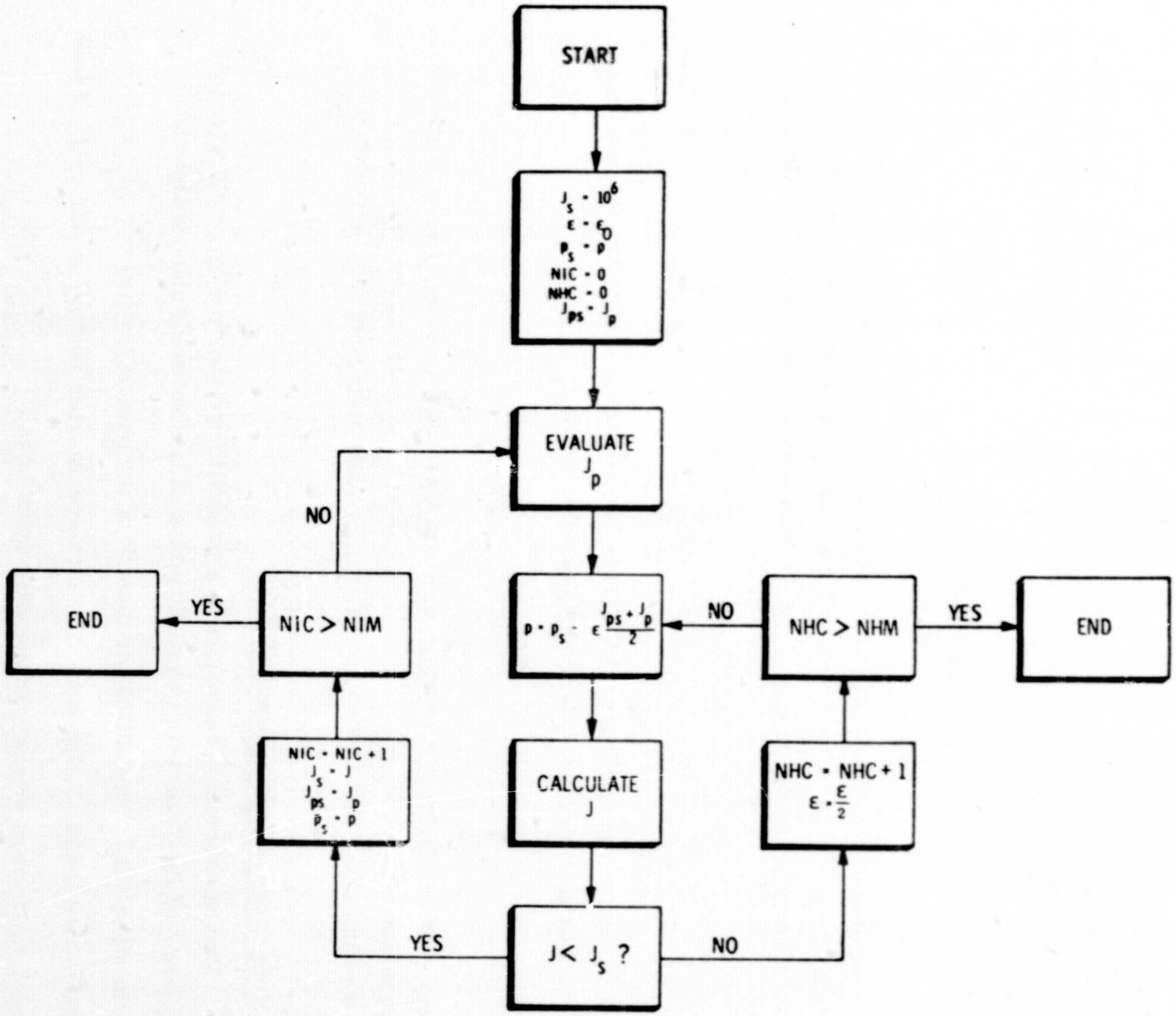


Fig. 4-4-1 Method of average gradient.

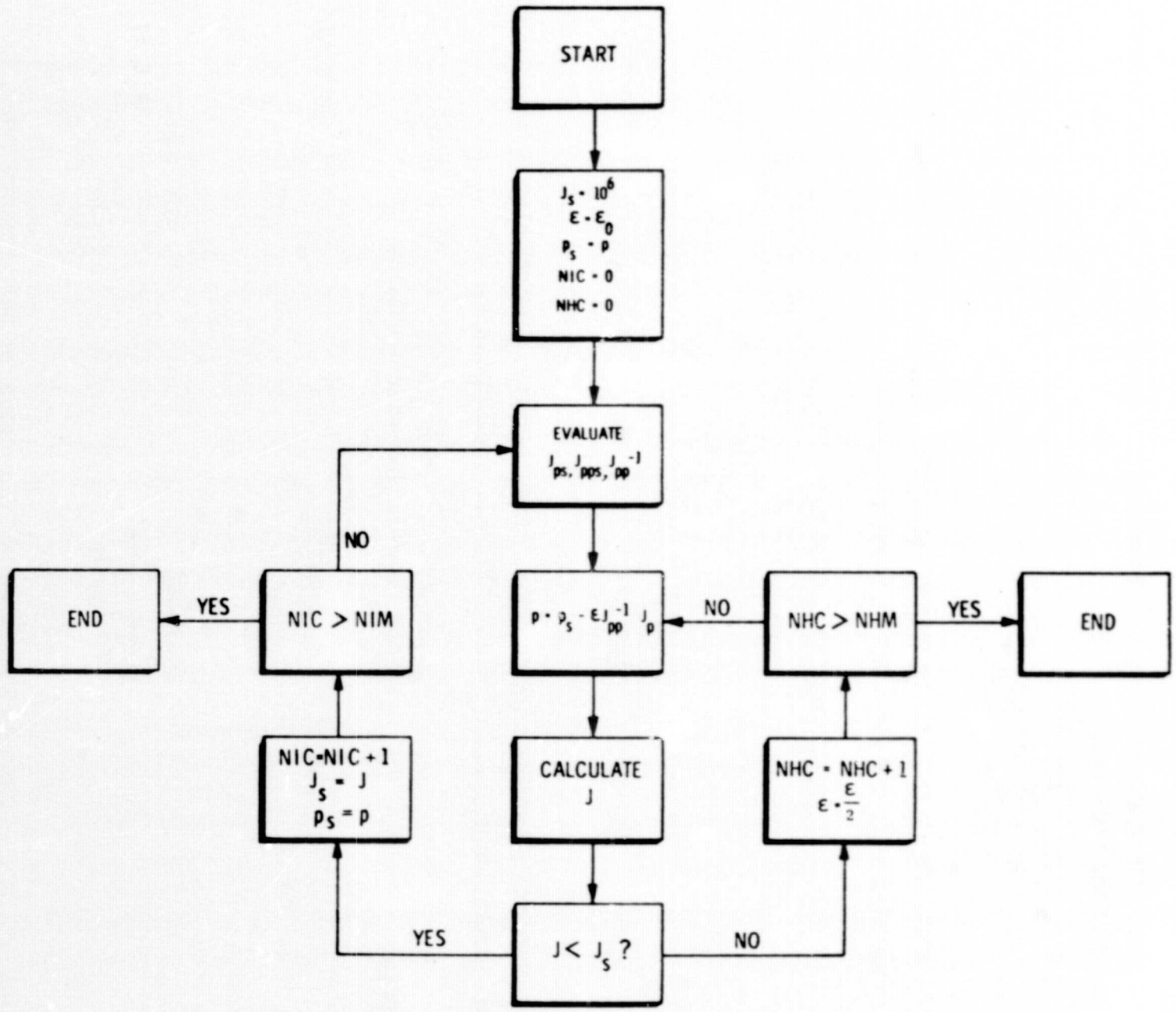


Fig. 4-5-1 Generalized method of Newton Raphson.

The matrix J_{pp} must be positive definite in which case

$$q_i J_{pp} q_j \begin{cases} = 0 & i \neq j \\ > 0 & i = j \end{cases} \tag{4.6.1}$$

As a result it can be shown that any vector p can be expressed as a linear combination of the vectors $q_1, \ldots, q_\ell$

$$p = \sum_{i=1}^{\ell} \beta_i \; q_i \tag{4.6.2}$$

where β_i is a scalar. If p_o is the initial value of p, p_o can be expressed in terms of the optimal value p_{opt} and the basis vectors by writing

$$[p_{opt} - p_o] = \sum_{i=1}^{\ell} \beta_i \; q_i, \tag{4.6.3}$$

where

$$\beta_i = \frac{[\, p_{opt} - p_o \,]' J_{pp} q_i}{q_i' J_{pp} q_i} . \tag{4.6.4}$$

The problems of finding the minimum thus reduces to the determination of the conjugate directions $q_1, \ldots, q_\ell$ and the Fourier coefficients $\beta_1, \ldots, \beta_\ell$.

A convenient set of "J_{pp}-conjugate" basis vectors may be constructed on the gradient vectors, J_p, using the following iterative procedure

$$p_{i+1} = - p_i + \alpha_i q_i \tag{4.6.5}$$

where

$$\alpha_i = \frac{- q_i' J_{p_i}}{q_i' J_{pp} q_i} \tag{4.6.6}$$

The value of α_i is conveniently generated by minimizing the performance index, J, along the straight line $p = p_i + \alpha_i q_i$. The value of α which minimizes J is α_i. The new basis vector is generated by orthogonalization with respect to the subspace spanned by the vectors $q_1, \ldots, q_i$.

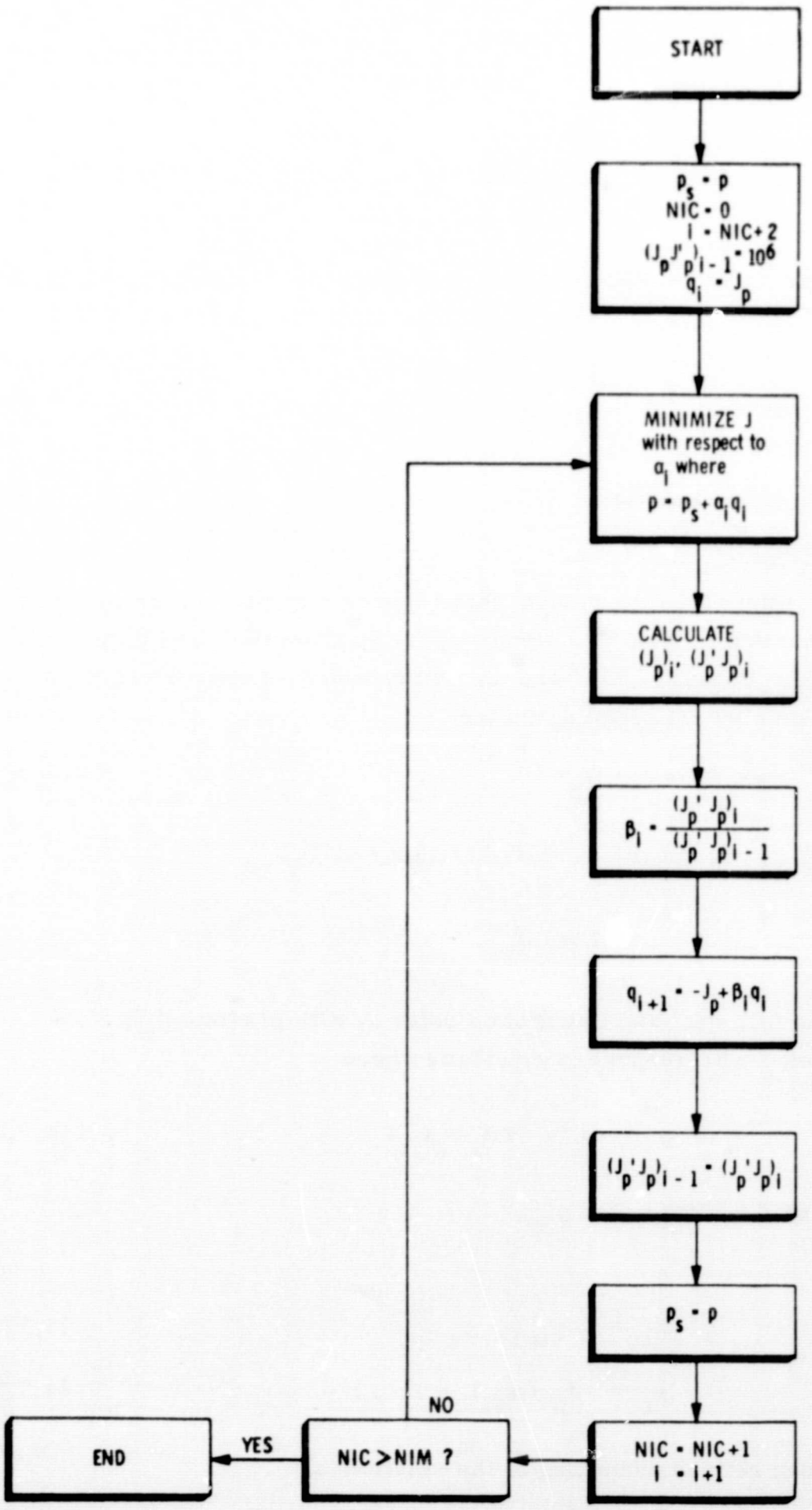


Fig. 4-6-1 Method of conjugate gradients.

$$q_{i+1} = -J_{p_{i+1}} + \beta_i q_i \tag{4.6.7}$$

where

$$\beta_i = \frac{J'_{p_{i+1}} J_{p_{i+1}}}{J'_{p_i} J_{p_i}} \tag{4.6.8}$$

The result is a sequence of operations which systematically satisfies the relationship

$$p_{opt} = p_o + \sum_{i=1}^{\ell} \alpha_i q_i. \tag{4.6.9}$$

The algorithm is illustrated in fig. 4-6-1.

4.7 Method of Davidon[17]

Another optimization technique which shares a number of the properties of the Conjugate Gradient method was suggested by Davidon (17) and further developed by Fletcher Powell (15). The algorithm searches iteratively for a matrix H which defines the optimum step size.

$$\delta p_{opt} = -H J_p \tag{4.7.1}$$

The matrix H is the inverse of the second variation matrix J_{pp}.

$$H = J_{pp}^{-1}. \tag{4.7.2}$$

The procedure is as follows: starting from a point p_i with gradient $J_p(p_i)$ the algorithm minimizes J with respect to a scalar ϵ where

$$p = p_i + \epsilon H_i J_p(p_i) \tag{4.7.3}$$

the optimum value of p is designated p_{i+1}.

Let

$$s_i = p_{i+1} - p_i \tag{4.7.4}$$

$$r_i = J_p(p_{i+1}) - J_p(p_i) \tag{4.7.5}$$

The matrix H_i is then refined according to the relationship

$$H_{i+1} = H_i + \frac{s_i s_i'}{s_i' r_i} - \frac{H_i s_i s_i' H_i}{r_i' H_i r_i} \tag{4.7.6}$$

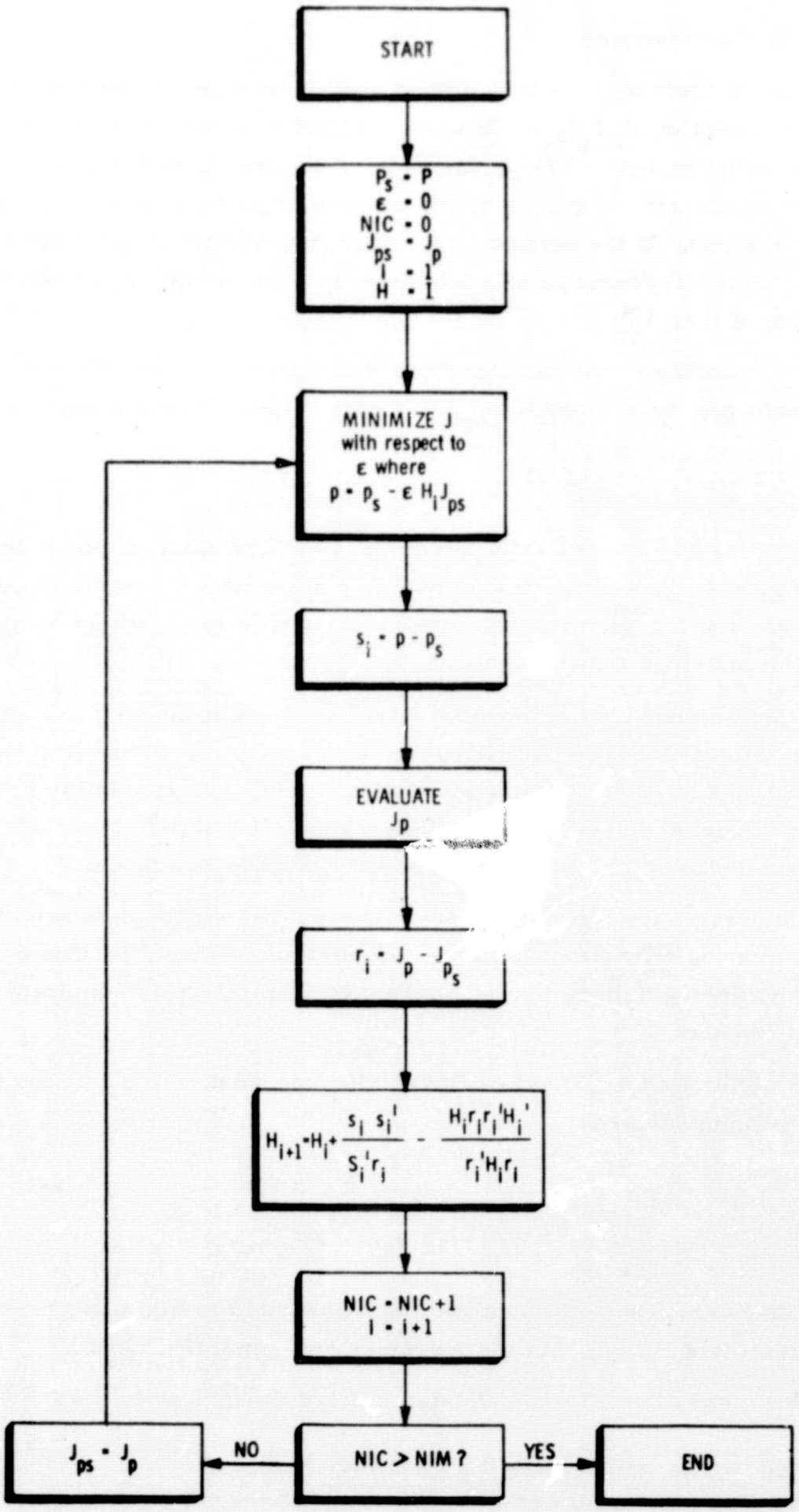


Fig. 4-7-1 Method of Davidon.

The process is then repeated.

It is possible to show that if the initial H is positive definite ($H_1 = I$ for example), the direction $H_i J_p(p_i)$ will always result in a reduction in J when the minimization with respect to ϵ is performed. Thus the algorithm generates a monotonically decreasing sequence of J's and convergence to at least a weak relative minimum is assured. If the performance index is quadratic in p, it can be shown that the algorithm will converge to a minimum in ℓ iterations, in which case the terminal value of H is J_{pp}^{-1}.

It is appparent that the algorithm will also have quadratic convergence properties when p is very close to p_{opt}. A flow diagram of the method is shown in fig. 4-7-1.

4.8 The Method of Powell[14]

This method is similar to the methods of Conjugate Gradient and Davidon, in as much as convergence can be achieved in ℓ steps where ℓ is the dimension of the parameter vector if the performance index is quadratic in p. There is also no necessity to evaluate the matrix of second derivatives J_{pp}.

In this method, each iteration requires one-dimensional minimizations down n linearly independent directions, $d_1, d_2, \ldots, d_\ell$. As a result of these minimizations, a new direction d is defined, which is linearly related to the coordinate values obtained during these minimizations. If d satisfies certain conditions, d replaces one of the original directions and the process continues.

In general, for the k^{th} iteration, the last k-1 directions used are conjugate. For quadratic functions, if p_1 is the minimum in the direction d_j, and p_2 the minimum along a direction parallel to d_j, then $p_2 - p_1$ is conjugate to d_j (parallel tangents).

The initial choice must be linearly independent. This implies that the matrix D of column vectors d_i

$$D = [d_1, d_2, \ldots . d_\ell] \qquad (4.8.1)$$

must be nonsingular ($D \neq 0$). The algorithm illustrated in fig. 4-8-1 is not the original statement of Powell, but the technique now generally adopted.

The convergence tests indicated in fig. 4-8-1 are as follows:

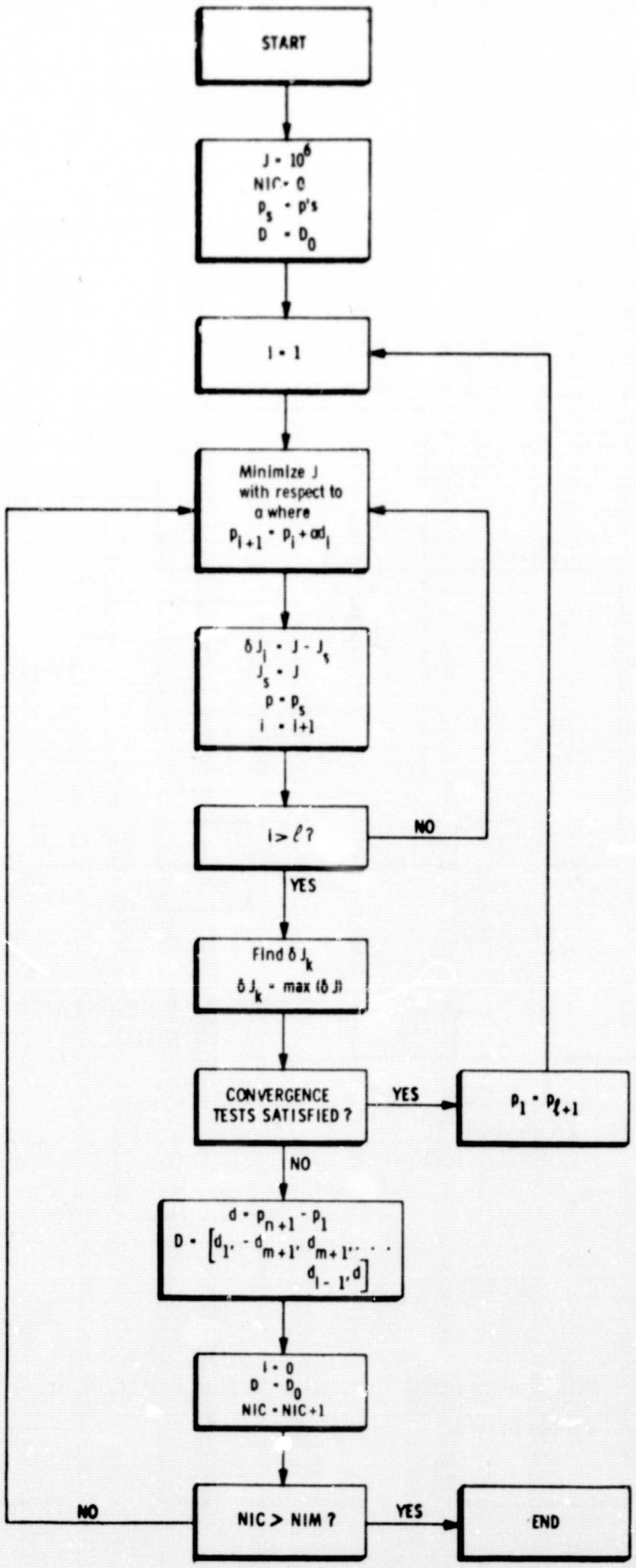


Fig. 4-8-1 Method of Powell.

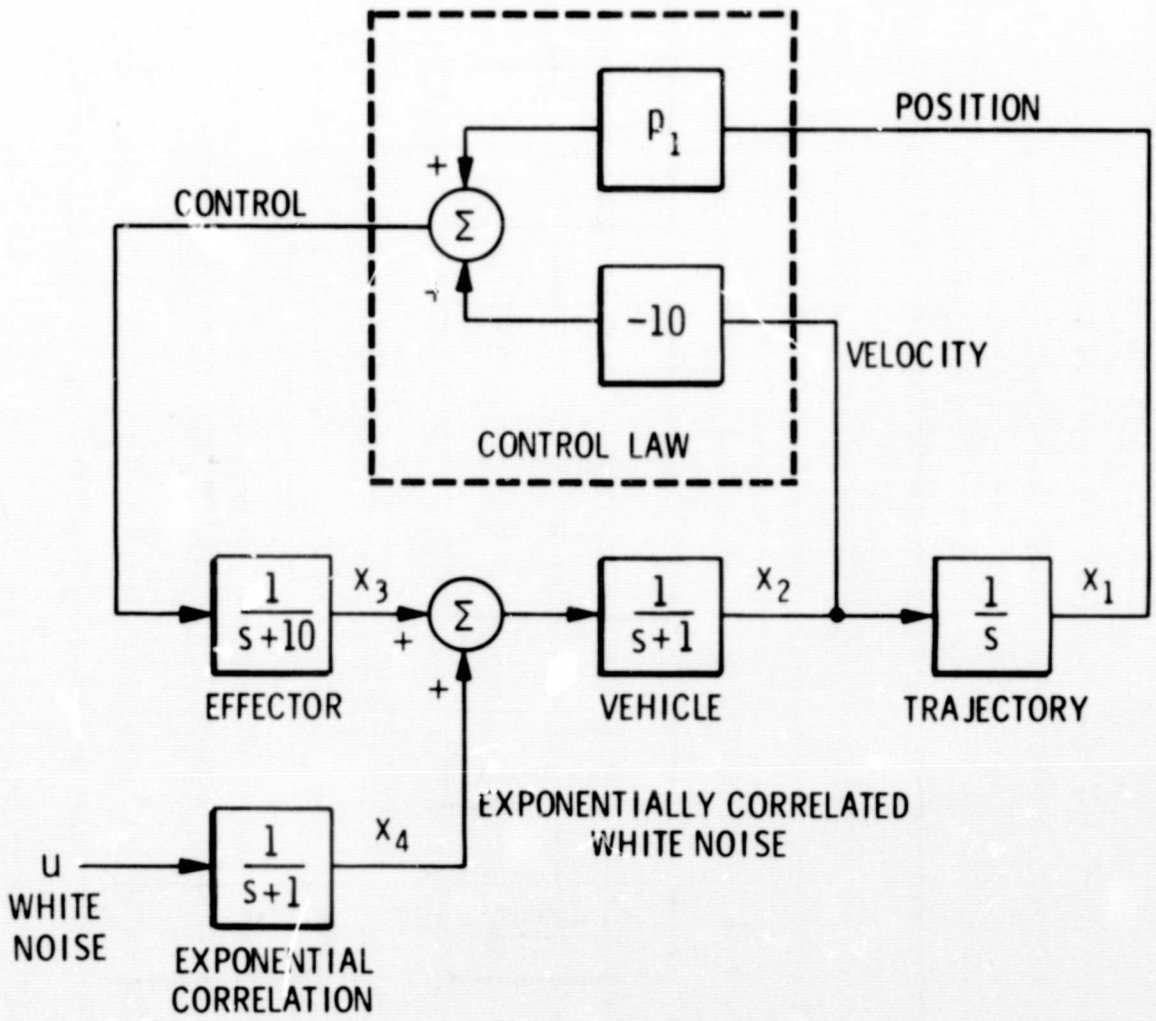


Fig. 4-9-1 Position control system with fixed control structure and a stochastic disturbance.

Define $J_1 = J(p_1)$ and $J_{\ell+1} = J(p_{\ell+1})$.

Calculate $J_2 = J(2p_{n+1} - p_1)$.

If $J_2 \geq J_1$

or if $[J_1 - 2J_{\ell+1} + J_2][J_1 - J_{\ell+1} - \Delta]^2 \geq \frac{1}{2}\Delta [J_1 - J_2]^2$

then set $p_1 = p_{\ell+1}$

and use the same set of directions, $d_1, d_2, \ldots, d_\ell$. If neither condition holds, accept a new direction defined as

$$d = p_{\ell+1} - p_1$$

and update the direction matrix as indicated.

4.9 A Simple Illustrative Example

The foregoing material is best illustrated by application to a simple example which is characterized by a fixed control structure which operates on a subset of the components of the state vector. The system is subject to an exponentially correlated disturbance.

Consider the block diagram in fig. 4-9-1 which may be interpreted as a position control system. The vehicle equations of motion are subject to a zero-mean, exponentially-correlated stochastic disturbance x_4 which produces random fluctuations in acceleration $\dot{x}_2$. The effects of the random variable u are counteracted by a control force x_3. The control law is defined by the adjustable parameter p_1.

The object of the parameter optimization is to minimize the mean square position response $E(x_1^2)$ subject to a penalty on the mean square control force $E(x_3^2)$.

$$\text{minimize } [E(x_1^2) + E(x_3^2)] \tag{4.9.2}$$

The system may be represented by

$$\dot{x} = Fx + Gu \tag{4.9.3}$$

where

$$x = \begin{bmatrix} x_1 \\ x_2 \\ x_3 \\ x_4 \end{bmatrix} \tag{4.9.4}$$

$$u_{vec} = [u] \tag{4.9.5}$$

$$F = \begin{bmatrix} 0 & 1 & 0 & 0 \\ 0 & -1 & 1 & 1 \\ p_1 & -10 & -10 & 0 \\ 0 & 0 & 0 & -1 \end{bmatrix} \tag{4.9.6}$$

$$G = \begin{bmatrix} 0 \\ 0 \\ 0 \\ 1 \end{bmatrix}$$

The performance index J has the form

$$J = \text{trace } CX \tag{4.9.7}$$

where

$$C = \begin{bmatrix} c_1 & c & 0 & 0 \\ c & 0 & 0 & 0 \\ 0 & 0 & 1 & 0 \\ 0 & 0 & 0 & 0 \end{bmatrix} \tag{4.9.8}$$

$$X = \begin{bmatrix} x_{11} & x_{12} & x_{13} & x_{14} \\ x_{21} & x_{22} & x_{23} & x_{24} \\ x_{31} & x_{32} & x_{33} & x_{34} \\ x_{41} & x_{42} & x_{43} & x_{44} \end{bmatrix} \tag{4.9.9}$$

The computations are initiated with a set of parameter values which result in an asymptotically stable solution. Initial solution stability is mandatory if the solutions for X and P are to exist. The initial value for p_1 was

$$p_1 = -3.0 \tag{4.9.10}$$

The initial position, velocity, and effector response to a white noise disturbance are shown in fig. 4-9-2. The optimal parameter value was

$$p_1 = -13.87 \tag{4.9.11}$$

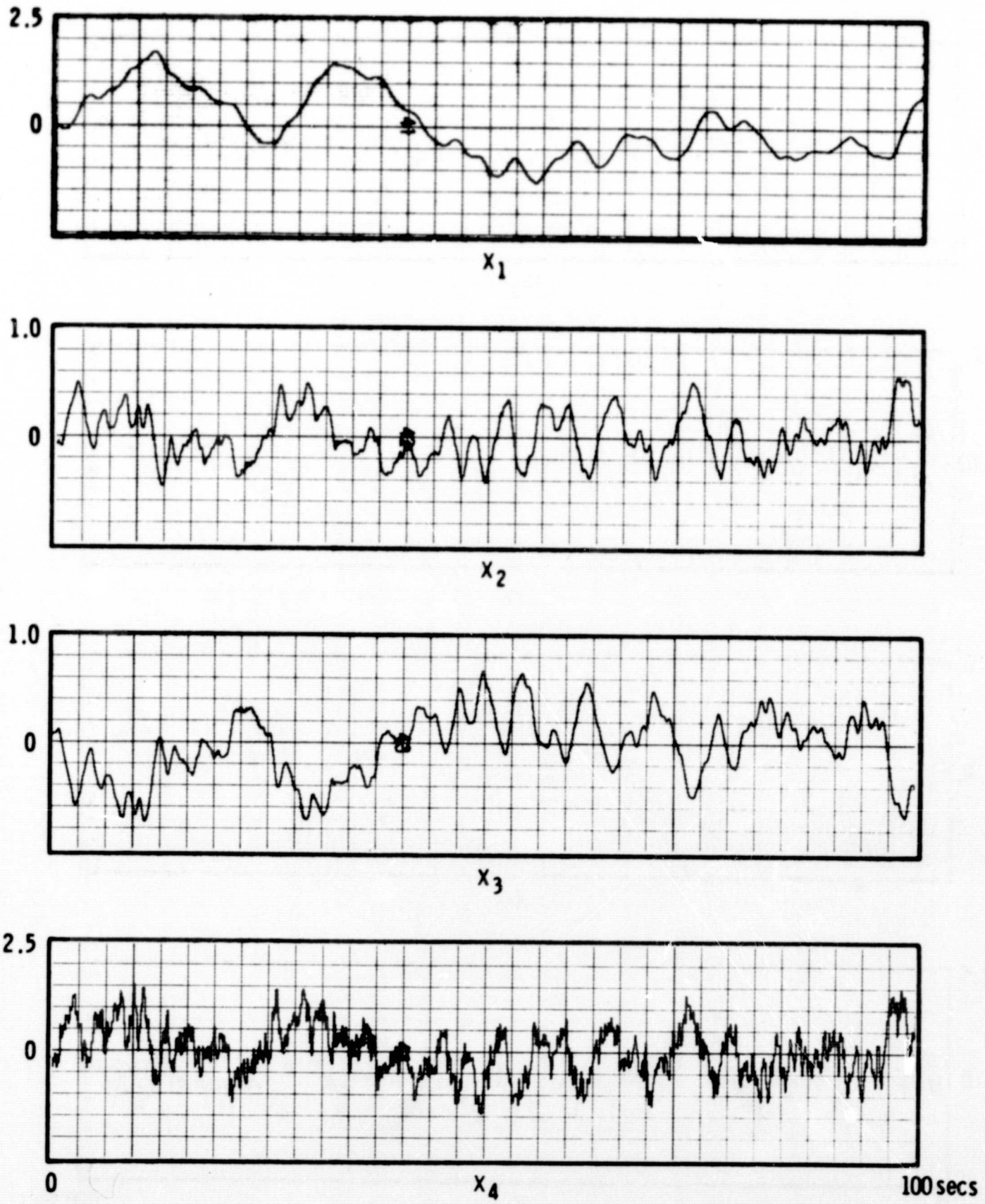


Fig. 4-9-2 Inertial system response to white noise. (p_1= -3.0)

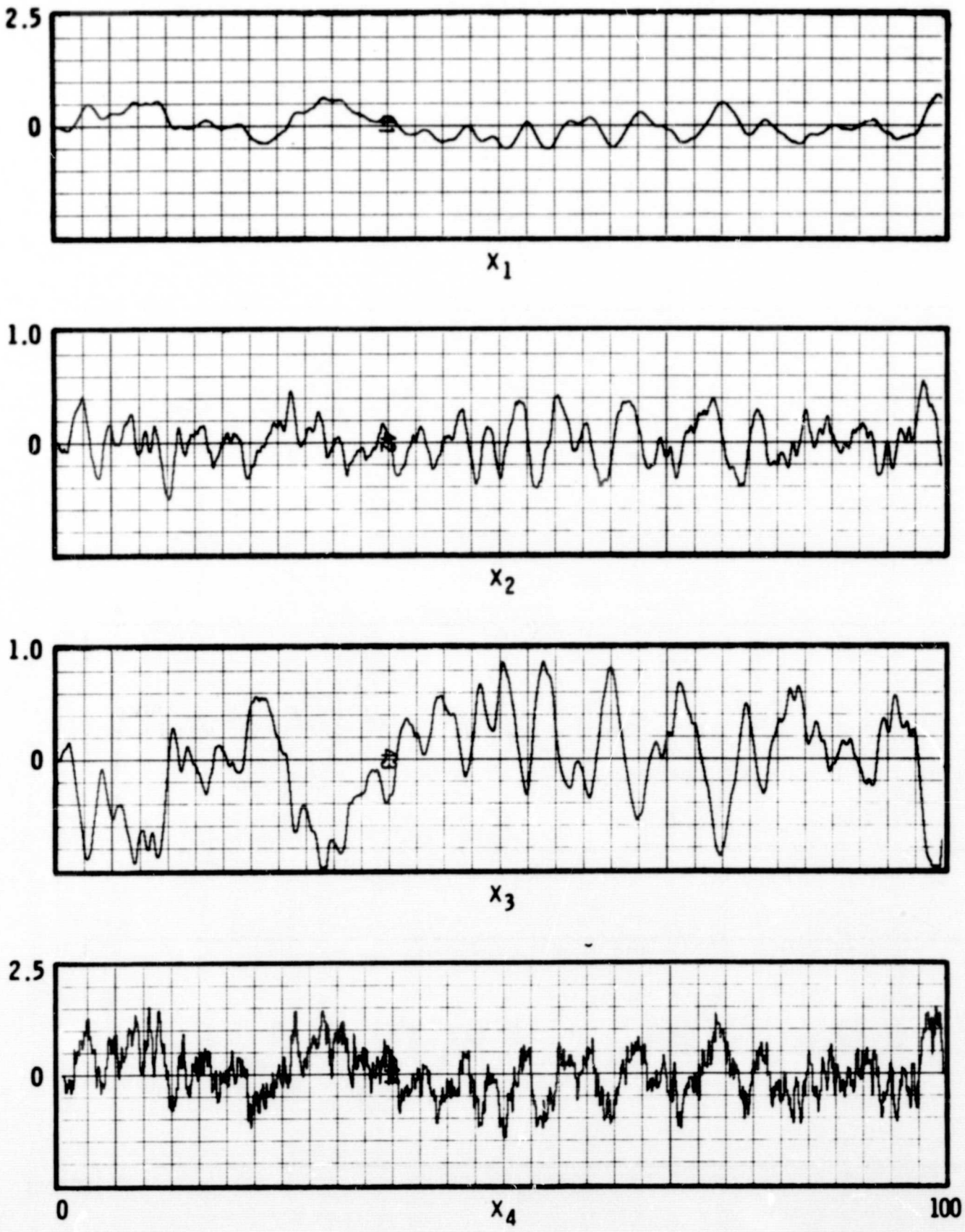


Fig. 4-9-3 Optimized system response to white noise. (p_1= −13.87)

Table 4-9.1

Initial and optimal mean square values.

	INITIAL SOLUTION	OPTIMAL SOLUTION
x_1	0.766	0.129
x_2	0.0805	0.0652
x_3	0.148	0.311
x_4	0.500	0.500

The corresponding responses for the optimal system are shown in fig. 4-9-3. The mean square values of the initial and optimal solutions is shown in table 4-9. 1.

The convergence characteristics of the various optimization algorithms may be compared by plotting J and the length of the gradient vector, $|J_p|$, and p_1 as a function of the iteration number NIC. These characteristics are illustrated in figs. 4-9-4, 4-9-5, and 4-9-6. The initial value of the step size control variable ϵ was 2.0. Computation was terminated at the end of 10 iterations.

Some conclusions may be drawn from these results:

1. The Steepest Descent and Average Gradient algorithms appear to converge rapidly when p is some distance from p_{opt} (J_p large). Convergence near the optimum value is very slow. (J_p small).
2. The quadratic convergence algorithms, Newton Raphson, Conjugate Gradient, Davidon, and Powell converge very quickly when p is near p_{opt} and if the problem is quadratic in p. However more care must be taken in their application to insure solution stability.

4.10 Selection of the Optimization Algorithm

The control scientist must select an algorithm from the preceeding array to solve the problem at hand. The choice is usually determined by considerations such as:

1. Convergence rate
2. Numerical errors
3. Computation time

Initial optimization from a suboptimal starting solution is efficiently carried out using the Steepest Descent* or Average Gradient* algorithms which display a high rate of convergence when p is some distance from the optimum value. As the optimum is approached, the slow convergence of Steepest Descent and Average Gradient algorithms weighs heavily in favor of algorithms such as Newton Raphson, Conjugate Gradient, Davidon, and Powell which display high rates of convergence where p is in the vicinity of p_{opt} justifying the increase in computation time per iteration. Numerical problems often preclude the application of the Generalized Newton Raphson technique as a result of errors arising in the estimation and inversion of the matrix J_{pp}.

---

*Considerable success has been achieved using accelerated versions of Steepest Descent and Average Gradient. (i.e. with algorithms which increase ϵ).

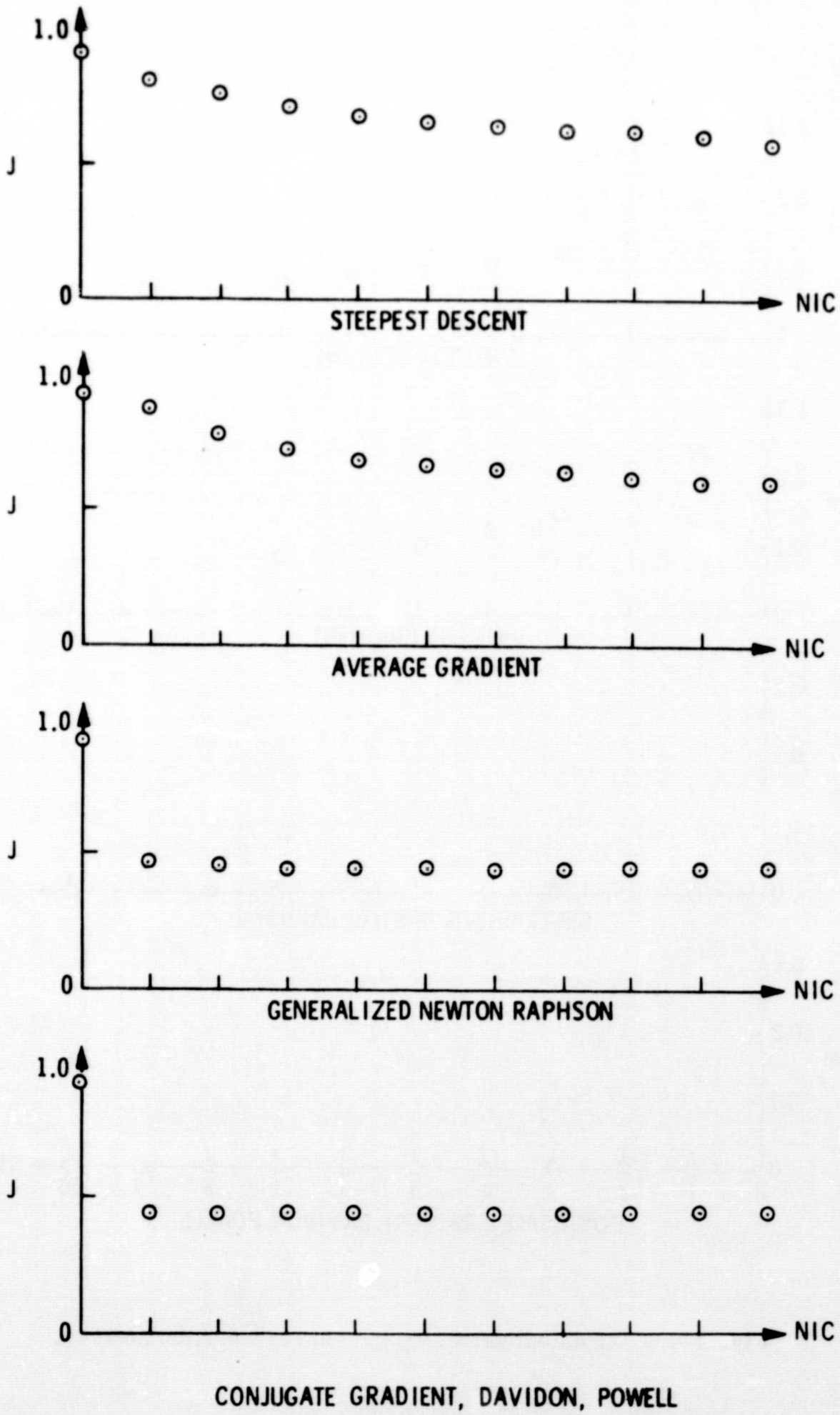


Fig. 4-9-4 Performance index versus iteration number.

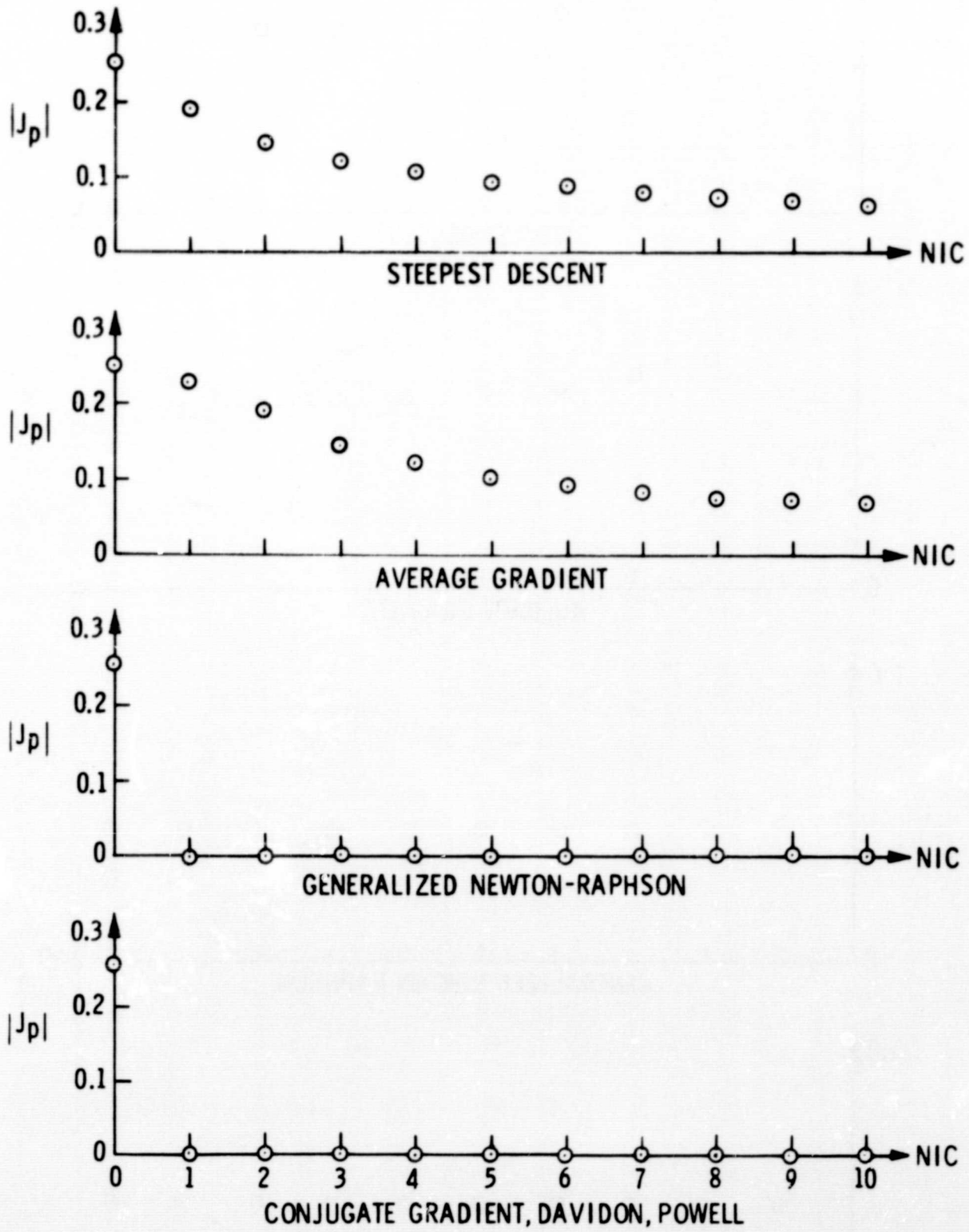


Fig. 4-9-5 Gradient vector length versus iteration number.

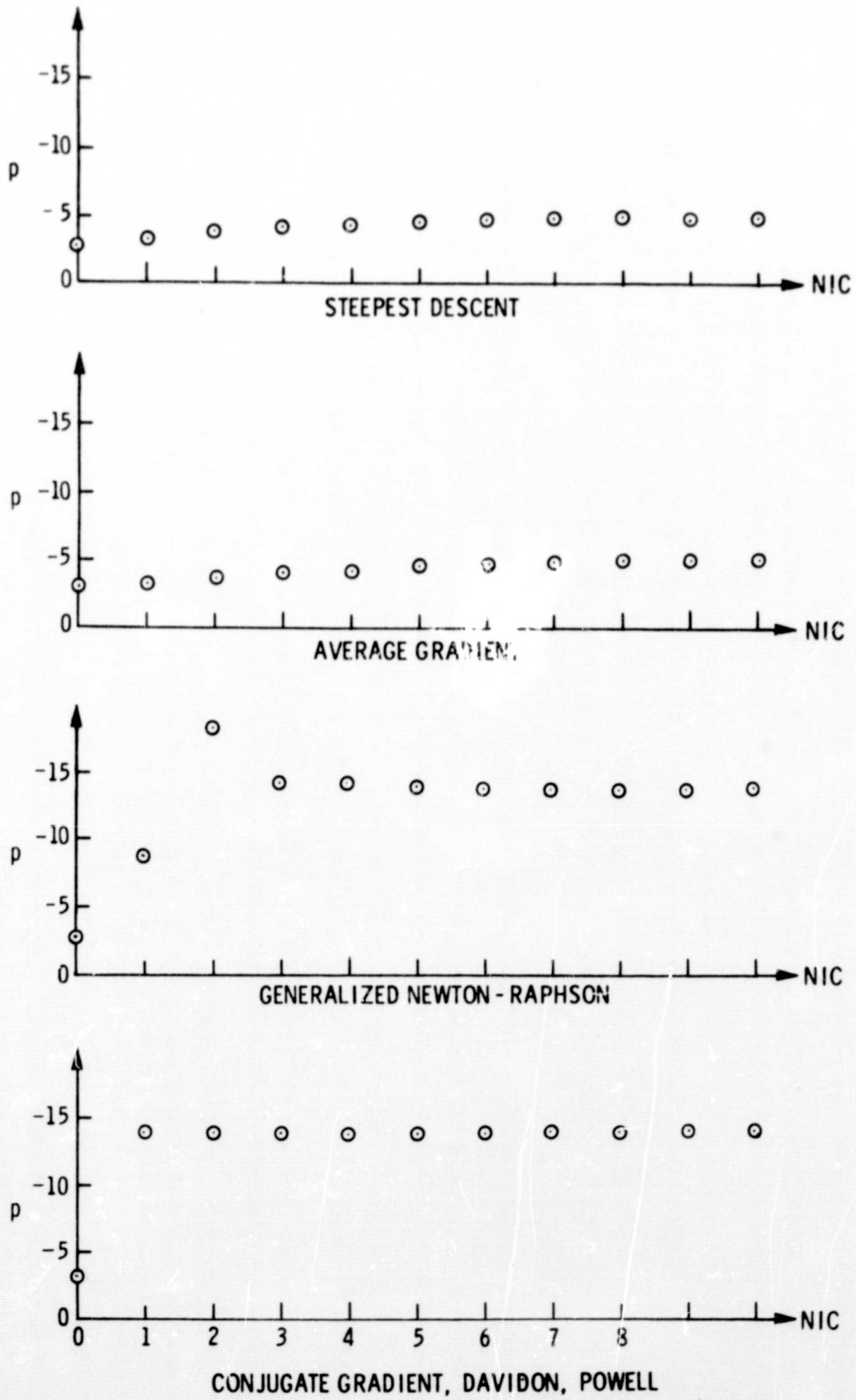


Fig. 4-9-6 Parameter value versus iteration number. (p_{opt} = 13.87)

PRECEDING PAGE BLANK NOT FILMED.

CHAPTER 5

OPTIMIZATION OF A VERTICAL POSITION CONTROL SYSTEM FOR AUTOMATIC LANDINGS

5.1 Introduction

Automatic landing system design may be dichotomized into vertical and lateral trajectory control components. Path control system design, from a classical point of view, has been dealt with in some detail in the preceeding two reports in this series (4, 5) . In this chapter, parameter optimization techniques are applied to the synthesis of a vertical path controller for the FAA Convair 880* vehicle. Control systems using elevators and elevators with direct lift spoilers are considered.

5.2 Vertical Trajectory Control

The vertical velocity, $\dot{z}$, of an aerodynamic vehicle is related to the path velocity v_p, the angle of attack α and the pitch angle θ by the equation

$$\dot{z} \approx v_p \, [\alpha - \theta] \qquad (5.2.1)$$

for small angles as shown in fig 5-1-1. The $\dot{z}$ may be modified by changing any combination of the variables α, θ, and v_p. In conventional systems the velocity v_p is normally held constant by the airspeed control system or autothrottle. The vertical control variables are thus θ and α.

The conventional method of achieving trajectory control utilizes the aircraft elevators (21, 22). The elevators produce a pitching moment about the y body axis. Control of θ is achieved by varying the pitching moment produced by the elevators. In order to satisfy the equation of static equilibrium, the aircraft weight W must balance the vertical component of lift L in the steady state.

$$L \cos [\theta - \alpha] = W \qquad (5.2.2)$$

Thus a change in α is required if θ is changed. Since the airspeed v_p is constant,

*The Convair 880 is a 4 jet commercial transport similar to the Boeing 707 in configuration.

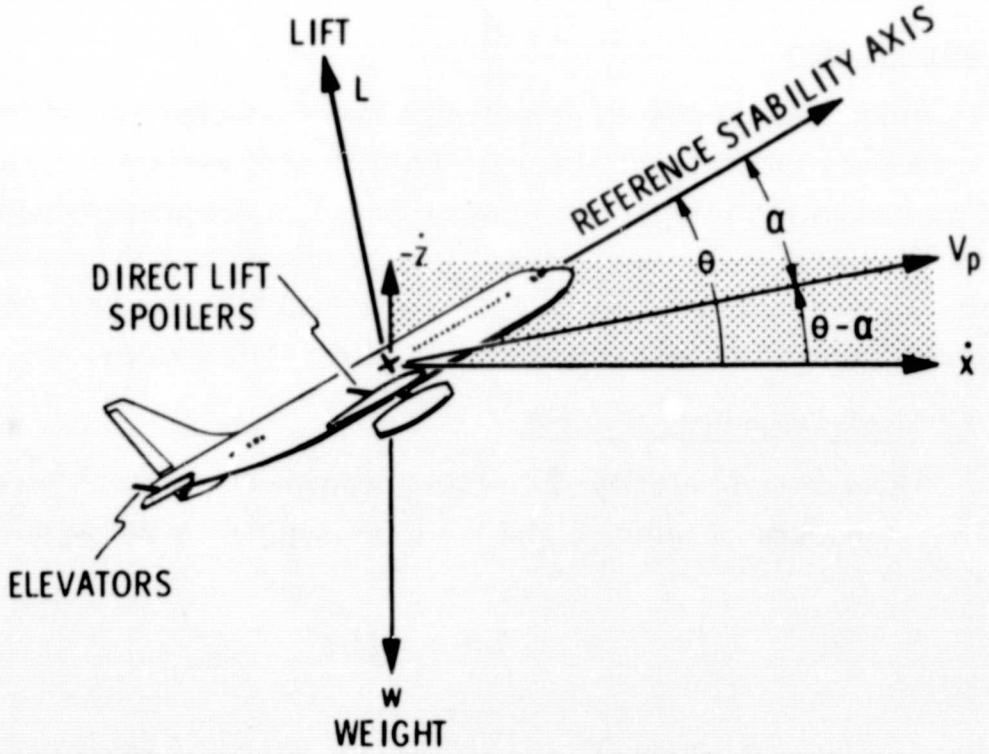


Fig. 5-1-1 Velocity relationships.

the change in lift is produced by a change in the angle of attack, α. The change is approximately proportional to the pitch perturbation

$$\alpha = K_{\alpha\theta}(\theta) \tag{5.2.3}$$

where $K_{\alpha\theta}$ is a positive constant less than unity in magnitude. Combining (5.2.3) and (5.2.1) gives

$$\dot{z} \approx v_p[K_{\alpha\theta}-1]\theta \tag{5.2.4}$$

Since $|K_{\alpha\theta}| < 1$, the steady state change in vertical velocity is proportional to the negative value of θ.

Another useful effector for vertical trajectory control is the direct lift spoiler (19, 20). A spoiler is generally a plate hinged at its leading edge to the top surface of the wing. When retracted the spoiler is flush with the normal surface of the wing and has no effect. When extended the spoiler disturbs the airflow over the wing reducing the coefficient of lift. Since v_p is constant, the lift is also reduced. This reduction in lift is countered by an increase in angle of attack which is roughly proportional to the spoiler deflection δ_s

$$\alpha = K_{\alpha\delta_s}\delta_s \tag{5.2.5}$$

Since the spoiler, correctly placed, produces very little pitching moment. θ remains essentially unchanged; and since v_p is constant, the change in angle of attack must produce a change in $\dot{z}$. Assuming $\theta = 0$ the static relationship for $\dot{z}$ becomes

$$\dot{z} = v_p K_{\alpha\delta_s}\delta_s \tag{5.2.6}$$

In a control system the average deflection of the direct lift spoilers is maintained at a fraction of the maximum spoiler range to permit positive and negative corrections in vertical velocity.

The range of θ is approximatily ± 6.0 degrees in the approach and landing phases; thus pitch angle control can produce rather large changes in vertical velocity as opposed to the rather small changes which can be achieved by CV880 direct lift mode spoiler actuation. Direct lift spoilers do offer the advantage of fast response. Thus

a vertical position control system using direct lift spoilers can cope more effectively with high frequency components in the stochastic environment. Direct lift spoilers also put the correcting force where the disturbance acts, thereby reducing structural loads.

It seems reasonable to attempt to combine the desirable properties of pitch angle and direct lift spoiler control by using pitch attitude to effect gross changes in trajectory while the direct lift spoilers are used to counter high frequency environmental disturbances. This goal may be achieved by using a control law which operates on z, $\dot{z}$, $\ddot{z}$, and θ to produce elevator and spoiler commands simultaneously. The spoiler command is then passed through a high pass filter which removes the low frequency components which characterize gross changes in vertical path.

5.3 Vertical Trajectory Control System Structure

The control laws for the elevator and direct lift spoiler inputs were assumed to be of fixed structure. The structure does not necessarily represent the configuration of the final control system but indicates how a structurally similar conventional system may be improved by the addition of direct lift spoilers and parameter optimization. The elevator servo command $\delta_e^{(sc)}$ is of the form

$$\delta_e^{(sc)} = p_1 z + p_2 \dot{z} + p_3 \ddot{z} + p_4 q \tag{5.3.1}$$

The high pass spoiler command filter is assumed to have the form

$$\frac{j\omega}{j\omega + \omega_f} \tag{5.3.2}$$

where ω_f is a constant. If ω_f is sufficiently small (less than 0.1 rad/s), the filter will have negligible effect on the response of the system to stochastic disturbances and may be omitted from the analysis for the moment. The direct lift spoiler servo input is

$$\delta_s^{(sc)} = p_5 z + p_6 \dot{z} + p_7 \ddot{z} \tag{5.3.3}$$

z, $\dot{z}$, and $\ddot{z}$ are perturbations in vertical position, velocity, and acceleration. The pitch rate, q, does not appear in (5.3.3) because the spoilers are assumed to produce a very small pitching moment on the vehicle.

A block diagram of the vertical trajectory control system is shown in fig. 5-3-1. The hybrid navigation system is discussed in Chapter 2. The pitch

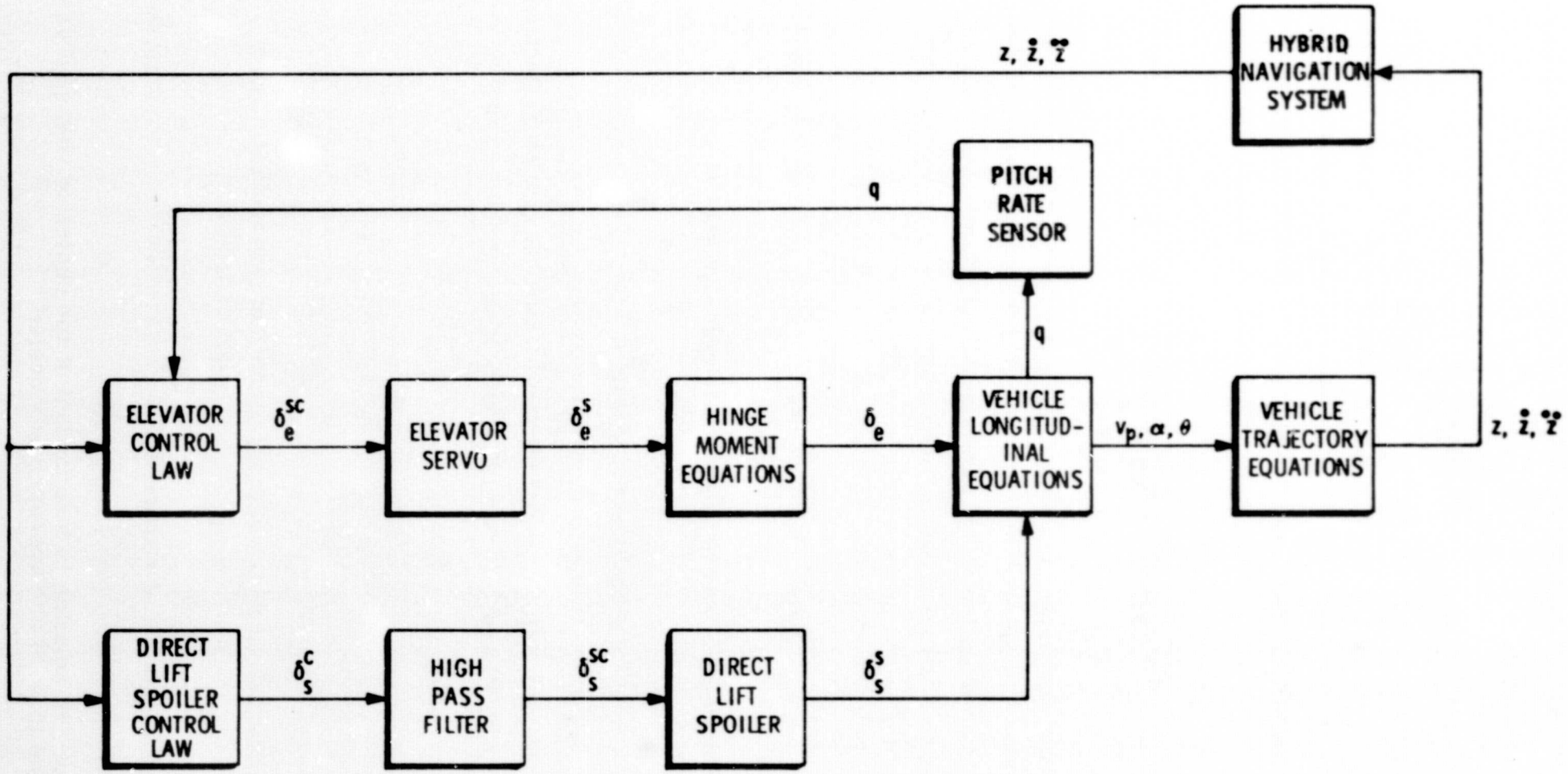


Fig. 5-3-1 Vertical position control system model.

rate sensor is normally a body-mounted rate gyro. The other blocks in the diagram are discussed in detail in Appendix A.

5.4 Optimizing the Vertical Position Control System

Two cases were considered: in the first, vertical control was provided entirely by the elevators ($p_5=p_6=p_7=0$); in the second, elevator control was augmented by the direct lift spoilers. The performance index was selected to minimize vertical path deviations subject to penalties on the mean-square elevator and spoiler servo deflections.

$$J = c_{33}E\left(z^2\right) + c_{66}E\left(\delta e_e^{s2}\right) + c_{77}E\left(\delta_e^{s2}\right) \qquad (5.4.1)$$

The parameter c_{33} was held constant. c_{66} and c_{77} were adjusted to vary the mean square values of the elevator and spoiler deflections. At the outset it was decided to use the mean-square elevator deflection of the original suboptimal Lear design as a design limit. Assuming that the root mean-square gust velocity is 0.49 ft/sec* the mean-square elevator deflection of the reference system is

$$E\left(\delta_e^{(s)2}\right) \approx 0.078 \text{ deg}^2 \qquad (5.4.2)$$

The mean-square spoiler deflection was constrained to a design goal of

$$E\left(\delta_S^{(s)2}\right) \approx 0.089 \text{ deg}^2 \qquad (5.4.3)$$

which reflects the behavior of the elevator and physical limits on spoiler deflection. As a result of the limits in (5.4.2) and (5.4.3) the optimization problem may be restated.

Problem:

Find a set of parameters p_{opt} which minimize the performance index

$$J = \text{trace } CX \qquad (5.4.4)$$

---

*Since the model is linear the solution is independent of the choice of rms gust velocity provided (5.4.2) and (5.4.3) are appropriately scaled.

subject to the constraints

$$FX + XF' + GQG' = 0 \tag{5.4.5}$$

and

$$|X| < L \tag{5.4.6}$$

where L is a matrix of limits.* The other terms are defined in Section 3.4.

The constraint set can be satisfied by the introduction of a term in the performance index which penalizes violation of the constraint limit or the introduction of an additional Lagrange multiplier and slack variables. Currently constraints are satisfied by adjusting the elements of the performance index matrix C.

The results of optimization are summarized in tables 5-4.1, 5-4.2, and 5-4.3. The initial parameter values correspond to the gains associated with the initial track mode of an experimental Lear Autoland System.

Table 5-4.1 illustrates the performance index coefficients and the initial and final parameter values, values of J and J_p are shown in table 5-4.2. The performance index J and gradient J_p vary as a result of changes in the performance index coefficients and the control system configuration.

The performance of the the optimization algorithm may be inferred from the reduction in J and the relative sizes of the initial and final values of J_p. The mean square values associated with the state x are summarized in table 5-4.3.

The response characteristics of the reference and optimized vertical postion control systems to the reference stochastic disturbance are shown in figs. 5-4-1, 5-4-2, and 5-4-3. The reduction in the magnitude of z achieved by optimization is apparent.

---

*The notation $|X| < L$ signifies that each element of X must satisfy the inequality $x_{ij} < \ell_{ij}$ where x_{ij} and ℓ_{ij} are the ij th elements of x and ℓ respectively.

Table 5-4.1

Optimization algorithm data and optimized parameter values.

		Optimized vertical control system with elevators	Optimized vertical control system with elevators and spoilers
VERTICAL POSITION WEIGHING c_{33}		3.3	10.0
ELEVATOR WEIGHING c_{66}		1.0	1.0
SPOILER WEIGHTING c_{77}		—	1.28
INITIAL PARAMETER VALUES FROM REFERENCE SYSTEM	p_1	-0.286	-0.286
	p_2	-1.25	-1.25
	p_3	-0.80	-0.80
	p_4	1.0	1.0
	p_5	0	0
	p_6	0	0
	p_7	0	0
OPTIMIZED PARAMETER VALUES	p_1	-0.08	0.176
	p_2	-7.5	-9.38
	p_3	-1.15	-1.20
	p_4	15.3	14.18
	p_5	0	-1.60
	p_6	0	-1.68
	p_7	0	-1.00

Table 5-4. 2

Optimization algorithm performance.

	Optimized Vertical Control system with elevators	Optimized vertical control system with elevators and spoilers
Initial value of J	0. 327	0. 830
Final value of J	0. 263	0. 372
$\frac{J \text{ initial}}{J \text{ final}}$	0. 804	0. 449
Initial value of $\lvert J_p \rvert^*$	0. 278	0. 940
Final value of $\lvert J_p \rvert$	≈0. 002	≈0. 002
$\frac{\lvert J_p \rvert \text{initial}}{\lvert J_p \rvert \text{final}}$	140.	470.

* $J_p = \left[J_p' J_p\right]^{\frac{1}{2}}$

Table 5-4. 3

Control system performance.

	Reference vertical control system	Optimized vertical control system with elevators	Optimized vertical control system with elevators and spoilers
$E(z^2)$ ft^2	0. 075	0. 056	0. 018
$E(\dot{z}^2)$ $(ft/s)^2$	0. 049	0. 040	0. 0168
$E(\ddot{z}^2)$ $(ft/s^2)^2$	0. 111	0. 103	0. 0566
$E(\theta^2)$ deg^2	0. 0115	0. 0102	0. 0067
$E(q^2)$ $(deg/s)^2$	0. 0092	0. 0086	0. 0063
$E(e^{\delta 2})$ deg^2	0. 078	0. 078	0. 078
$E(s^{\delta 2})$ deg^2	-----	-----	0. 089
$E(\alpha_n^2)$ deg^2	0. 010	0. 010	0. 010
$\frac{E(z^2)_{reference}}{E(z^2)_{final}}$	1. 0	0. 747	0. 240

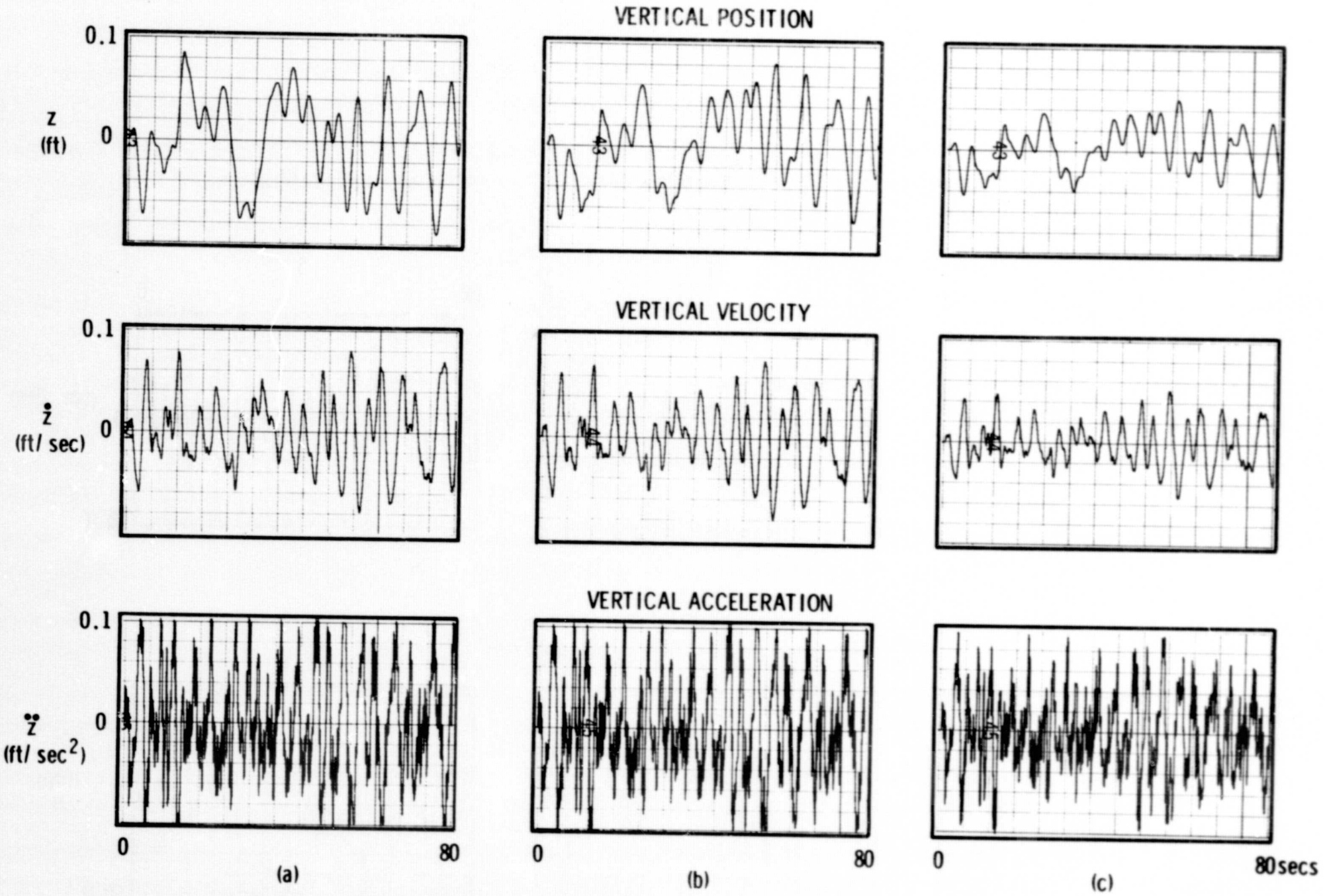


Fig. 5-4-1 Responses of reference system (a), optimized reference system (b) and optimized reference system with spoilers (c).

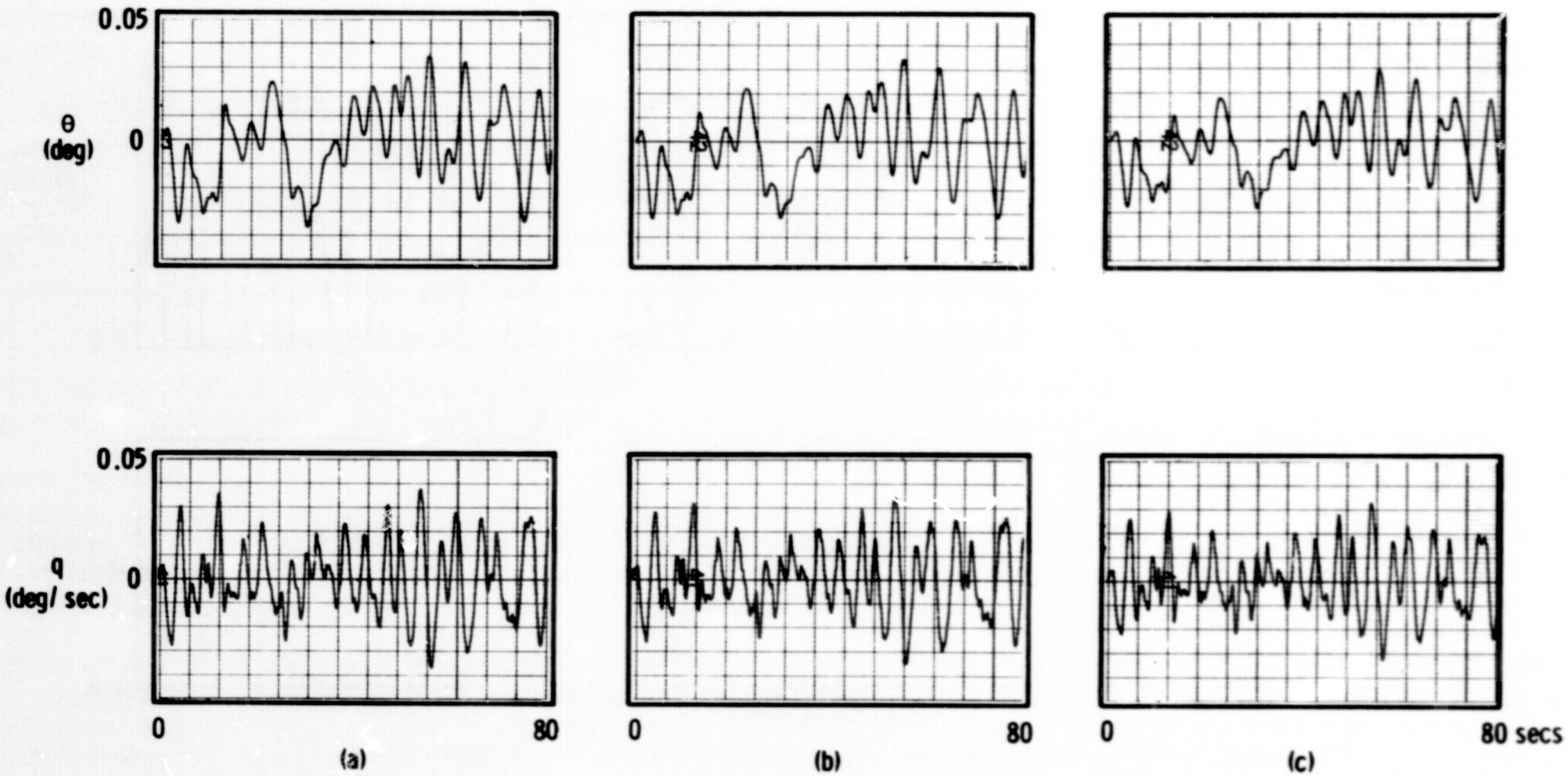


Fig. 5-4-2 Responses of reference system (a), optimized reference system (b) and optimized reference system with spoilers (c).

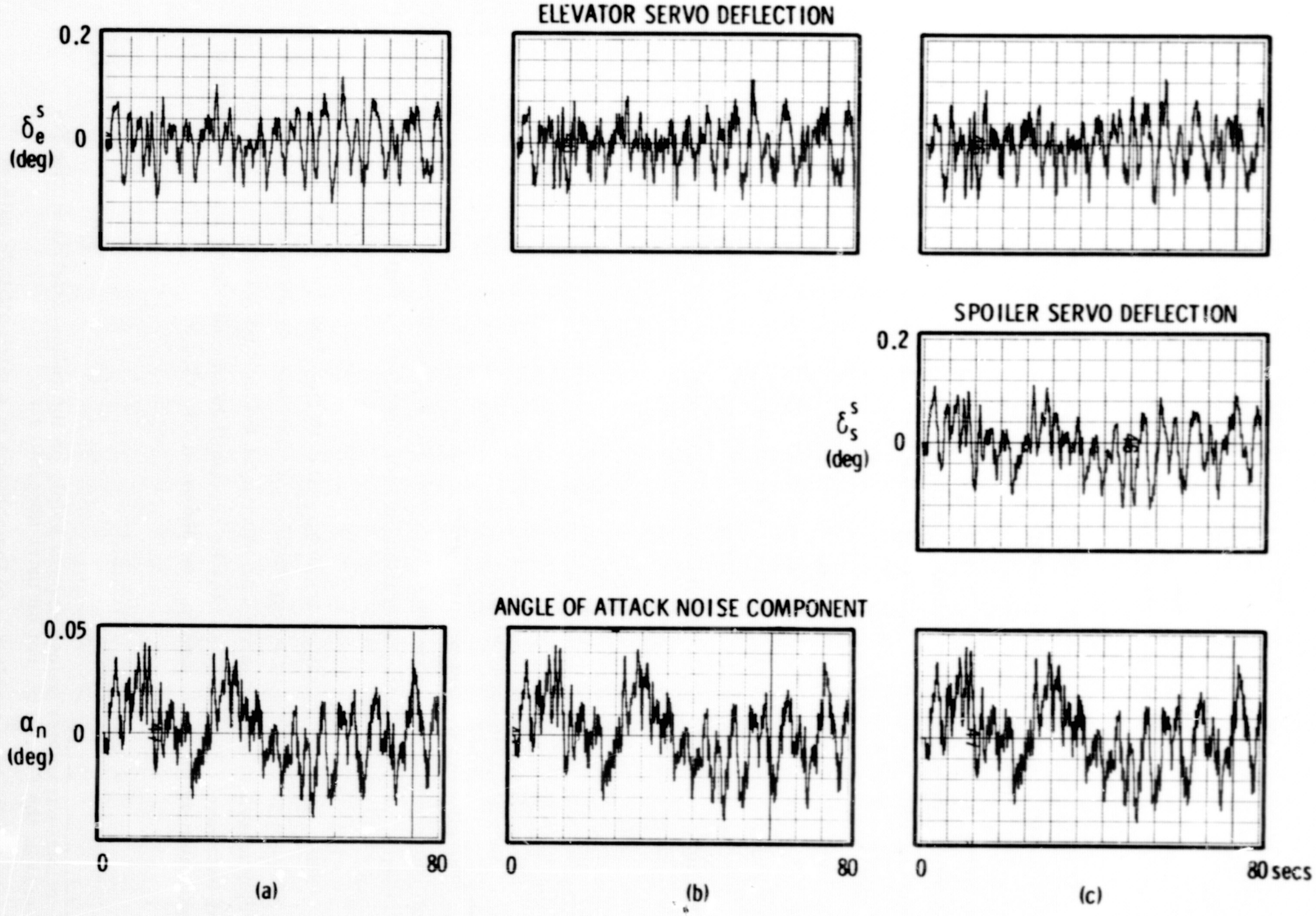


Fig. 5-4-3 Responses of reference system (a), optimized reference system (b) and optimized reference system with spoilers (c).

The effect of varying the ratio* between vertical position weight C_{33} and elevator weight C_{66} without spoilers is delineated in figures 5-4-4 and 5-4-5. The effect of varying spoiler weight in a vertical control system augmented by spoilers is illustrated in figures 5-4-6 and 5-4-7. Figures 5-4-4 to 5-4-7 provide a basis for the investigation of the effects of control system specification changes such as the value of $E(\delta_e^2)$ for example.

The transient response characteristics of the systems described in Tables 5-4.1, 5-4.2, and 5-4.3 to an initial error in vertical position are shown in figs. 5-4-8 and 5-4-9. The relatively slow response characteristics of the optimized control systems are a result of the low position gains, p_2 and p_5, and the greatly increased pitch rate and velocity gains, p_4 and p_2. The small decrease in $E(z^2)$ obtained by optimizing the elevator-based control system shows the inherent limitations of the system.

The addition of spoilers results in a rather dramatic improvement in performance. However, the present spoiler configuration in (5.3.3) results in an undesirable pitch attitude reversal in response to an error in vertical position**. This problem is being counteracted by applying spoiler-elevator feedforward compensation to eliminate the spoiler-pitch coupling and a new control configuration similar to the one used in R-628

$$\delta_s^{(sc)} = p_5 \delta_e^{(sc)} \qquad (5.4.7)$$

where p_5 is an adjustable parameter.

The effect of the low position gain on trajectory following accuracy should not be too important if reference trajectory velocity and acceleration are fed forward into the vertical velocity and acceleration control loops, and integral compensation is used in the position loop.

The correction of initial trajectory errors may take too long with the optimized position gain. This problem may be circumvented by increasing the position gain trading a loss in performance with stochastic disturbances for an improvement in transient response. The increase may be accomplished by adjoining a soft constraint on the minimum value of p_1 and p_5 as shown in ref. 11 .

---

* The optimal parameter values depend solely on the ratios existing among the elements of the C matrix, not on their absolute size.

** This peculairity is probably due to the absence of a pitch attitude gain in control law (5.3.1).

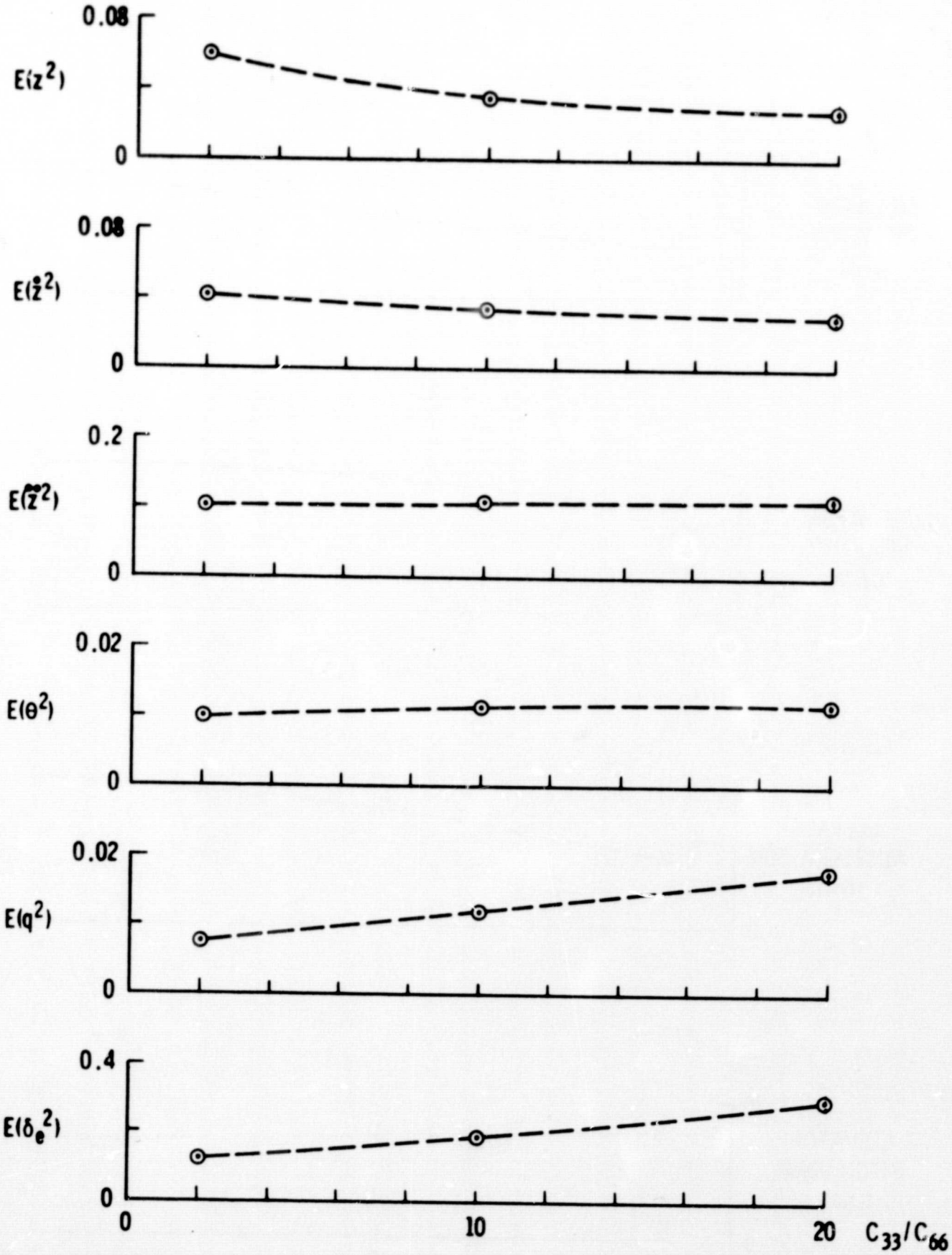


Fig. 5.4-4 Mean square values of optimal system state variables as a function of C_{33}/C_{66} where $J = C_{33}\, E(z^2) + C_{66}\, E(\delta_e{}^2)$.

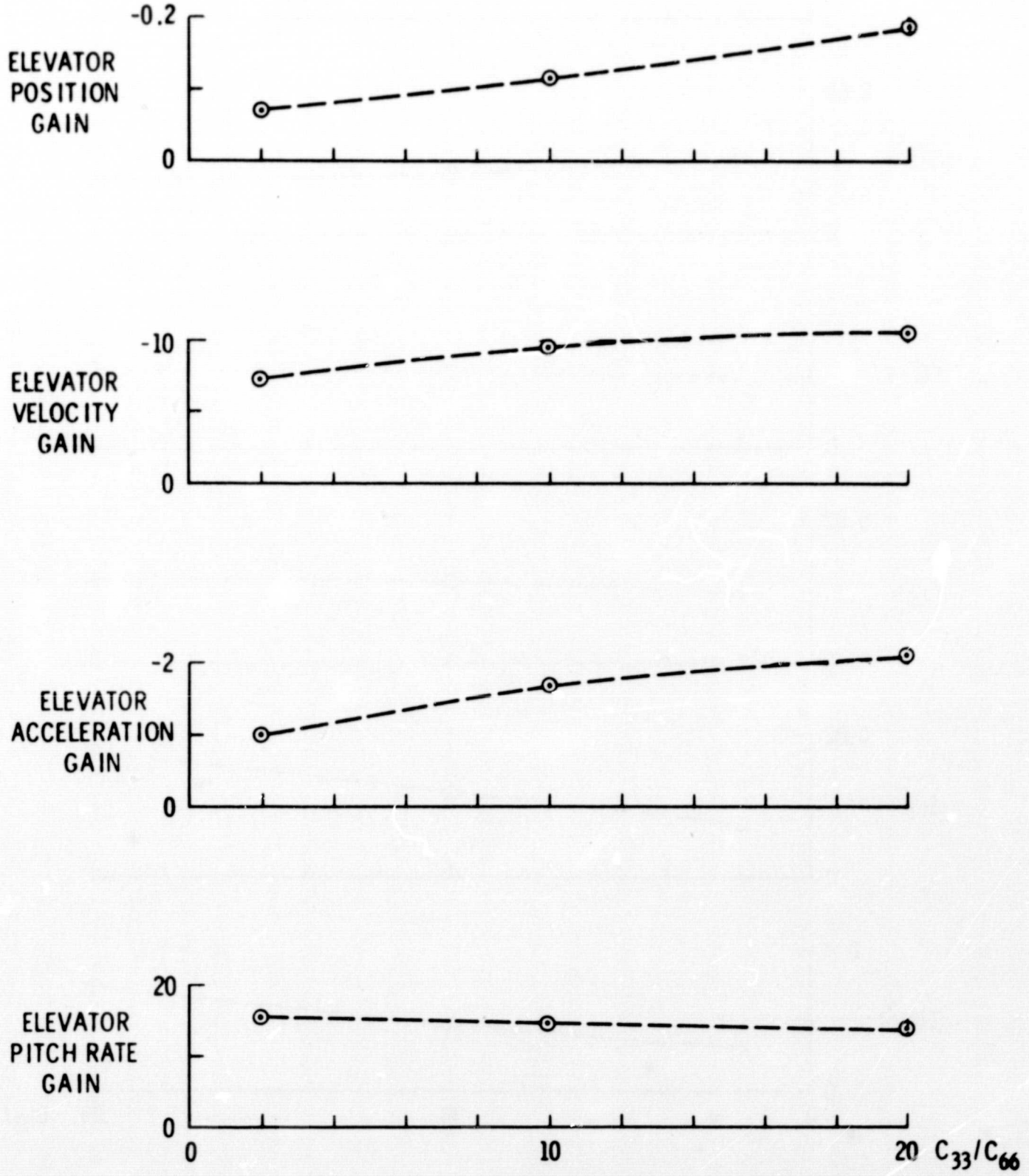
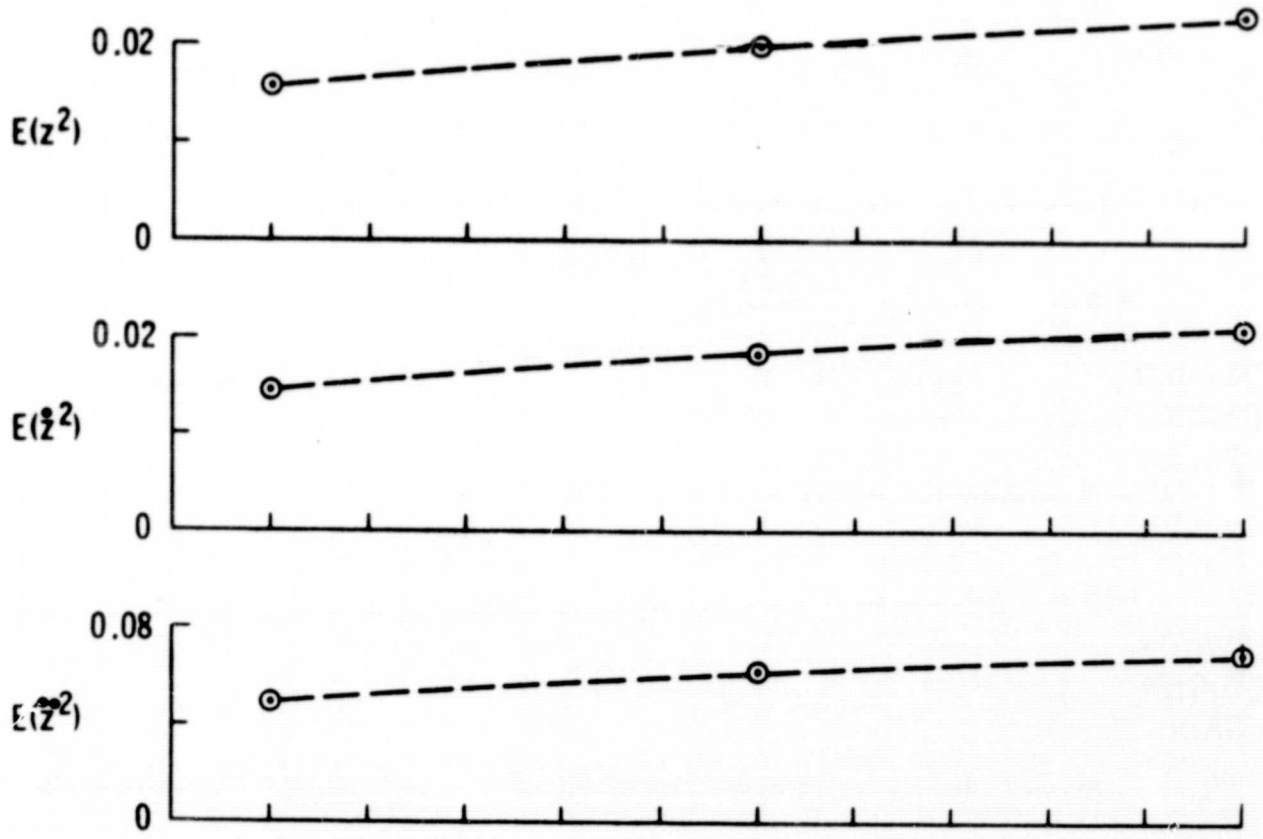


Fig. 5-4-5 Optimum parameter values as a function of C_{33} / C_{66} where $J = C_{33} E(z^2) + C_{66} E(\delta_e{}^2)$.



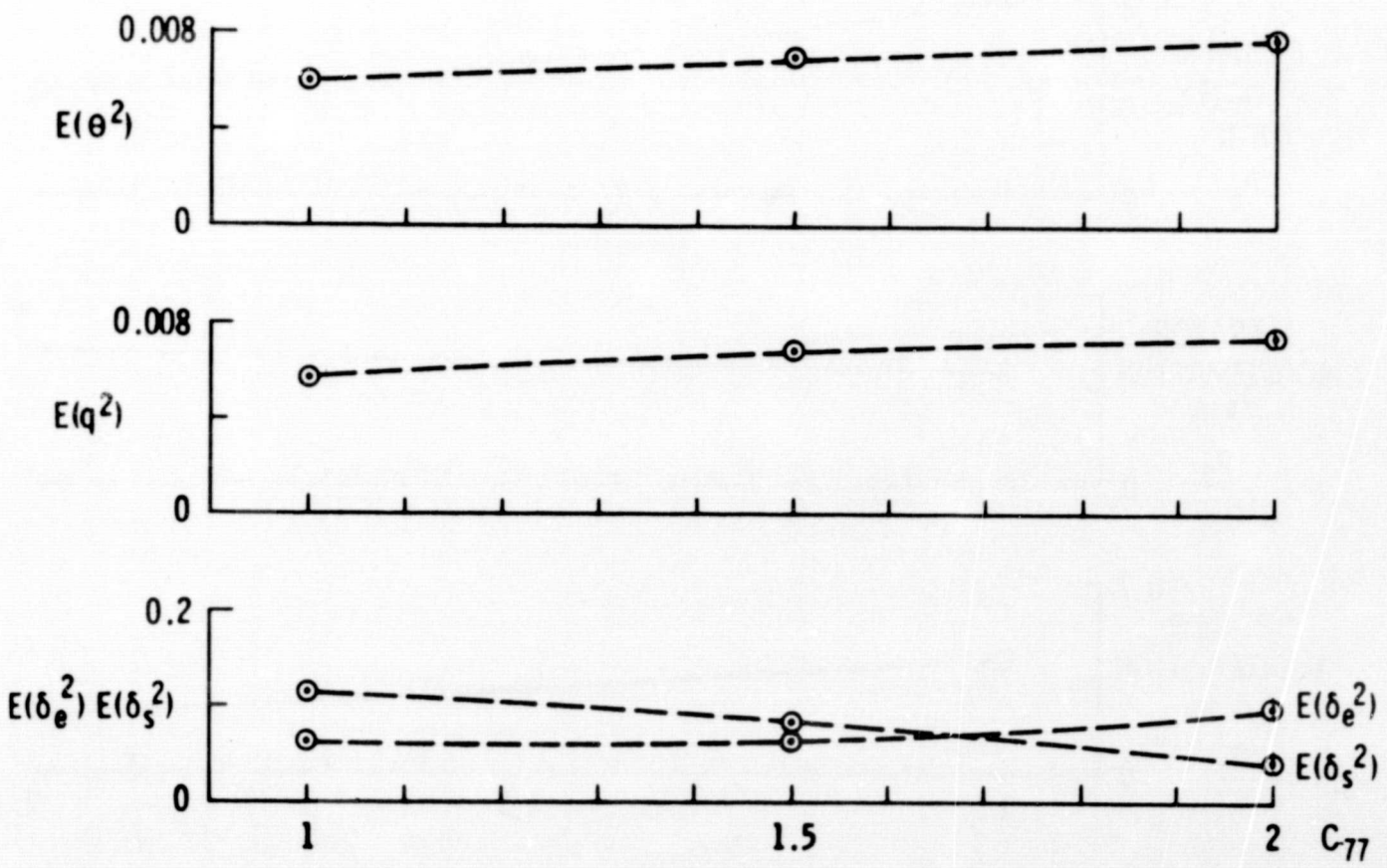


Fig. 5-4-6 Mean square values of optimal system state variables versus C_{77} where $J = 10\ E(z^2) + E(\delta_e^2) + C_{77}\ E(\delta_s^2)$.

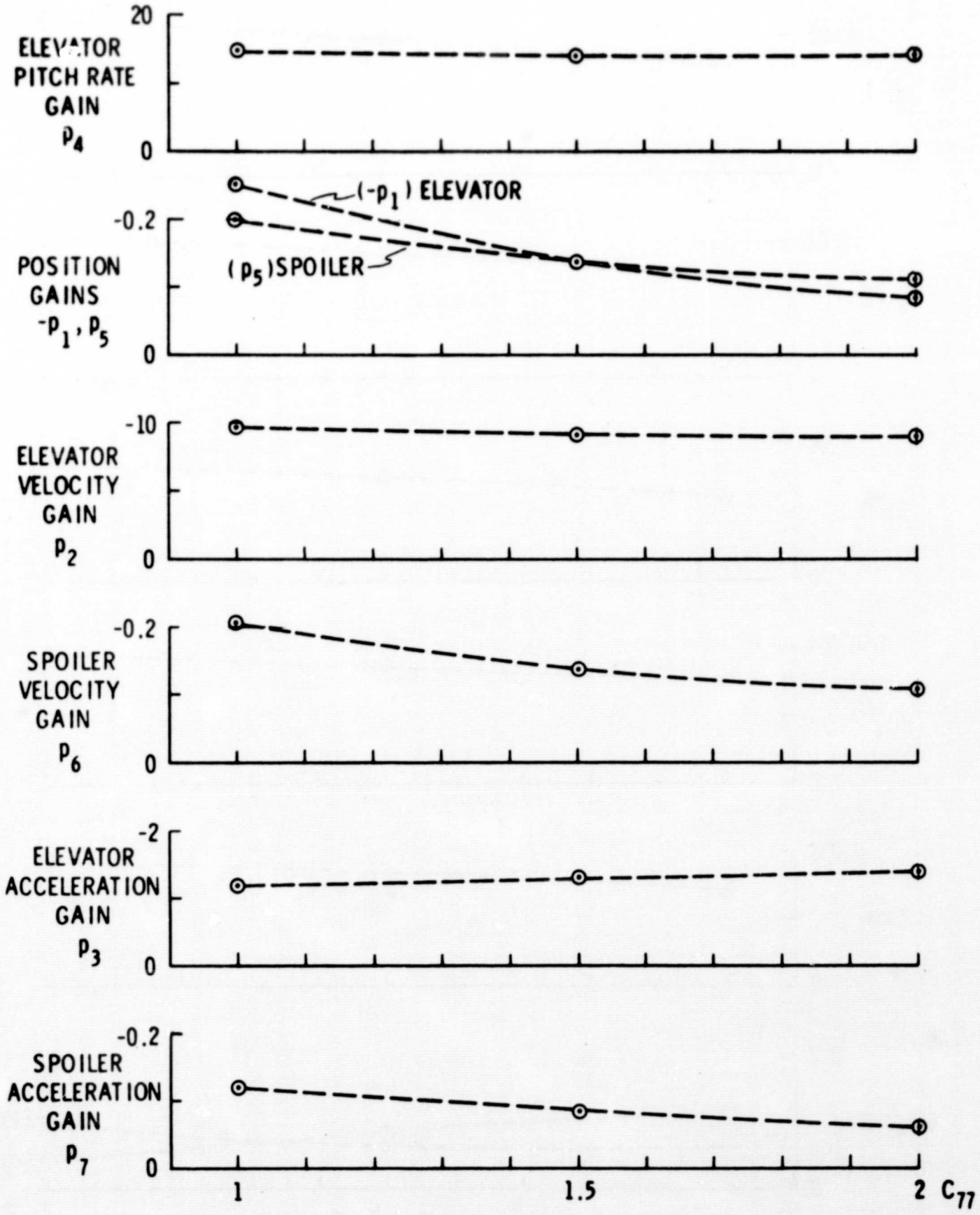


Fig. 5-4-7 Optimum parameter values as a function of C_{77} where $J=10\ E(z^2) + E(\delta_e{}^2) + C_{77}\ E(\delta_s{}^2)$.

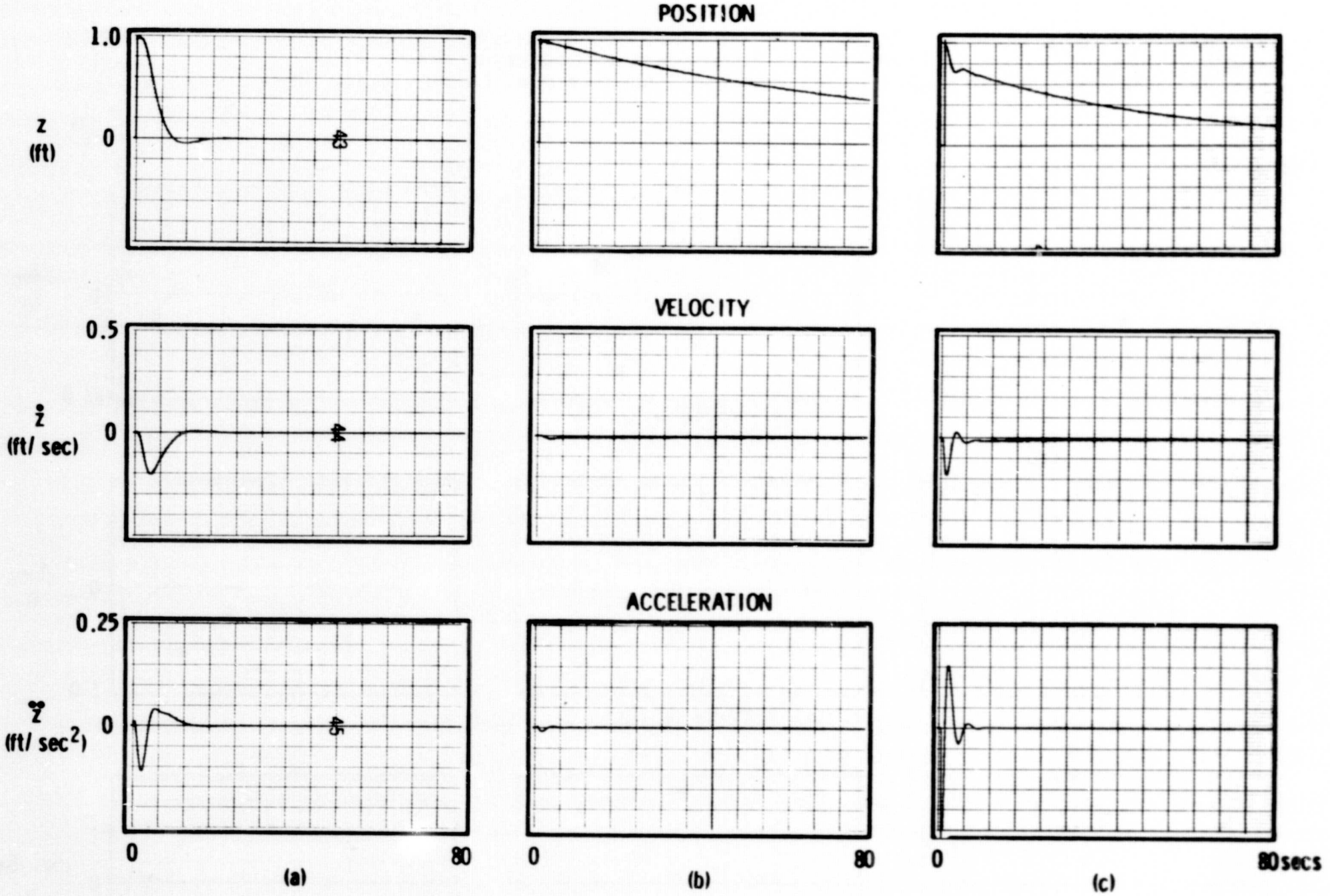


Fig. 5-4-8 Responses of reference system (a), optimized reference system (b) and optimized reference system with spoilers (c).

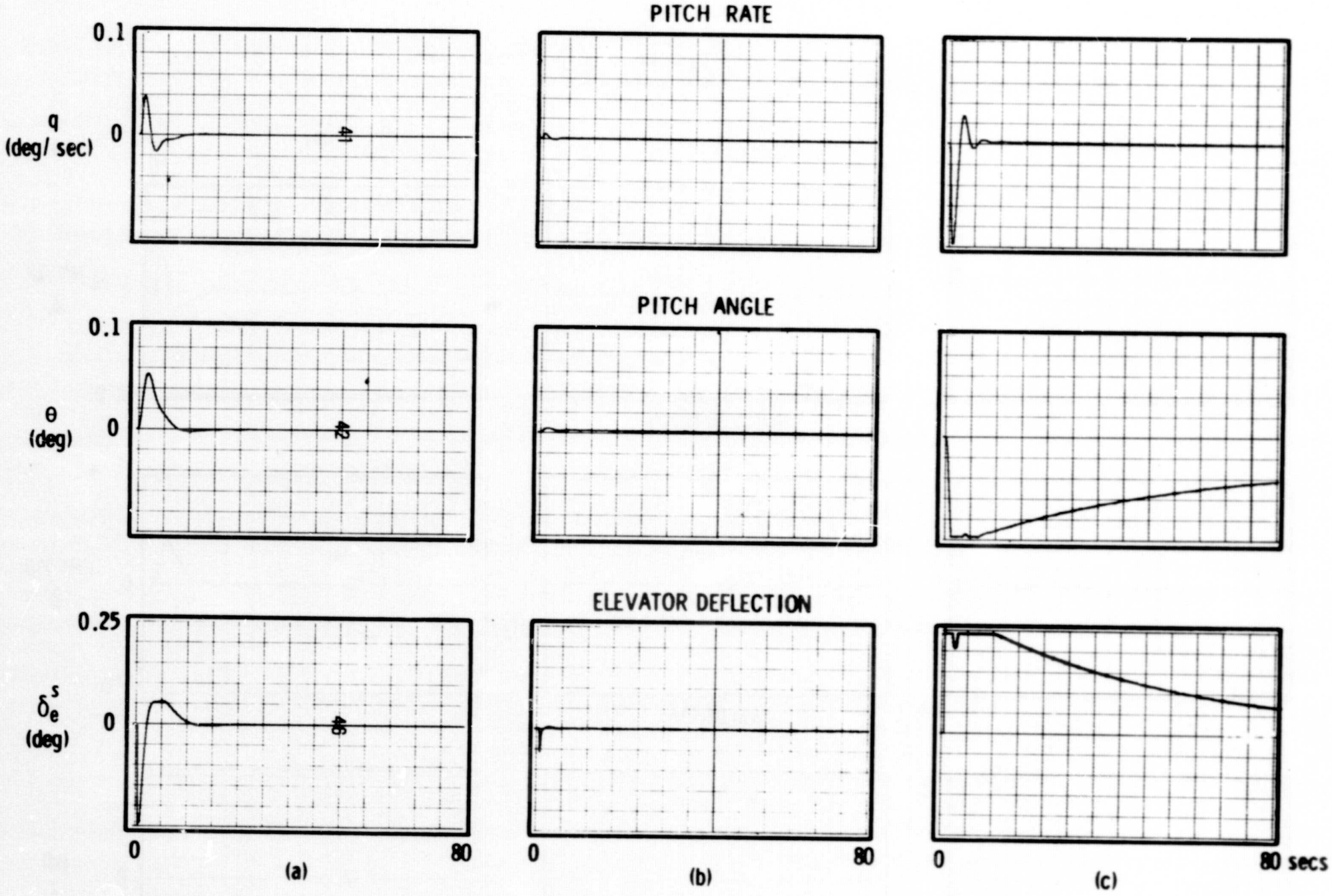


Fig. 5-4-9 Responses of reference system (a), optimized reference system (b) and optimized reference system with spoilers (c).

CHAPTER 6

SUMMARY CONCLUSIONS AND AREAS FOR FURTHER INVESTIGATION

The application of mathematical optimization theory to two aspects of the Automatic Landing Problem has been demonstrated.

Optimum estimation using radio aid and inertial measurements, when applied to integrated navigation system design, yielded relatively noise-free estimates of inertial navigator errors in position, velocity, and acceleration. The resulting errors could then be subtracted from the actual inertial system position, velocity, and acceleration outputs to yield relatively noise-free estimates of true position, velocity, and acceleration.

Two different estimation procedures were used. The Kalman-Bucy Estimator provided information which was superior in a mean square error sense; however, it was less effective in supressing high frequency components of radio aid noise than the Minimum ISE filter. The transient response characteristics of the sample minimum ISE estimator to inertial bias estimate errors was superior to the Kalman filter for initial errors in velocity and acceleration; however, errors in position, which will typically be the greatest, result in large transients in the case of the minimum ISE estimates. Computationally the Kalman-Bucy solution is far superior since no matrix inversion is required. The discrete versions of the estimator algorithms which would probably be used in a real system were mentioned briefly.

The improved position, velocity and acceleration data provided by the integrated navigation system is the foundation for an improved control system design. In this report a method is presented which systematically refines the trajectory precision of a vehicle control system subject to stochastic disturbances.

The necessary conditions for optimum stochastic control were developed and mathematical parameter optimization techniques were introduced to generate minima satisfying the necessary conditions.

Sufficient conditions were not delineated since such conditions are extremely hard to apply in practice, and do not contribute to the development of the optimization algorithms presented here.

Parameter optimization design techniques were then applied to the synthesis of a vertical position control system for the Convair 880 vehicle to establish feasibility. A control system relying on elevators as the main effector source was optimized. The approach was then extended to the optimization of a vertical control system configuration using direct-lift spoilers as well as elevator control. The performance of the reference and optimized control systems is summarized in Table 5-4.3.

While the above designs are incomplete since the vehicle model did not include the effects of elastic bending, control surface hinge moment equations and sensor noise, they do demonstrate the feasibility of applying parameter optimization to problems of the magnitude associated with aircraft trajectory control.

In addition to its value as a design tool, parameter optimization yields solutions which may be compared to those obtained using other configurations, if care is taken in the definition of the environment and the mean square values of the common actuator outputs.

Computation time is the main drawback of the parameter optimization techniques described in Chapters 4 and 5. While considerable time was saved by a judicious combination of numerical integration and state transition techniques computer runs with 8 state variables typically required 2-3 hours of SDS 9300 computer time to generate the solutions described in Chapter 5. This was not felt to be a serious problem since efficient programming permits the algorithm to be run on relatively small machines (less than 64 thousand bytes of memory). There is also a definite down trend in the relative cost of computer time per operation since computer speed is increasing and computer cost is falling.

The performance results tended to validate the general conclusions reached in R628 which stated that a significant improvement in vertical position control performance cannot be achieved unless direct lift control is utilized.

During the course of this project a number of interesting challenges arose which must be pursued in future phases of this work.

1. Apply parameter optimization to refine lateral and longitudinal flight path control system designs using a more sophisticated vehicle model incorporating hinge moment equations and airframe flexibility.

2. Study the feasibility of low power, noise abatement approaches using drag producing devices for airspeed control.

3. Utilize mathematical optimization techniques to generate optimal landing abort procedures and control systems.

4. Consider the problems associated with steep STOL and stepped approaches which may be realized with new terminal area navigation aids.

5. Consider trajectory control of a vehicle utilizing trajectory commands generated by a ground based computer which also observes the position of the vehicle.

6. Investigate the affect of sampling (due to the use of a digital computer as the main control system algorithmic component) on the performance of trajectory control systems.

7. Demonstrate the application of parameter optimization techniques to the synthesis of optimal digital controllers.

8. Design an inertially aided roll out control system using parameter optimization techniques.

Some of the topics are currently under investigation at M.I.T.

PRECEDING PAGE BLANK NOT FILMED.

APPENDIX A

LONGITUDINAL EQUATIONS OF MOTION WITH AUTOMATIC TRAJECTORY CONTROL

by

Paul A. Madden

A.1 Introduction

The Convair 880M longitudinal equations of motion have been linearized and some simplifications have been made to reduce the order of the state. The simplifications include the assumption of automatic airspeed control ($u = 0$), reduction of the servo models from second to first order, and substitution of the hinge-moment equations by quasi-steady relationships deduced from full nonlinear simulation studies. The effectiveness of the resultant set of equations was established by very good agreement between the step responses of the simplified linear and the full nonlinear simulator equations which included second order servos and hinge-moment equations.

In addition, a direct lift control is incorporated, currently envisaged as the existing spoiler controls operating in unison.

Construction of the simplified vehicle, servo, noise and trajectory equations is outlined and finally set in the state variable form

$$\dot{x} = Fx + Gu \qquad (A.1.1)$$

for parameter optimization.

A.2 Vehicle Trajectory Equations[22]

The linearized trajectory equations are

$$\ddot{z} = V_p [\dot{\alpha} - q]/57.3 \qquad (A.2.1)$$

$$\dot{z} = \int_0^t \ddot{z}(\tau)\, d\tau \qquad (A.2.2)$$

$$z = \int_0^t \dot{z}(\tau)\, d\tau \qquad (A.2.3)$$

where α is the perturbation angle-of-attack measured in degrees, and q is the perturbation pitch rate measured in degrees/second. Since $\ddot{z}$ was computed explicitly for use as a feedback variable, the $\dot{\alpha}$ equation is redundant (for small angles) and may be eliminated by substituting the equation for into equation (A.2.1).

A.3 Vehicle Longitudinal Equations of Motion[23,24]

The equations of motion used in this study corresponded to an approach to landing flight condition. The linearized perturbation equations may be written

$$\dot{u} = C_u u + C_\alpha \alpha + C_\theta \theta + C_{\alpha_n} \alpha_n + C_{\delta_s} \delta_s + C_{\delta_t} \delta_t \qquad (A.3.1)$$

$$\dot{\alpha} = C_u u + C_\alpha \alpha + C_q q + C_{\alpha_n} \alpha_n + C_{\delta_e} \delta_e + C_{\delta_s} \delta_s + C_{\delta_{te}} \delta_{te} \qquad (A.3.2)$$

$$\dot{q} = C_\alpha \alpha + C_{\dot{\alpha}} \dot{\alpha} + C_q q + C_{\alpha_n} \alpha_n + C_{\delta_t} \delta_t + C_{\delta_e} \delta_e + C_{\delta_{te}} \delta_{te} + C_{\delta_s} \delta_s + C_{\dot{\delta}_e} \dot{\delta}_e \qquad (A.3.3)$$

$$\dot{\theta} = q \qquad (A.3.4)$$

where u is measured in feet/second, q in degrees/second, and θ in degrees.

The control variables are defined as:

- δ_e - elevator angle in degrees
- δ_{te} - elevator tab angle in degrees
- δ_s - direct lift spoiler angle in degrees
- δ_t - engine thrust in pounds

The coefficient values are:

u equation

$C_u = -0.0271$

$C_\alpha = 18.15$

$C_\theta = -32.2$

$C_{\alpha_n} = 18.15$

$C_{\delta_s} = -1.737$

$C_{\delta_t} = 0.000255$

α equation

$C_u = -0.000855$

$C_\alpha = -0.778$

$C_q = 0.955$

$C_{\alpha_n} = -0.778$

$C_{\delta_e} = -0.036$

$C_{\delta_s} = 0.0678$

$C_{\delta_{te}} = -0.009$

q equation

$C_\alpha = -1.288$

$C_{\dot{\alpha}} = -0.2005$

$C_q = -0.586$

$C_{\alpha_n} = -1.288$

$C_{\delta_t} = 0.000000414$

$C_{\delta_e} = -0.909$

$C_{\delta_{te}} = -0.227$

$C_{\delta_s} = 0.0485$

$C_{\dot{\delta}_e} = -0.000845$

A.4 Velocity Control System [22]

The aircraft is assumed to have a velocity control system such that $u = \dot{u} = 0$. Making this substitution in equation (A.3.1) results in an expression for the change in thrust, δ_t, required to maintain this condition. This expression is substituted into (A.3.1, A.3.2), simultaneously setting $u = 0$ in those equations.

A.5 Hinge Moment Equations [23,24,25]

The hinge moment equations were replaced by quasi-steady expressions relating control surface and tab displacements to servo output displacement. These relationships were deduced from full nonlinear simulation of the CV880 M at the same flight condition and are given by

$$\delta_e = 0.47\ \delta_e^s \qquad \text{(A.5.1)}$$

$$\delta_{te} = -0.53\ \delta_e^s \qquad \text{(A.5.2)}$$

where δ_e^s is the elevator servo output.

A. 6 Control Surface Servo

The elevator and spoiler servos were modeled by the first order system

$$\dot{\delta}^{s} = \frac{1}{\tau} \left[\delta^{sc} - \delta^{s}\right] \qquad \text{(A. 6. 1)}$$

where δ^{sc} is the servo command; τ was set at 0.08 seconds.

A. 7 Aerodynamic Noise [5]

The lateral and vertical components of atmospheric turbulence may be characterised by the power spectral density function

$$\Phi_g(\omega) = \sigma^2 \left[\frac{L}{2\pi V_p}\right] \frac{1 + 3\left(\frac{L\omega}{V_p}\right)^2}{\left[1 + \left(\frac{L\omega}{V_p}\right)^2\right]^2} \qquad \text{(A. 7. 1)}$$

where σ is the root mean square gust quantity, V_p the flight path velocity, L the scale of turbulence and ω the frequency in radians/sec.

This expression can be approximated by

$$\Phi_g(\omega) = \sigma^2 \left[\frac{L}{3^{1/2}\pi V_p}\right] \frac{1}{1 + \left[\frac{L\omega}{3^{1/2} V_p}\right]^2} \qquad \text{(A. 7. 2)}$$

Exponentially correlated noise may be modeled by passing white noise through a suitable shaping filter whose dynamics adjoin the existing system to produce a new system with expanded state subject only to white noise input.

In the system investigated, only vertical gusts (α_n) were introduced, but a simple extension would allow input gusts whose intensity varied along the length of the aircraft (α_n and q_n inputs).

Let the white noise autocorrelation function be given by

$$\phi(\tau) = Q\, \delta(\tau)$$

then its power spectral density is

$$\Phi(\omega) \approx \frac{1}{2\pi} Q \qquad \text{(A. 7. 4)}$$

Passing gaussian white noise through a filter F produces an output whose power spectral density is

$$\Phi_n(\omega) = \left|F\right|^2_{s = i\omega} \Phi(\omega)$$

For the filter $F = \frac{a}{s + a}$, the output is given by

$$\Phi_n(\omega) = \frac{Q}{2\pi} \frac{1}{1 + \left[\frac{\omega}{a}\right]^2} \qquad \text{(A. 7. 5)}$$

Equivalencing (A. 7. 2) and (A. 7. 5)

$$a \equiv \frac{3^{1/2} V}{L} p$$

$$Q \equiv 2\sigma^2 [1/a] \qquad \text{(A. 7. 6)}$$

where the quantity 1/a is the correlation time.

The noise equation may now be written

$$\dot{\alpha}_n = -a\alpha_n + aw \qquad \text{(A. 7. 7)}$$

where w is a gaussian white noise input.

For a mean turbulence scale length of L = 600 feet and V_p = 278.4 feet per second, a = 0.807.

A. 8 Sensor Noise

In addition to the noise created by instruments sensing the position, velocity, and acceleration of the craft, further noise is generated by the attitude sensors. For this example, it is assumed that this noise may be ignored.

The matrices F and G are identified:

$$F = \begin{bmatrix}
-0.7019 & 0.0521 & 0 & 0 & 0.345 & -0.2843 & -0.0758 & 0 \\
1.0 & 0 & 0 & 0 & 0 & 0 & 0 & 0 \\
0 & 0 & 0 & 1.0 & 0 & 0 & 0 & 0 \\
0 & 0 & 0 & 0 & 1.0 & 0 & 0 & 0 \\
\begin{bmatrix}-0.74p_4 \\ -3.662\end{bmatrix} & -0.01138 & \begin{bmatrix}4.11p_5 \\ -0.74p_1\end{bmatrix} & \begin{bmatrix}4.11p_6 \\ -0.74p_2\end{bmatrix} & \begin{bmatrix}4.11p_7 \\ -0.74p_3 \\ -0.854\end{bmatrix} & 0.7987 & -4.093 & 3.05 \\
12.5p_4 & 0 & 12.5p_1 & 12.5p_2 & 12.5p_3 & -12.5 & 0 & 0 \\
0 & 0 & 12.5p_5 & 12.5p_6 & 12.5p_7 & 0 & -12.5 & 0 \\
0 & 0 & 0 & 0 & 0 & 0 & 0 & -0.807
\end{bmatrix}$$

$$G = \begin{bmatrix} 0 \\ 0 \\ 0 \\ 0 \\ -3.05 \\ 0 \\ 0 \\ 0.807 \end{bmatrix}$$

A.9 Control Law

The control law is divided into two sections which generate control inputs for the elevator and direct lift spoiler servos respectively

$$\delta_e^{sc} = p_1 z + p_2 \dot{z} + p_3 \ddot{z} + p_4 q \qquad (A.9.1)$$

$$\delta_s^{sc} = p_5 z + p_6 \dot{z} + p_7 \ddot{z} \qquad (A.9.2)$$

The q term is eliminated for the direct lift spoiler because spoiler coupling into the pitch equation is negligible.

A.10 State Variable Equations

Collecting the trajectory, vehicle, actuator, noise, and control law equations together results in a set of eight first-order linear differential equations which may be written in the form

$$\dot{x} = Fx + Gu \qquad (A.10.1)$$

where x is an eight dimension state vector, and u is a one dimension white noise driving term.

$$x = \begin{bmatrix} q \\ \theta \\ z \\ \dot{z} \\ \ddot{z} \\ \delta_e^s \\ \delta_s^s \\ \alpha_n \end{bmatrix} \qquad (A.10.2)$$

$$u = \begin{bmatrix} w \end{bmatrix} \qquad (A.10.3)$$

REFERENCES

1 Litchford, G. B., "Low Visibility Landing: The Systems Challenge", Astronautics and Aeronautics, Volume 6, numbers 11 and 12, November and December 1968.

2 MacKinnon, D., "Automatic Landing System Optimization using Inertial Navigation Data and Modern Control Theory", presented at the NATO-AGARD Conference on Automatic Landing, Boston, Massachusetts May 1969.

3 MacKinnon, D., "Quasi-Optimization of a Localizer Acquisition System", Proceedings of the Joint Automatic Control Conference of the American Automatic Control Council, Boulder, Colorado, 1969.

4 Broxmeyer, C., D. MacKinnon, and P. Madden, "Application of Inertial Navigation and Modern Control Theory to the All-Weather Landing Problem", MIT Instrumentation Laboratory Report R-613, June 1968.

5 MacKinnon, D., "Improving Automatic Landing System Performances Using Modern Control Theory and Inertial Measurements", MIT Instrumentation Laboratory Report R-628, January 1969.

6 Erzberger, H., and H.Q. Lee, "Optimum Horizontal Guidance Techniques for Aircraft", to be published, NASA Ames Research Center.

7 Kalman, R.E., and R.S. Bucy, "New Results in Linear Filtering and Prediction Theory", Journal of Basic Engineering Transactions of the ASME, March 1961.

8 Burrows, J.W., "Combined Radio-Dead Reckoning Navigation Systems", Proceedings of the ION Conference on Supersonic Navigation, 1967.

9 "Advanced Scanning Beam Guidance System for All-Weather Landing", FAA Report No. RD-68-2.

10 Broxmeyer, C., and D. MacKinnon, "Terminal Phase Navigation", Navigation, Volume 15, Number 4, Winter 1968-69.

11 Merriam, C.W., Optimization Theory and the Design of Feedback Control Systems, McGraw-Hill, New York, N.Y., 1964.

12 Merriam, C.W., "Unpublished Lecture Notes", Cornell University 1966.

13 Gelfand, M., and S.V. Fomin, "Calculus of Variations", Prentice Hall, 1963.

REFERENCES (Cont.)

14. Bellman, K., (Editor) "Modern Analytic and Computational Methods in Science and Mathematics", American Elsevier Publishing Company, Inc., New York, 1968.

15. Rediess, H A., "A New Model Performance Index for the Engineering Design of Control Systems", MIT Thesis TE - 26, December 9, 1968.

16. Mehra, R. K., and A. E. Bryson, Jr., "Conjugate Gradient Methods with an Application to V/ STOL Flight - Path Optimization", AIAA Journal of Aircraft, Volume 6, Number 2, March - April 1969.

17. Widnall, W. S., "Applications of Optimal Control Theory to Computer Controller Design", MIT Research Monograph No. 48, MIT Press 1968.

18. Bryson, A. E., and Y. C. Ho, Applied Optimal Control, Blaisdell Publishing Company, 1969.

19. Lorenzetti, K. C., G. L. Nelson, and K. N. Johnson, "Computerized Design of Optimal Direct Lift Controllers", AIAA Journal of Aircraft, Volume 6 Number 2, March - April 1969.

20. Lorenzetti, K. C., "Direct Left Control for Approach and Landing", presented at the NATO - AGARD Conference on Automatic Landing, Boston, Massachusetts, May 1969.

21. Etkins, B., Dynamics of Flight, Stability and Control, John Wiley and Sons, 1959.

22. Blakelock, J. H., Automatic Control of Aircraft and Missiles, John Wiley and Sons, 1965.

23. "CV 880 M Data", Lear Siegler Report ADR - 595.

24. "Model 32 Revised Longitudinal Stability Derivatives", General Dynamics, Convair Report DC - 22 - 104, Revision II, Sept 1956.

25. "Model 22 DATA For Autopilot Design" General Dynamics, Convair Report DC - 22 - 104 Revision 1 October 1957.

26. Pogust, F. B., "Status of Microwave Scanning Beam Landing System Developments", 1969 Electronics and Aerospace Systems Convention and Exposition, Washington, D. C.

27. Newton, G. C., L. A. Gould and J. F. Kaiser, Analytical Design of Linear Feedback Controls, John Wiley and Sons, 1961.